

**Dispersion of inorganic fillers in
polymeric matrices for food
packaging applications**

Valeria Bugatti



Unione Europea



*Ministero dell'Istruzione,
dell'Università e della Ricerca*



UNIVERSITÀ DEGLI
STUDI DI SALERNO

Department of Industrial Engineering

***Ph.D. Course in Chemical Engineering
(X Cycle-New Series)***

**Dispersion of inorganic fillers in
polymeric matrices for food
packaging applications**

Supervisor

Prof. Vittoria Vittoria

Ph.D. student

Valeria Bugatti

Scientific Referees

Prof. Francesco Pilati

Prof. Loredana Incarnato

Ph.D. Course Coordinator

Prof. Paolo Ciambelli

To my dear family...

Publications list

Publications

1. "Synthesis and physical properties of Layered Double Hydroxide based on Ionic Liquids: Application to a Polylactide matrix", Sébastien Livi and **Valeria Bugatti**, Luis Estevez, Jannick Duchet-Rumeau, Emmanuel. P Giannelis; *Submitted*.
2. "Bio-Nanocomposites Based on Layered Double Hydroxides and active molecules into pectins: preparation, characterization and physical properties", Giuliana Gorrasi, **Valeria Bugatti**, Vittoria Vittoria; *Carbohydrate Polymers*, *Accepted*.
3. "Physical And Water Sorption Properties Of Chemically Modified Pectin With An Environmentally Friendly Process", Luca Monfregola, **Valeria Bugatti**, Pietro Amodeo, Stefania De Luca, Vittoria Vittoria, *Biomacromolecules*: 06/2011; 12(6):2311-8
4. "Modified Layered Double Hydroxides In Polycaprolactone As A Tunable Delivery System: In Vitro Release Of Antimicrobial Benzoate Derivatives"; **Valeria Bugatti**, Gorrasi, Montanari, Nocchetti, Tammaro, Vittoria; *Applied Clay Science* 52 (2011) 34–40.
5. "Water Barrier Properties Of Epoxy-Clay Nanocomposites" Luigi Vertuccio, Andrea Sorrentino, Liberata Guadagno, **Valeria Bugatti**, Marialuigia Raimondo, Carlo Naddeo, Vittoria Vittoria, Generoso Iannuzzo, Erika Calvi, Salvatore Russo. *Submitted*
6. "Thermo-Oxidation Stability Of Poly(Butylene Terephthalate) And Catalyst Composition" A.Massa, **Valeria Bugatti**, A. Scettri, S. Contessa. In: Polymer Aging, Stabilizers And Amphiphilic Polymer- Isbn: 978-1-60692-928-5. Editor: Liudvikas Segewicz And Marijus Petrowsky. © 2010 Nova Science Publishers, Inc.
7. "Synthesis And Characterization Of New Photoluminescent Oxadiazole/Carbazole Containing Polymers," Simona Concilio, **Valeria Bugatti**, Pio Iannelli, Stefano Piotto, *International Journal Of Polymer Science Vol. 2010, Article Id 581056, 6 Pages, 2010*.
8. "Nano-Hybrids Incorporation Into Polycaprolactone For Active Packaging Applications: Mechanical And Barrier Properties"

Valeria Bugatti, Umberto Costantino, Giuliana Gorrasi, Morena Nocchetti, Loredana Tammaro, Vittoria Vittoria. *European Polymer Journal* 46 (2010) 418–427.

9. “New Polymeric Composites Based On Poly(E-Caprolactone) And Layered Double Hydroxides Containing Antimicrobial Species” Umberto Costantino, **Valeria Bugatti**, Giuliana Gorrasi, Francesca Montanari, Morena Nocchetti, Loredana Tammaro And Vittoria Vittoria. *Acs Appl. Mater. Interfaces*, 2009, 1 (3), 668-677;
10. “The Effect Of Additives And Complexing Agents On The Synthesis And Thermo-Oxidation Stability Of Poly(Butylenes Terephthalate)” Antonio Massa, **Valeria Bugatti**, Arrigo Scettri, Socrate Contessa; *Macromolecules: An Indian Journal*, Vol. 4, Issue 1, 2008

Patents

1. Vittoria V, Gorrasi G., Sorrentino A Tammaro L, **V. Bugatti**, Costantino U, Nocchetti M. (2008). Italian Patent Filed On 08.08.2008 At The Office Of The Chamber Of Commerce Industry And Agriculture Of Salerno For The Invention Entitled “Polymeric Materials For The Production Of Active Food Packaging That Protect And Enhance The Food And To Reduce Treatments For The Storage Of Foods. (SA2008A/000024)
2. Vittoria V.; Sorrentino A.; Gorrasi G.; Tammaro L.; **Bugatti V.**; Costantino U.; Nocchetti M.. Polymeric Materials For Active Food Packagings Able To Protect And To Enhance The Quality Of The Contained Food Products And To Reduce Their Preservation Treatments. (WO2010/016034 A2 (11.02.2010)
3. Vittoria V.; Tammaro L.; **Bugatti V.**; Bianchi R. “Preparation Process Of A Polymeric Composition Comprising Hydrotalcites Intercalated With Active Molecules, Composition So Obtained And Shaped Articles Including The Same”. N. MI2011A00192

Awards and Spin-off

- 16-06-2011: “**Nice Filler**” **Society Srl Constitution**- Production And Marketing Of Polymeric Materials For Food Packaging, Spin-Off Based At The Department Of Industrial Engineering, University Of Salerno, Via Ponte Don Melillo, 84084 Fisciano (SA)

- 27 November 2009: **1° Award At Polymer Challenge 2009**, *Veneto Nanotech Ed Imast*, Padova, *Business Plan "Nice Filler"*: "Polymeric Compounds For Active Food Packaging To Increase The Shelf Life Of Food Products And Reduce The Use Of Preservatives And Sterilization Of Foods"

- 7 October 2009: **2° Award - Start Cup Unisa 2009**; Project: "Vulcano S.R.L." Composite Material With Properties Of Self-Healing And Release Of Active Ingredients For Biomedical Applications

Conference

I. Vth International Conference On Times Of Polymers (Top) And Composites 2010, Ischia 20-23 June 2010; Synthesis And Characterization Of New Photoluminescent Oxadiazole/Carbazole Containing Polymers. Concilio, Simona; **Bugatti, Valeria**; Iannelli, Pio; Piotto, Stefano P.

II. Biopolpack: Parma, 15-16 Aprile 2010; Poster Dal Titolo: Nuovi Compositi Polimerici Biodegradabili A Base Di Pectina E Idrotalciti Contenenti Specie Antimicrobiche, **Valeria Bugatti**, Giuliana Gorrasi, Loredana Tammaro, Vittoria Vittoria.

III. Nano_Mates Meets Cncd: 15-16 Dicembre 2009; Università Di Salerno, Presentazione Dal Titolo: Self-Healing Dental Resins And Scaffolds

IV. Workshop Ingegneria Chimica E Alimentare, 30-09-09: Università Di Salerno: Poster Dal Titolo Poly (ϵ -Caprolactone) Composites For Active Packaging Applications

V. Edimburgo: 25-31 Luglio 2009; Water Barrier Properties Of Epoxy-Clay Nanocomposites

VI. Workshop Ingegneria Chimica E Alimentare, 29-06-09: Università Di Salerno: Poster Dal Titolo Mechanical And Barrier Properties Of Poly (ϵ -Caprolactone) Composites For Active Packaging Applications

VII. VII Convegno Nazionale Instm – Tirrenia, 9-12 Giugno 2009: Presentazione Dal Titolo: Mechanical And Barrier Properties Of Poly (ϵ -Caprolactone) Composites For Active Packaging Applications. **Valeria Bugatti**, Umberto Costantino, Giuliana Gorrasi, Morena Nocchetti, Loredana Tammaro, Vittoria Vittoria

Index

Chapter I	
Introduction.....	1
I.1 Preface.....	1
I.2 Phases of the project.....	3
I.3 Materials	5
I.4 Food packaging.....	8
I.5 Packaging as active barrier.....	9
I.6 Release of antimicrobial.....	11
I.7 Preparation of materials with enhanced barrier properties.....	10
I.8 Inorganic filler dispersion method.....	12
I.8.1 Nanocomposites.....	12
I.8.1.1 High energy ball milling (HEBM).....	14
I.8.2 Coating system.....	14
I.8.2.1 Acrylic resin.....	15
I.8.2.2 Plasma.....	15
I.9 Inorganic filler.....	16
I.9.1 Main types of nano-fillers.....	16
I.9.2 Anionic clay.....	16
I.9.3 Methods of synthesis.....	17
I.9.3.1 Urea method.....	18
I.9.3.2 Coprecipitation method.....	19
I.10 Types of polymers for food packaging.....	19
I.10.1 Biodegradable polymers in food packaging field.....	21
I.10.2 Natural polymers.....	22

Chapter II	
Layered Double Hydroxides.....	25
II.1 Preparation of LDHs.....	25
II.1.1 Synthesis of hydrotalcite (LDHBz and derivatives) by urea method..	25
II.1.2 Synthesis of hydrotalcite modified with active molecule by coprecipitation method.....	26
II.2 Characterization and comparison of preparative methods.....	27
II.2.1 X-ray diffraction.....	27
II.2.2 Infrared spectroscopy.....	28
II.2.3 Thermogravimetry (TGA).....	29
II.2.4 Elemental Analysis.....	31
Chapter III	
Polycaprolactone composites.....	33
III.1 PCL/nano-hybrids preparation.....	34
III.2 Film preparation.....	34
III.3 X-Ray analysis.....	34
III.4 Water vapor barrier properties.....	36
III.5 Release kinetics.....	39
III.5.1 Release of Benzoate.....	39
III.5.2 Comparison of PCL composites with hydrotalcite synthesized by different methods.....	40
III.5.2.1 X-ray diffraction analysis.....	41
III.5.2.2 Kinetics of release.....	42
Chapter IV	
Polyethyleneterephthalate composites.....	45
IV.1 Selection of fillers used.....	45
IV.2 Incorporation of modified inorganic fillers in PET by "High Energy Ball Milling".....	46
IV.3 PET composites characterization.....	46
IV.3.1 X-ray diffraction of PET-filler composites.....	46
IV.3.2 Thermogravimetric Analysis of PET Filler Composites.....	47
IV.3.3 Oxygen barrier properties.....	48
IV.4 Antimicrobial test of PET composites.....	50
IV. 4. 1 Evaluation of antimicrobial activities of LDH-active molecule powder.....	50
IV. 4. 2 Evaluation of antimicrobial activities of LDH-salicylate in film....	52
IV. 4. 2. 1 Evidence of contact between films and microorganisms in liquid.....	52
IV. 4. 2. 2 Evidence of contact between films and microorganisms in solid.....	53
IV.5 Release kinetics.....	54
Chapter V	
PET/hydrotalcites coating.....	55
V.1 PET/ active filler coatings characterization.....	56

V.1.1 X-ray diffraction.....	56
V.1.2 Release of salicylate from PET/adhesive/12% LDHsal.....	57
V.1.3 Microbiological Test of PET/adhesive/12 %LDHsal.....	57
V.2 Application of system PET+ (adhesive / LDH-active molecules) on extending the shelf life of food.....	58
V.2.1 Mozzarella.....	58
V.2.1.1 Project phases.....	59
V.2.1.2 First results.....	59
V.2.2 Other foods.....	61
V.2.2.1 Milk.....	63
Chapter VI	
Polylactic acid coating.....	65
VI.1 Objectives of this part of the project.....	65
VI.2 Idea.....	66
VI.3 Research outline.....	66
VI.4 Advantages.....	67
VI.5 Organic molecules incorporated in the hydrotalcites.....	67
VI.5.1 Phosphonium ionic liquid salts.....	67
VI.6 Hydrotalcite (LDH) synthesis.....	69
VI.7 Characterization of hydrotalcite LDH-active molecule.....	69
VI.7.1 X ray diffraction.....	69
VI.7.2 Thermogravimetric analysis (TGA).....	71
VI.8 PLA characterization.....	72
VI.8.1 X ray diffraction.....	72
VI.9 Study of the best plasma treatment conditions for PLA.....	73
VI.10 Deposition process of LDH nanoparticles on plasma treated PLA....	74
VI.11 Coating characterization.....	74
VI.11.1 X-ray photoelectron spectroscopy.....	74
VI.11.2 Scanning electron microscope.....	75
VI.11.3 Contact angle.....	76
VI.11.4 Stability and durability.....	77
VI.11.5 Selection of LDH nanoparticles.....	77
VI.11.6 Water permeability.....	78
VI.11.7 Thermal analysis.....	80
VI.11.8 TEM.....	81
Chapter VII	
Polylactic acid composites.....	83
VII.1 Materials preparation.....	83
VII.2 PLA composites film preparation.....	84
VII.3 Research outline.....	84
VII.4 Characterization of PLA composites.....	84
VII.4.1 X-ray diffraction.....	84
VII.4.2 Thermal analysis.....	85
VII.4.3 Mechanical properties.....	87

VII.4.4 Barrier properties: water permeability.....	88
VII.4.5 Morphology of PLA/LDH nanocomposites.....	89
Chapter VIII	
Pectin composites.....	91
VIII.1 Objectives.....	91
VIII.2 Composites and film preparation.....	91
VIII.3 Results and discussion.....	92
VIII.3.1 X-ray analysis.....	92
VIII.3.2 Thermogravimetric analysis (TGA).....	93
VIII.3.3 Mechanical properties.....	94
VIII.3.4 Transport properties of water vapour.....	95
VIII.3.5 Antimicrobial behaviour.....	98
Chapter IX	
Methods of investigation.....	101
IX.1 High Energy Ball Milling.....	101
IX.2 Twin screw extruder mini lab Haake.....	102
IX.3 X-ray diffraction.....	102
IX.4 Thermogravimetric analysis (TGA).....	102
IX.5 Differential scanning calorimetry (DSC).....	102
IX.6 Infrared spectroscopy (FT-IR).....	102
IX.7 Ultraviolet spectrophotometry (UV).....	103
IX.8 Mechanical properties.....	103
IX.9 Water vapor barrier properties.....	103
IX.10 Oxygen transport properties.....	104
IX.11 Elemental analysis.....	105
IX.12 Antimicrobial test.....	105
IX.13 Contact angle.....	106
IX.14 Plasma.....	106
IX.15 Xps surface science instrument sxx-100.....	106
IX.16 Leo 1550 FESEM.....	106
IX.17 FEI T12 TWIN TEM.....	107
Conclusion.....	109
References.....	113

Figures Content

Figure I.1 <i>Hydrotalcite structure</i>	5
Figure I.2 <i>Organic molecules incorporated in hydrotalcite</i>	7
Figure I.3 <i>Schematically illustration of three different types of thermodynamically achievable polymer/clay nanocomposites</i>	13
Figure I.4 <i>Generation of reactive species on oxygen plasma treated polymeric surface</i>	15
Figure II.1 <i>Comparison between X-Ray spectra of LDH from Urea and from Coprecipitation for LDHsal (a) and LDHBz(b)</i>	27
Figure II.2 <i>Comparison between Infrared spectra of LDH from Urea and from Coprecipitation for LDHsal (a) and LDHBz(b)</i>	29
Figure II.3 <i>Comparison between TGA of LDH from Urea and from Coprecipitation for LDHsal (a) and LDHBz(b) (thermal cycle from 30 to 800 ° C at 5 ° C / min, in air flow)</i>	30
Figure III.1 <i>X-ray powder diffraction patterns of: (A) ZnAl-Bz and composites; (B) ZnAl-BzDC and composites; (C) ZnAl-p-BzOH and composites; (D) ZnAl-o-BzOH and composites</i>	35
Figure III.2 <i>Diffusion coefficient of water vapor for: PCL and PCL/ZnAl-Bz composites (A); PCL and PCL/ZnAl-BzDC composites (B); PCL and PCL/ZnAl-p-BzOH composites (C); PCL and PCL/ZnAl-o-BzOH composites (D)</i>	37
Figure III.3 <i>The logarithm of thermodynamic diffusion coefficient, $D_0(\text{cm}^2/\text{s})$ versus the inorganic content of the nano-hybrid</i>	38
Figure III.4 <i>Release kinetics of Bz anion from PCL/ZnAl-Bz6 and PCL-Bz/1.6 in a physiological saline solution, as a function of time</i>	40

Figure III. 5 Comparison between X-Ray spectra of PCL/LDH from Urea and from Coprecipitation for LDHsal (a) and LDHBz(b).....	41
Figure III.6 Release kinetics as a function of time of Sal(a) and Bz(b) anion from LDH from coprecipitation and Urea, incorporated in PCL	42
Figure IV.1 X-Ray diffraction patterns of PET/3%LDHsal composite.....	47
Figure IV.2 TGA curve of PET composite (thermal cycle from 30 to 800 ° C at 5 ° C / min, in air flow).....	47
Figure IV.3 Oxygen sorption coefficients of PET composites.....	48
Figure IV.4 Oxygen diffusion coefficients of PET composites.....	49
Figure IV.5 Oxygen Permeability coefficients of PET composites.....	49
Figure IV.6 Apples Test of PET composites.....	50
Figure IV.7 Antimicrobial activities of LDH-active molecule powder.....	51
Figure IV.8 Antimicrobial activities of LDH-active molecule in film before (A) and after(B) incubation in liquid.....	53
Figure IV.9 Antimicrobial activities in solid of LDH-active molecule in film.....	53
Figure IV.10 Kinetics of release of salicylate from PET composites.....	54
Figure V.1 X-ray diffraction patterns of PET/adhesive/12%LDHsal.....	56
Figure V.2 kinetics of release of salicylate from PET/adhesive/12%LDHsal.....	57
Figure V.3 Antimicrobial test of PET/adhesive/12%LDHsal film.....	58
Figure V.4 pH variation for mozzarella in PET and in PET/active system.....	60
Figure V.5 Yeast growth in PET (a) and in PET/active system (b).....	60
Figure V.6 Total bacterial growth in PET/active system (a) and in PET (b).....	61
Figure V.7 Organoleptic characteristic for Mozzarella after 34days for the control (a) and antimicrobial agent (b).....	61
Figure V.8 Grapes after 21 days: control(a) and antimicrobial system (b).....	62
Figure V.9 Cherries after 21 days: control(a) and antimicrobial system (b).....	62
Figure V.10 Cheese after 21 days: control(a) and antimicrobial system (b).....	62
Figure VI.1 Possible interaction between hydrotalcites nanoparticles and Plasma treated surface PLA	66
Figure VI.2 Ionic liquid (IL) salts structures.....	68
Figure VI.3 IL103:tetradecyl(trihexyl)phosphonium decanoate (P1) structure.....	68
Figure VI.4 Comparison between X ray diffraction of LDHnitrate and LDH-IL103.....	70
Figure VI.5 Comparison between Tga of LDHnitrate and LDH-IL103: [30-800°C at 20°C/minute under nitrogen].....	71

Figure VI.6	PLA structure.....	72
Figure VI.7	X-ray diffraction patterns of PLA.....	73
Figure VI.8	Contact angle ($^{\circ}$) values for different conditions (power/time) of plasma treatment.....	73
Figure VI.9	Xps spectra for PLA untreated, PLA after plasma (AP) and PLA AP after coating with LDHIL103.....	75
Figure VI.10	SEM images for PLA untreated, PLA AP, PLA AP after coating with LDHnitrate and LDH-IL103.....	76
Figure VI.11	Contact angle ($^{\circ}$) values for PLA, PLA AP and PLA after coating with different LDH.....	77
Figure VI.12	SEM images of PLA AP after coating with LDH after 1 hour in solvent.....	77
Figure VI.13	SEM images of PLA after coating with LDHnitrate filtered...78	
Figure VI.14	Weight loss in function of the time for sample PLA AP AC+LDHP1.....	79
Figure VI.15	Water Permeability coefficients for PLA untreated, PLA AP and PLA after coating with different LDH.....	79
Figure VI.16	TEM images of LDH nanoparticles.....	81
Figure VI.17	TEM images of the plasma treated PLA surfaces coated with a multilayer of LDH nanoparticles after a one-step deposition.....	82
Figure VII.1	X-ray diffraction patterns of PLA composites.....	85
Figure VII.2	Elastic Modulus of PLA composites.....	87
Figure VII.3	Tensile strength and Tensile strain of PLA composites.....	87
Figure VII.4	Stress-strain curve for PLA+2%LDHP1 composite.....	88
Figure VII.5	Water Permeability for PLA composites.....	89
Figure VII.6	TEM images of (a) PLA/LDH-P1, (b) PLA/LDH-P2.....	90
Figure VIII.1	X-ray diffraction pattern of (a) Pectin, (b) Pectin/LDH-Bz, (c) Pectin/LDH-DCBz, (d) Pectin/LDH-o-OHBz, (e) Pectin/LDH-p-OHBz.....	92
Figure VIII.2	TGA analysis of (a) Pectin, (b) Pectin/LDH-Bz, (c) Pectin/LDH-DCBz, (d) Pectin/LDH-o-OHBz, (e) Pectin/LDH-p-OHBz.....	94
Figure VIII.3	Elastic moduli evaluated on pure pectin and nano composite films.....	95
Figure VIII.4	Sorption isotherms of water vapour of pure pectin and composites with different nanohybrids.....	97
Figure VIII.5	Diffusion coefficients of water vapour as function of $C_{eq}(g/100g)$ for pure pectin and composites with different nanohybrids.....	98
Figure VIII.6	Pictures from cast film of pectin and composites with nanohybrids after storage 12 months at ambient temperature.....	99

Table Content

Table II.1 Values for elemental analysis of LDHsal.....	31
Table III.1 Composition of hydrotalcites incorporated on PCL.....	33
Table III. 2 Transport parameters for all the composites.....	38
Table IV. 1 <i>E. coli</i> counts after time of incubation for all the samples.....	52
Table V.1 Reduction time of blue methylene indicator on PET and PET/12 Mix samples.....	63
Table VI.1 Reagents quantities for LDH ionic exchange reaction.....	69
Table VI.2 TGA of PLA and PLA coatings[30-800°C at 20°C/minute under nitrogen].....	80
Table VI.3 DSC of PLA and PLA coatings[30-250°C at 10°C/minute under nitrogen].....	80
Table VII.1 Tga of PLA composites: [30-800°C at 20°C/minute under nitrogen]	85
Table VII.2 DSC of PLA composites: [30-250°C at 10°C/minute under nitrogen].....	86
Table VIII.1 Degradation temperature (°C) evaluated at 50% of weight loss from TGA.....	94
Table VIII.2 Transport parameters extracted from the curves of Figures VIII.4 and VIII. 5.....	98

Abstract

The objective of this PhD project regards the formulation, preparation and characterization of polymeric materials in which lamellar inorganic solids containing potentially active molecules are dispersed.

In particular the present work was aimed at the preparation and characterization of "Active Food Packaging Materials" using inorganic fillers modified with active molecules (antimicrobials, antioxidants) dispersed in polymeric matrices for the realization of:

- 1) Materials with improved barrier properties to gases and vapors
- 2) Systems for controlled release of active molecules, act to protect and extend the shelf life of food products.

Two techniques of dispersion of active inorganic fillers in polymer matrices have been used, generating:

- 1) polymeric nanocomposites
- 2) coatings of polymeric surfaces.

A screening of different polymers, from biodegradable and thermoplastic to natural, was done to compare the effect of the fillers and of the dispersion technique on the properties mentioned above.

Chapter I

Introduction

I.1 Preface

The need to extend the shelf life of packaged food has brought the research into innovative solutions along with the changing needs of consumers, making the "packaging" a constantly evolving field. This evolutionary process has changed the concept of packaging. Today, the package must meet increasingly strict requirements, not always all compatible, which affect not only product protection, ease of use, low cost but also the hygienic, health, nutritional, organoleptic and aesthetic quality.

For this reason, packaging is increasingly taking a leading role in preserving and improving the characteristics of food to the point of being considered itself a respectable product.

More than half of the materials which are most commonly used in the sector of food packaging are glass, aluminum, cardboard and plastic cards.

The last 50 years have been characterized by the implacable advance of plastics that are gradually taking the place of traditional materials, especially glass and metal. This is because the plastics are very versatile in terms of processability (low specific gravity, transparency, shatterproof, etc.) and performance, keeping costs more or less down. For this reason, the research in the field of plastic packaging is always pushing towards the development of new solutions that could meet the growing needs of the market, particularly of the food one.

The current trend is directing the research towards the development of innovative solutions both for functional packaging (active packaging and nanocomposite materials) and low environmental impact (biodegradable materials, recyclable packaging with reduced size).

Packaging and food are not seen anymore as separate entities but as elements that can interact and are always pursuing the goal of improving the acceptability of the packed product.

A possible strategy to improve the mechanical properties, heat resistance and the barrier properties of these systems is the incorporation of inorganic materials at the nanometer level, in polymeric matrices. The research on polymer-based nanocomposite systems by oil and biodegradable polymers has shown that the dispersion of inorganic materials at the nanometer level in the polymer improves its properties.

The incorporation of inorganic fillers in the polymeric matrix can improve the mechanical properties (eg elastic modulus and energy at break), thermal (eg, increased glass transition temperature and the temperature of thermal degradation of the polymer) and liquid permeability gases and vapors, allowing the creation and the processing of products that have a high mechanical module and a good toughness. Other interesting prospects concern some specific properties, such as controlled release, a better control of thermal expansion and a highly effective flame retardants inherent.

High quality and microbiologically safer foods, as well as longer product shelf-life, are continuously required by consumers and this is compelling the research, both academic and industrial, to develop, more and more, new food preservative strategies. The packaging of food products, aimed at reducing the spoilage by bacteria and at protecting from the pollutant environment, is quite different from the packaging of other products and requires more specific properties.

The realization of new materials, in which an inorganic component is dispersed, impose the necessity of knowing the structural organization of the polymer and the resulting physical properties. In fact, the properties of the material depend on the properties of the components and on the interfacial interactions between the different phases. A crucial point for understanding many properties of the composites and the prevision of their behavior is the analysis of the structure and the interface polymer/inorganic compound. In this sense the analysis of the structural organization of the polymer and the correlation with the physical properties will be of fundamental importance. Moreover, the release of the active molecules will be dependent on: interaction molecule-inorganic lamella, composition, type of dispersion of the modified inorganic material into the polymer, contact with food. The new approach of introducing inorganic particulates containing active molecules into polymeric matrices can lead to a synergism of properties typical for organic and for inorganic compounds with tuneable molecular delivery. The inorganic compound is introduced into the polymer not only to

improve the properties but mainly because active molecules that can be released with controlled kinetics, depending on electronic structure, interaction, concentration, morphology and polymorphism of the matrix, are fixed on it. The methods of immobilization of the active compounds in the hybrid compounds was modelled and developed and the processing procedures to incorporate the nano-hybrids into the polymeric matrices was explored. The release kinetics and the release models was correlated to the structure and morphology of the polymeric matrix.

The methodology to incorporate the inorganic compound with the active molecule into the polymeric material are those currently used such as melt blending at high temperatures. However an innovative method like High Energy Ball Milling (HEBM) at room temperature, and without solvent is used in the last years. The last method seems to be potentially the most suitable for natural polymers that in many cases undergo degradation phenomena before melting.

The characterization of films obtained was carried out using different experimental techniques:

- The X-rays diffraction, to determine the degree of intercalation of polymer between the layers of the charge.
- The infrared spectroscopy (FT-IR), to investigate which molecules are present in the layers.
- The degradation temperature and composition of the filler were determined by thermogravimetric analysis (TGA).
- The study of the kinetics of release was made using the UV-visible.
- Morphological analysis by SEM and TEM

I.2 Phases of the project

The principal phases of the PhD project were:

1) **Synthesis of Hydrotalcite** (LDH) modified with organic molecules with specific action (antimicrobial and antioxidant) by Urea method and Coprecipitation method: characterization and comparison

2) Incorporation by High Energy Ball Milling (HEBM) of LDH modified with molecules with antimicrobial properties (LDHBenzoate (LDHBz), LDHp-hydroxybenzoate (LDHpOHBz), LDHortho-hydroxybenzoate (LDHsal), LDH2,4-dichlorobenzoate (LDHDCB)) on **Polycaprolactone (PCL)**:

- Study of water barrier properties of composites (from LDHpOHBz and LDHDCB)

- Study of controlled release from composites and comparison of release from LDH obtained from 2 different method of synthesis (LDHsal and LDHBz)

3) Incorporation by HEBM of LDH modified with active molecules with antioxidant and antimicrobial properties on **Polyethyleneterephthalate (PET)** to obtain materials with oxygen barrier properties and antimicrobial activity:

- Thermal and structural characterization
- Study of the oxygen barrier properties
- Study of antimicrobial properties of composite and release kinetics of antimicrobial

4) Preparation and characterization of **coatings on PET** film, dispersing the inorganic filler (LDH) in an adhesive for food application, to develop antimicrobial and antioxidant systems:

- Study of antimicrobial properties, oxygen barrier properties and kinetics of release of the PET coating
- Application of the system PET coating + LDH-active molecule on fresh foods such as mozzarella, grapes, cherries, milk, to demonstrate the effectiveness of controlled-release on extension of the food shelf life

5) Preparation and characterization of antimicrobial **coatings on plasma treated Polylactic acid (PLA)** (procedure developed during the period spent at Cornell University, Ithaca NY):

- Preparation of inorganic filler (LDH) modified with active molecules: Ionic liquids based on tetraalkylphosphonium salts combined with different anions (decanoate and dodecylsulfonate) have been used as intercalating agents of layered double hydroxides (LDHs) by ion exchange. The synthesized phosphonium-treated LDHs display a dramatically improved thermal degradation and a significant increase of the interlayer distance as confirmed by thermogravimetric analysis (TGA) and X-Ray Diffraction (XRD).

- Deposition of modified filler on plasma treated polymeric surface and characterization for the realization of systems with antimicrobial activity and systems with improved water barrier properties

6) **Incorporation by extrusion** of LDH modified with active molecules on **PLA** (procedure developed during the period of time spent at Cornell University, Ithaca NY) to obtain materials with improved mechanical, barrier properties and antimicrobial activity. To highlight the effect of thermostable ionic liquids, a very low amount of LDHs have been introduced on a polylactid acid (PLA) matrix and PLA/LDHs

nanocomposites have been processed in melt by twin screw extrusion. Then, Transmission electron microscopy (TEM) analysis has been used to investigate the influence of ILs on the different morphology of these nanocomposites. Even if the thermal stability of PLA matrix decreased, an excellent stiffness-toughness compromise has been obtained.

7) **Incorporation by High Energy Ball Milling (HEBM)** of LDH modified with molecules with antimicrobial properties (LDHBenzoate (LDHBz), LDHp-hydroxybenzoate (LDHpOHBz), LDHortho-hydroxybenzoate (LDHsal), LDH2,4-dichlorobenzoate (LDHDCB)) on natural polymers such as **Pectin from apple** to realize system of composites or coating for food packaging:

- Thermal and structural characterization
- Study of the mechanical properties
- Study of the water barrier properties
- Study of antimicrobial properties of composite

I.3 Materials

The polymeric materials used include a polymeric matrix (polycaprolactone (PCL), polyethylene terephthalate (PET), polylactic acid (PLA) and an inorganic component dispersed within said matrix, the hydrotalcite (LDH), a double-layered aluminum and zinc hydroxide modified with active organic molecules.

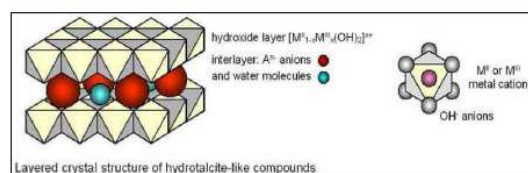


Figure I.1 Hydrotalcite structure

1) For the realization of water barrier systems and release of antimicrobials were prepared nanocomposites based on poly (ϵ -caprolactone) (PCL) and hydrotalcites. Were synthesized hydrotalcites, (ZnAlLDH)-benzoate, pOHBz, DCB and salicylate by Urea method at the University of Perugia and by the method of coprecipitation at our laboratories.

Poly (ϵ -caprolactone) (Mn = 50000), sodium benzoate and derivatives were used without further purification.

The sodium benzoate and derivatives are used as preservatives in food. Sodium salicylate is an antiseptic in toothpaste, and is the key-ingredient of aspirin.

Chapter I

2) To obtain materials with enhanced gas barrier properties were prepared nanocomposites based on polyethylene terephthalate (PET); were used PET CLEARUF 8006 of M&G, high molecular weight polymer with a 0.80 intrinsic viscosity (IV) and various fillers chosen to act as an oxygen barrier layer and replace high barrier:

- Are synthesized various hydrotalcites, (LDH)-organic molecule by the method of coprecipitation. Organic molecules incorporated in hydrotalcite are:

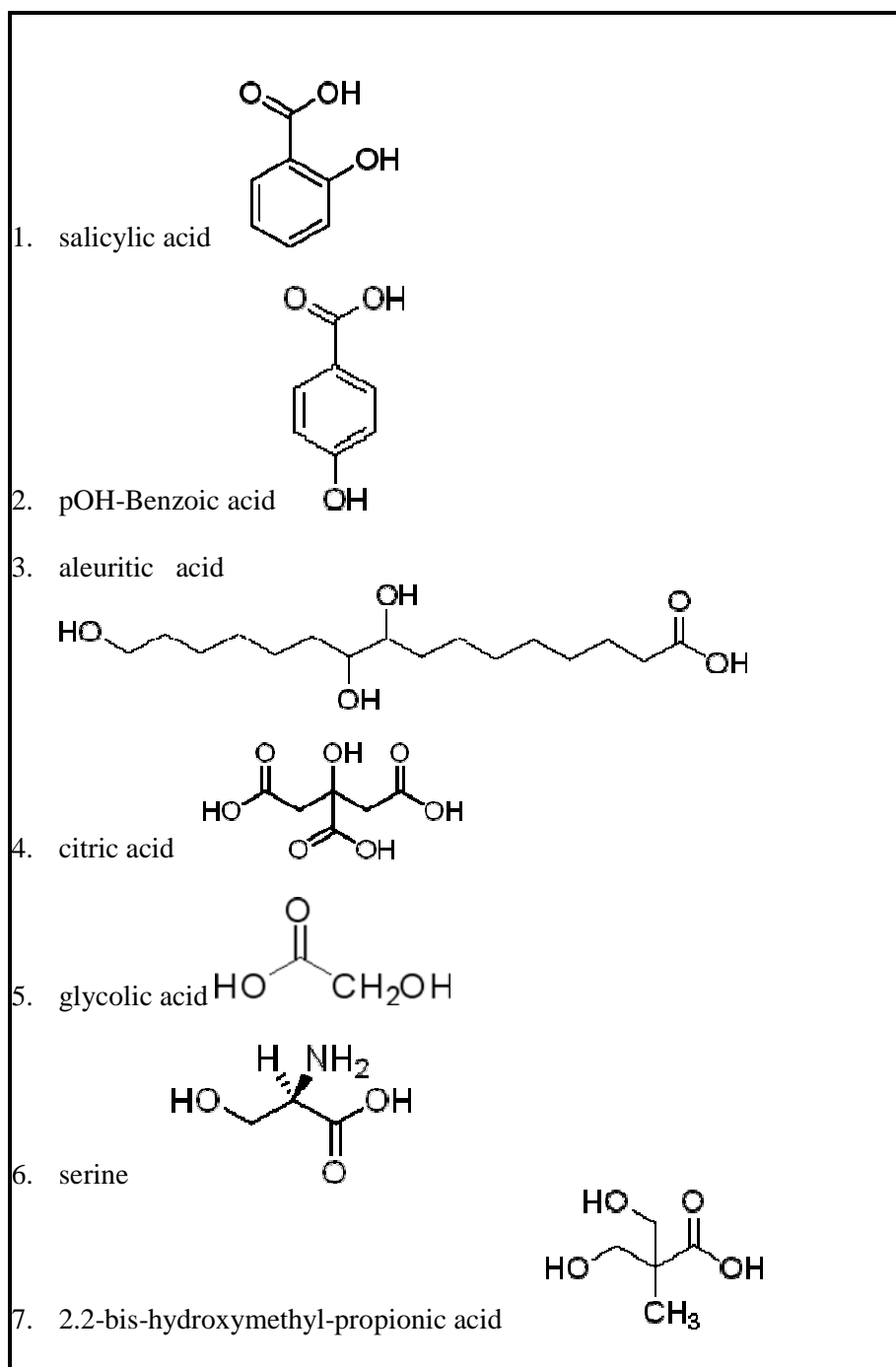


Figure I.2 Organic molecules incorporated in hydrotalcite

3) For the realization of antimicrobial release systems from PET coating, were prepared coating on PET film, using an acrylic adhesive for food, normally used as an adhesive in poly laminated (Novacote HS-8256, COIM spa, weight 3.8g/m^2) in which was dispersed active filler (LDH-anion-LDH-carbonate) to allow a release faster than when the filler is dispersed in the melt polymer.

4) For the realization of antimicrobial coatings on plasma treated PLA and PLA composites the organic molecules used to modify the hydrotalcite and give a target activity, are polystyrenesulfonate (PSS) and phosphonium ionic liquid salts (IL) such as IL 103 tetradecyl(trihexyl)phosphonium decanoate (P1) and IL 201: tetradecyl(tributyl)phosphonium dodecylsulfonate (P2) provided by Cytec Industries Inc, to increase the hydrophobicity of PLA surface and to have an antimicrobial coating. The PLA polymer used is 7032D from NatureWorks. It is a semicrystalline PLA, had reported a Tg of $57\text{ }^\circ\text{C}$, specific gravity of 1.25 and a melt flow index of 10-25g/10 min.

5) For the realization of barrier and antimicrobials systems from pectin nanocomposites, the apple peel Pectin was purchased from Sigma Aldrich. It is a powder sample with high molecular weight (30,000–100,000) and a high degree of esterification (70–75%) on a dry basis. For the nano-hybrids were synthesized hydrotalcite, (ZnAILDH)-benzoate, pOHBz, DCB and salicylate by Urea method at the University of Perugia.

I.4 Food packaging

Earlier food packaging materials were used to provide only barrier and protective functions. Polymers have been widely used in different packaging applications, and nowadays the incorporation of antimicrobial substances in polymeric matrices is gaining more and more field in technical processes. These materials include new biodegradable polymers, polymers with both hydrophilic and hydrophobic characteristics, and hydrogels able to respond to temperature or pH variations (Cabedo *et al*, 2006). Various kinds of active substances can be incorporated into packaging materials to improve their functionality. Such active packaging technologies are designed to extend the shelf life of foods while maintaining their nutritional quality and safety. Active packaging technologies involve interactions between food, packaging material, and the internal gaseous atmosphere. The extra functions they provide include oxygen scavenging, antimicrobial activity, moisture scavenging, and others.

When antimicrobial agents are incorporated into a polymer, they retard or prevent microbial growth. This application could be used for foods effectively, not only in film forms but also as containers and utensils and this

approach can reduce the addition of larger quantities of antimicrobials that are usually incorporated into the bulk of the food. Nevertheless, the incorporation of low molecular weight antimicrobial molecules in polymer matrices has the disadvantage that the migration and the release of the molecules cannot be easily predicted and controlled. More often, it leads too rapidly to an initial high concentration of the active constituent in the food, limiting at the same time the duration of the surface activity of the polymeric matrix. The morphology of the polymer matrix plays an important role to the active molecule release rate. However the diffusion parameter can change in a narrow interval, not allowing prolonged times for complete exit of the molecules (Goodburn *et al*, 1988).

Controlled release systems are currently being developed in many fields of science and technology with the aim to lead to more efficient processing and targeting of active molecules. Drugs in medical devices, antimicrobial and oxygen scavenging for food packaging applications, biocides for agricultural purposes are currently intensely being investigated (Kester *et al*, 1986).

Recently great attention has emerged around the hybrid organic-inorganic systems and, in particular to those in which layered silicates are dispersed at a nanometric level in a polymeric matrix. Such nanohybrid composites possess very unusual properties that are very different from their microscale counterparts. In particular layered double hydroxide (LDHs) or hydrotalcite like compounds, have received considerable attention as active molecule delivery vehicle, because of their anion exchange properties. These compounds, also known as "anionic clays" have general formula $[M(II)_1 \cdot_x M(III)_x(OH)_2](A_{x/n}) \cdot mH_2O$ where M(II) is a divalent cation such as Mg, Ni, Zn, Cu or Co and M(III) is a trivalent cation such as Al, Cr, Fe or Ga, A^{n-} an anion of charge n such as CO_3^{2-} , Cl^- , NO_3^- or organic anion.

These hybrid organic-inorganic systems can ensure the migration and the release of the molecule in a controlled and tuneable way, keeping preserved for as long as the food does before degradation starts.

A big effort to extend the shelf life and enhance food quality while reducing packaging waste, has encouraged the exploration of new bio-based packaging materials such as edible and biodegradable films. The use of these materials, due to their biodegradable nature, could solve the waste problem, at least to some extent.

I.5 Packaging as active barrier

The packaging indicates those functional packaging solutions in which involves the use of a material, container or packaging of an accessory, that can play an active and an additional containment solution rather than a traditional generic product protection (Ravi Kumar *et al*, 2001). The definition of "active" was associated with all the solutions of "packaging" that constantly and actively interact with the atmosphere inside a package:

by varying the composition and quantitative headspace or directly with the product it contains, by releasing from the material of antimicrobials, antioxidants, or other useful substances to improve their quality. The solution of "active packaging" consists of placing inside the box bags containing special agents that interact continuously with the internal atmosphere and / or with the product or absorption through the release of suitable substances.(Lu et al, 2004). Such systems, however, find it difficult to succeed in European countries for at least two reasons:

- The national and European regulations are not yet ready to face legislative action, such a development of food packaging;
- The consumer himself is not well prepared psychologically to buy packaged food that contain not only the product but some objects inside that one could think as "strangers."

In view of psychological denial that European customers would have in respect of such system, the food packaging industry is taking steps in the next few years to better hide the view of these liberators / gas absorbers. The solution was found by developing new packaging materials that enclose the active agents (gas emitters and absorbers, antimicrobials). The main active packaging technologies relate to the use of specific substances able to absorb oxygen, adjust the humidity, emit or absorb carbon dioxide, act with antimicrobial effects on the food, absorb ethylene, flavors or smells. Applications of "active packaging" materials provide the addition of active substances released into the product by increasing its shelf life (Giavaresi et al, 2004).

I.6 Release of antimicrobial

More and more the research focus on developing active packaging sterile film that is able to have an antimicrobial effect on food and beverages. In general, antimicrobial packaging approaches are of two types: the first one is to bind the reagent to the surface of the packaging with the aid of a molecular structure which is large enough to maintain microbial activity even when trapped in the plastic and whilst the second one is about the release of agents in the food or the removal of a localized food ingredient essential for microbial growth. The major application of antimicrobial films is about the packaging of meat, fruit and vegetables. (Zweers et al, 2006) The most common antimicrobial agent is represented by zeolites replaced by Ag ions that have a strong antimicrobial activity. Another antimicrobial agent is potassium sorbate which is added and extruded with LDPE at high temperatures to prevent thermal decomposition of the sorbate to produce "masterbatch". (DelNobile et al, 2003). These are developing systems to gradually release SO₂ to control the growth of mould on certain fruits. Another compound that exhibits antimicrobial effects is ethanol. While the removal of oxygen and the removal of ethylene and the release of ethanol

represent an opportunity to limit food additives with chemical preservatives of all kinds, the "active packaging" may also be a way to release the same preservatives on the packaged food. In this case it's possible to capitalize on the ability of the material to allow the diffusion from molecules of low molecular weight, and the diffusion and release mechanisms on the food are regulated by factors including the nature of the polymer matrix, the nature of the diffusing molecule, the temperature, the partition material/food. In perspective to this application, active packaging can modulate, quantitatively and in respect of time, the preservative effect. There are many references regarding this use and its effectiveness has always been demonstrated (Appendini *et al*, 2002).

I.7 Preparation of materials with enhanced barrier properties

The polymeric materials used nowadays for packaging have several weaknesses, including: poor mechanical properties, low thermal resistance, poor barrier property (Jasse *et al*, 1997).

The standard polymeric resins do not have sufficient barrier properties to protect the shelf life of products. The substrate must then be coupled, co-extruded or coated with materials "high barrier". The easiest way to get food packaging with high performance is to combine multiple materials, of which the outer layer is made of polyester or polypropylene (high melting point) whilst the interior is a gas barrier material such as aluminum, metallized films, copolymers cyclic olefin, etc (Brun *et al*, 2008). An important objective is the reduction of multiple incompatible materials in the same articles. While the foil is widely used as barrier material, the coupling of sheets is not always the best solution to ensure the right combination of required features, especially for packaging where transparency is the primary requirement.

The packaging manufacturers claim that, along with barrier properties, the materials that ensure good mechanical properties, long life, are welded and / or printed (Salame *et al*, 1986).

A possible strategy to improve the physical properties of conventional packaging is to disperse inorganic materials at the nanometer level, in polymer matrices, such as organic-inorganic hybrid systems. The dispersion of filler in the polymer matrix is generally more economical than the one required in coupling and guarantees:

- Improved mechanical properties (increased modulus and toughness) could allow the use of film with lower thickness.
- Improved barrier properties: elimination of the layer "high barrier" in the multilayer film (eg aluminum and EVOH) (Gorrasi *et al*, 2003). The determination of the barrier properties of a polymer is crucial to estimate and predict the product-package shelf-life. The specific barrier requirement of

the package system is related to the product characteristics and the intended end-use application. (Robertson et al, 1993) Generally plastics are relatively permeable to small molecules such as gases, water vapour, organic vapours and liquids and they provide a broad range of mass transfer characteristics, ranging from excellent to low barrier value, which is important in the case of food products. Water vapour and oxygen are two of the main permeants studied in packaging applications, because they may transfer from the internal or external environment through the polymer package wall, resulting in a continuous change in product quality and shelf-life. Carbon dioxide is now important for the packaging in modified atmosphere (MAP technology) because it can potentially reduce the problems associated with processed fresh product, leading to a significantly longer shelf-life. For example, for fresh product, respiration rate is of a great importance in MAP design so identifying the best packaging is a crucial factor (Sorrentino *et al*, 2006).

I.8 Inorganic filler dispersion method

I.8.1 Nanocomposites

Nanocomposites are a new class of composites consisting of polymers loaded with dispersed particles having at least one dimension in the order of nanometers (Dubois *et al*, 2000).

There are three types of nanocomposites, depending on how many dimensions of the dispersed particles are in the order of nanometers. When the three dimensions are in the order of the nanometer, it comes to nanoparticles such as spherical silica nanoparticles or semiconductor nanoinclusions. When two dimensions are in the nanometer scale and the third is larger, forming an elongated structure, let's talk of nanotubes or "whiskers." The third type of nanocomposites is characterized by only one dimension of in the order of nanometers, in which case the reinforcement is present in the form of sheets with thickness of few nanometers and a length that can vary from hundreds to thousands of nanometers. Going from two-dimension to one nanometer dimension of particles it's possible to maximize the interaction between the nanofillers and the matrix, which form the basis of the unique properties of nanocomposites (Giannelis *et al*, 1999).

In general when a modified inorganic phase is dispersed in a polymer, nanocomposites can be achieved by three main structures depending on the nature of the components used (solid laminated, organic cation and polymer matrix) and the preparation method used:

- structure with separate phases. The polymer is not between the lamellae of the solid, in this case the properties of the composite are the same as microcomposites.

- intercalated structure. One or more polymer chains are intercalated between the layers forming a morphologically well-ordered multilayer structure with alternating organic and inorganic part of the part.
- exfoliated structure. Represents an extreme case of the intercalated structure in which the efficiency of intercalation is massive. The layers are completely and uniformly dispersed in the polymer matrix.

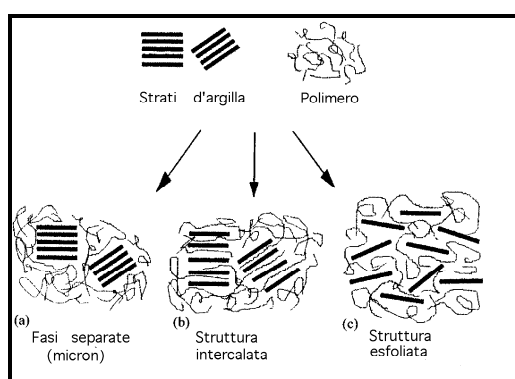


Figure I.3 Schematically illustration of three different types of thermodynamically achievable polymer/clay nanocomposites

Exfoliation of the nanosheets in polymer matrix leads to an improvement in the tensile, barrier and thermal stability of the material. Due to a more tortuous path for the permeating agents, the nanocomposite has excellent intrinsic properties such as flame retardant, high mechanical and chemical resistance, and reduced permeability to gases and vapors (Calvert *et al*, 1997).

Two complementary techniques are used to characterize the structures of the nanocomposites:

1) The X-ray diffraction (XRD) is used to identify hybrids with intercalated structure, exfoliated or separate. The multilayer is well preserved and the distance between the layers is well determined. Generally, the intercalation of the polymer chain leads to an increase of the distance between the layers, when compared with the solid laminated departure. In the diffractogram of an exfoliated structure there is no visible peak at low angles of diffraction, possibly due to excessive space between layers (greater than 8 nm in the case of an orderly exfoliated structure) or possibly because the nanocomposite is no longer aligned and precise. The presence of a widened peak at low angles of diffraction indicates the existence of intermediary organizations due to the systems well intercalated.

2) The electronic transmission spectroscopy (TEM) is used to characterize the morphology of the nanocomposite, allowing to clearly distinguish when a nanocomposite is exfoliated or intercalated. In the former case it can identify the lamellae of the solid that have no order.

1.8.1.1 High energy ball milling (HEBM)

The technique of "High Energy Ball Milling" (HEBM) to incorporate powders on polymeric matrices has attracted a great interest in recent years, because this technique allows to transfer high-energy mechanical mixtures of powdered parts or alloys, in order to induce structural transformations, with the formation of nanostructured alloys (Suryanarayana et al, 2001).

The technique of "ball milling" may be used for:

- change the structure of materials by reducing the grain size;
- homogenizing a composition;
- increase the solubility of an element within a metal alloy;
- create a metastable crystalline phase;
- to produce metal alloys;
- produce metallic crystals.

The technique of "ball milling" may be used whenever necessary to supply energy to the system in order to obtain a reaction product, a polymer blend, a metal alloy. The technique of the HEBM can be used to induce the intercalation or exfoliation of clay in a polymer matrix.

Only recently the "ball milling" was used for the production of polymer nanocomposites comprising a thermoplastic polymer and an inorganic phase. This technical innovation in this field, has a number of advantages over traditional methods of preparation of nanocomposites (ie the mixing time, mixing as a solution) because the process occurs at ambient temperature and in the absence of solvents. Are avoided, therefore, problems of disposal of solvents and fillers can be used with thermally sensitive molecules (Sorrentino *et al*, 1998).

1.8.2 Coating system

Coating technologies are continuously being developed in an attempt to meet a diverse range of very specific requirements and applications. Full or partial coatings are applied to surfaces for a number of different reasons including aesthetic or functional finishes and protective layers. Current trends in this field have focused on introducing nanoparticles to coating formulations.

An other method of dispersion of inorganic filler on polymeric matrices consists in use of coating system. Several physical methods of surface modification of polymers are common. The first type of treatment requires the generation of reactive species such as radicals, ions, molecules in excited electronic states.

In this category belong to the flame treatment, corona and plasma (hot and cold), and UV treatments, X-ray, laser, and ion-beam e-beam. The coating methods involve the deposition of key species, atoms or molecules on the surface of the polymer. This includes plasma treatments (sputtering and PECVD) methods and physical vapor deposition (electron beam or thermal activation), deposition of polymer films from solution: dip-coating, roll coating, spin-coating (Pilati *et al*, 2009)

1.8.2.1 Acrylic resin

The development of active systems for protection of substrates is an issue of prime importance for many industrial applications.

Several attempts were made to introduce different species in polymer coatings for controlled release of active molecules. It was used (Buchheit *et al*, 1985) Al-Zn-decavanadate hydrotalcite as anticorrosion pigment, adding it to epoxy-based organic coating (Fabbri *et al*, 2006).

The application of protective polymer coatings is the most widespread approach used nowadays for protection of different materials (Ferreira *et al*, 2007 and 2010).

1.8.2.2 Plasma

Oxygen plasma generates reactive species such as radicals, ions, molecules in electronic excited states, to create hydrophilic surface with oxygen functional groups. The principal species generated are:

- Neutral atoms or molecules
- Electrons bonded to the nucleus
- Charged atoms or molecules
- Electron(s) detached from nucleus (ionization)
- Requires additional supply of energy
- Electron attached to a neutral (negative ions)

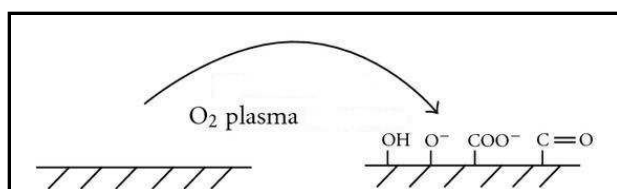


Figure I.4 Generation of reactive species on oxygen plasma treated polymeric surface

The plasma treatment is used for different application such as Hydrophilic properties , Barrier coatings, Adhesion promotion and Biocompatibility.

I.9 Inorganic filler

1.9.1 Main types of nano-fillers

Great attention has recently emerged around the hybrid organic–inorganic systems and in particular to those in which layered fillers are modified by substituting the inorganic ions between the lamellae by organic ions.

Such nano-hybrids firmly bind the organic molecules with ionic bonds, and can be considered as a reservoir where guest species are stored, protected from oxidation and photolysis, and released *on demand* by a chemical signal, that is by a de-intercalation process.

For these reasons research in intercalation chemistry has shifted from the study of the insertion mechanism to the preparation of new materials, with very specific properties, not obtainable through other synthetic procedures. For example, insertion of dyes and chromophores into lamellar hosts has so far produced materials as tuneable lasers, fluorescent and non-linear optics devices.

Materials, that are cheap and naturally occurring, as natural clays or synthetic layered phosphates acquire a great added value after intercalation of molecules with special functionalities.

The most common nano-fillers are:

- POSS (polyhedral silsesquioxane): 0.7-50 nm diameter particles with reactive functional groups.
- Expanded graphite (EG): lamellar porous structure with pores from 10 nm to 10 μ m.
- Carbon nanotubes: the wall may be single or multiple, typically have lengths from 100 nm to tens of μ m and diameters from 1 to 20 nm.
- Lamellar crystals (exfoliated) hydroxides include dual-layer laminated also called anionic clays (hydrotalcite), but, above all, natural phyllosilicates (montmorillonite, hectorite and saponite) and synthetic (Fluoro-mica).

1.9.2 Anionic clay

Among the different types of lamellar solids, in this PhD thesis the attention was focused on anionic clays (or hydrotalcite LDH). They are prepared with different procedures with high levels of purity, economic and environmentally friendly, used to prepare hybrid organic-inorganic polymeric materials and they have at least a nanometric dimension of the lamellae (Rives *et al.*, 2001). This filler offers different advantages such as the possibility to fix, by ionic bonds, organic molecules on the lamellar layers of clay. Such molecules may improve compatibility with the polymer matrix, be released in controlled way, having a target action. (Tammaro *et al.*, 2009)

Anionic clays, mixtures of natural or synthetic lamellar hydroxides containing exchangeable anions in the interlayer region, are much less known and popular in the nature of cationic clays. To understand the structure of these compounds it is necessary to understand the brucite mineral lamellar formula $\text{Mg}(\text{OH})_2$. In brucite Mg^{2+} ions six-fold coordinated by OH-ions identify octahedra that share edges to form infinite planes. These plans are packed on each other and are held together by Van der Waals forces. When the Mg ions are replaced by a trivalent cation, (as Fe^{3+} and Al^{3+} for hydrotalcite), a positive charge is generated in the plan. This is compensated by carbonate anions located in the interlayer region, where there is also the water of crystallization. The plans contain the cations, therefore, are like those of brucite, and the two different cations occupy randomly the octahedral sites. The anions and water are located in the interlayer region. The general formula that is attributed to the hydrotalcite-type compounds is as follows: $[\text{M}(\text{II})_{1-x}\text{M}(\text{III})_x(\text{OH})_2]^{x+}(\text{A}^{n-})_x \cdot n\text{H}_2\text{O}$, where M (II) = Group II metal, M (III) = metal of Group III A = interlayeranion.

The possibility of replacing these anions with simple ion exchange procedures, makes hydrotalcite solid ideal for a class of molecules potentially active incorporated, leading a negative charge: they are good candidates for active food packaging. The value added of these nanocomposite systems, from the consideration that the layers of the inorganic compound can be fixed through ionic bonds, active molecules, such as antimicrobials, antioxidants, oxygen scavengers, through a process of anion exchange resin may bond with active sites that can provide anions, typically carboxyl groups, phenolic derivatives, phosphonic acid (Tammara *et al*, 2005).

1.9.3 Methods of synthesis

Interest in the use of mixed oxides of Mg and Al has increased notably. These solids are used as catalysts in reactions of basic character and as catalysts supports, due to their structural properties.

Mesoporous hydrotalcites, with the formula $\text{Mg}_6\text{Al}_2(\text{OH})_{16}\text{CO}_3 \cdot 4\text{H}_2\text{O}$, have been synthesized by two techniques: first, an innovative one, the mechanical milling (MM) and second, the conventional coprecipitation method (CM). The synthesis by CM was prepared from $\text{Mg}(\text{NO}_3)_2 \cdot 6\text{H}_2\text{O}$ and $\text{Al}(\text{NO}_3)_3 \cdot 9\text{H}_2\text{O}$ over a solution of NaOH and Na_2CO_3 , with a Mg/Al molar ratio of 3.

The MM technique was employed over the hydrotalcites in an aqueous media previously prepared by CM. In this case, the milling retained the pillared lamellar structure and resulted in the formation of hydrotalcites with refined thickness layers and higher specific areas, compared with those that

were prepared by CM. The materials obtained by both methods were calcined at 500 °C and analyzed (Kloprogge *et al.*, 2001).

New synthesis method of hydrotalcites by microwave irradiation is used, which avoids the autoclave high temperature treatment as well as the long crystallization time. The crystallite size of the obtained solids is smaller than in the conventionally prepared hydrotalcites. The highest irradiation time provided the lowest aluminium incorporation to the hydrotalcite network. Diminishing microwave irradiation time produces purer hydrotalcites. If the gel is irradiated only for two minutes a well crystallized hydrotalcite is obtained.

Hydrotalcites also have been synthesized by three different procedures: conventional precipitation-aging, aging under microwave irradiation, and sonication during the coprecipitation step. The synthesis procedure has an effect on the crystal size and textural properties of the hydrotalcite (HT) and the Al₂O₃-MgO mixed oxides formed upon calcination. HT samples prepared under sonication at 298°K are formed by dispersed and homogenous particles of 80nm average particle size. They also produce upon calcinations the mixed oxides with the largest surface area. This method of preparation increases not only the surface area but also the number of defects in the solid, leading to sites of higher basicity. This was determined by means of catalytic reactions such as Knoevenagel and aldol condensations which demand basic sites of different strengths. Hydrotalcites were regenerated from mixed oxides by hydration while giving Brönsted basic sites. Samples originally prepared by sonication present smaller crystallite size and have a larger number of accessible active sites. With these samples acetone/citral condensations with 96% and 99% conversion and selectivity, respectively, are achieved in a 15-min reaction time.

Costantino (Costantino *et al.* 1998) innovated a new synthetic route to hydrotalcite (2:1) synthesis via thermally induced urea hydrolysis

1.9.3.1 Urea method

In this method, solid urea was added to aqueous solutions of magnesium chloride and aluminum chloride and the clear homogeneous solutions were heated under stirring at temperatures between 60 and 100 °C. The slow decomposition of urea produces an alkaline pH, which is a prerequisite for HTlc precipitation. The same author successfully used this urea method to prepare ZnAl-LDH and NiAl-LDH. Urea hydrolysis of cobalt nitrate melts at 80 8C yielded a HTlc like Co(II,III) hydroxide and further increase in temperature produced a compound with a new phase. In a recent work by Oh *et al.*, hydrotalcite particles were prepared by two methods, urea hydrolysis and hydrothermal synthesis and the particle sizes were compared. Hexagonal plates of monodispersed hydrotalcite (4:1) particles were obtained by urea hydrolysis at 120 °C. At lower temperatures particle sizes are larger while at

high temperatures particle sizes are smaller and uniform. When the concentrations of metal chlorides and urea were increased, a deviation from 4:1 ratio of Mg/Al was observed (Valcheva, 1993).

Urea hydrolysis is basically a modification of hydrothermal method where the precipitating agent remains to be urea. The advantage of using urea against NaOH is that the urea hydrolysis progresses slowly, which leads to a low degree of super saturation during precipitation. Urea is a very weak Bronsted base. It is highly soluble in water and its controlled hydrolysis in aqueous solutions can yield ammonium cyanate or its ionic form (NH_4^+ , NCO^-). Prolonged hydrolysis results in either CO_2 in acidic medium or to CO_3^{2-} in basic medium as shown below.

1.9.3.2 Coprecipitation method

Co-precipitation is the most widely used method to prepare hydrotalcites.

Often co-precipitated samples are subsequently subjected to hydrothermal treatment to obtain well-crystallized samples. Hydrothermal synthesis is a well-known and established method to prepare transition metal oxides, ternary systems and inorganic-organic hybrid materials. A series of Ni-Al-Cr and Ni-Al-Fe HTICs were prepared by co-precipitation at 60°C, followed by hydrothermal treatment at 150 °C.

Layered materials, especially hydrotalcite-like materials or layered double hydroxide (LDH) are amongst attractive materials for the preparation of a controlled release formulation.

The insertion of guest anions into the inorganic interlamellae, can be accomplished by spontaneous self-assembly or coprecipitation technique. In this method, the host and the guest species are included in the mother medium, followed by aging process to form a well-ordered nanolayered structure. On the other hand, insertion of the guests can also be done by first preparing the host followed by modification or further treatment of the host and finally insertion of the guest molecule into the interlayer (Frunza et al, 2008).

1.10 Types of polymers for food packaging

For a long time polymers have supplied most of common packaging materials because they present several desired features like softness, lightness and transparency. However, increased use of synthetic packaging films has led to a serious ecological problems due to their total non-biodegradability. Although their complete replacement with eco-friendly packaging films is just impossible to achieve, at least for specific applications like food packaging the use of bioplastics should be the future (Soroka et al, 1995).

The current global consumption of plastics is more than 200 million tonnes, with an annual growth of approximately 5%, which represents the largest field of application for crude oil. It emphasizes how dependent the plastic industry is on oil and consequently how the increase of crude oil and natural gas price can have an economical influence on the plastic market. It is becoming increasingly important to utilize alternative raw materials. Until now petrochemical-based plastics such as polyethylene (PE), polypropylene (PP), polystyrene (PS) and polyamide (PA) have been increasingly used as packaging materials because their large availability at relatively low cost and because of their good mechanical performance such as tensile and tear strength, good barrier to oxygen, carbon dioxide, anhydride and aroma compound, heat sealability, and so on. But nowadays their use has to be restricted because they are not non-totally recyclable and/or biodegradable so they pose serious ecological problems. Plastic packaging materials are also often contaminated by foodstuff and biological substance, so recycling these materials is impracticable and most of the time not economically convenient. As a consequence several thousands of tons of goods, made on plastic materials, are landfilled, increasing every year the problem of municipal waste disposal (Piergiovanni et al, 1994).

The growing environmental awareness imposes both user-friendly and eco-friendly attributes to packaging films and process. As a consequence biodegradability is not only a functional requirement but also an important environmental attribute. The compostability attribute is very important for biopolymer materials because while recycling is energy expensive, composting allows disposal of the packages in the soil. By biological degradation it produced only water, carbon dioxide and inorganic compounds without toxic residues. According to the European Bioplastics, biopolymers made with manufactures renewable resources have to be biodegradable and especially compostable, so they can act as fertilizers and soil conditioners. Whereas plastics based on renewable resources do not necessarily have to be biodegradable or compostable, the second ones, the bioplastic materials, do not necessarily have to be based on renewable materials because the biodegradability is directly correlated to the chemical structure of the materials rather than the origin.

Bioplastics, like plastics, present a large spectrum of application such as collection bags for compost, agricultural foils, horticultures, nursery products, toys, fibres, textiles, etc. Other fields such as packaging and technical application are gaining importance. Several University Research Centers in the world (Italy, Ireland, France, Greece, Brazil, USA and so on) and several Industry like NatureWorks LLC, are focusing their attention to the study of these bio-based materials. From our point of view, it is important to understand not only the physical and mechanical properties of such materials for the task but also the compatibility with the food, which

has been recognized as a potential source of loss in food quality properties (Piergiovanni et al, 1987).

1.10.1 Biodegradable polymers in food packaging field

The field of application of biodegradable polymer in food-contact articles includes disposable cutlery, drinking cups, salad cups, plates, overwrap and lamination film, straws, stirrers, lids and cups, plates and containers for food dispensed at delicatessen and fast-food establishments.

These articles will be in contact with aqueous, acidic and fatty foods that are dispensed or maintained at or below room temperature, or dispensed at temperatures as high as 60 °C and then allowed to cool to room temperature or below. In the last few years, polymers that can be obtained from renewable resources and that can be recycled and composted, have garnered gained increasing attention. Also their optical, physical and mechanical properties can be tailored through polymer architecture so as a consequence, biodegradable polymers can be compared to the other synthetic polymers used in fresh food packaging field, like the most common oriented polystyrene (OPS) and polyethylene terephthalate (PET).

Depending on the production process and on the source, biopolymers can have similar properties to traditional ones. They are generally divided into three groups: polyesters; starch-based polymer; and others. Polyesters:

- i. Polymers directly extracted from biomass like proteins, lipids, polysaccharides, etc.
- ii. Polymeric materials synthesized by a classical polymerization procedure such as aliphaticaromatic copolymers, aliphatic polyesters, polylactide aliphatic copolymer (CPLA), using renewable bio-based monomers such as poly(lactic acid) and oil-based monomers like polycaprolactones.
- iii. Polymeric materials produced by microorganisms and bacteria like polyhydroxyalkanoates.

a) Polycaprolactone (PCL)

It is a fully biodegradable polymer coming from the polymerization of not renewable raw material, like crude oil. It is a thermoplastic polymer with good chemical resistance to water, oil, solvent and chlorine, with a melting point of 58-60°C, low viscosity, easy to process and with a very short degradation time. It is not used for food application but if mixed with starch it is possible to obtain a good biodegradable material at a low price, used for trash bags.

b) Poly(lactic acid) (PLA)

One of the most promising biopolymer is the poly (lactic acid) (PLA) obtained from the controlled depolymerisation of the lactic acid monomer obtained from the fermentation of sugar feedstock, corn, etc., which are renewable resources readily biodegradable (Cabedo et al, 2006). It is a versatile polymer, recyclable and compostable, with high transparency, high

molecular weight, good processability and water solubility resistance. In general commercial PLA is a copolymer between poly(L-lactic acid) and poly(D-lactic acid). Depending on the L-lactide/Dlactide enantiomers ratio, the PLA properties can vary considerably from semicrystalline to amorphous ones. Researches carried out to improve the performance quality of this material are made on PLA with D-lactide content less than 6%, which is the semicrystalline polymer. However the amorphous one, containing 12% of D-lactide enantiomer, is easy to process by thermoforming, which is the actual technology in the food packaging sector, and it shows properties like polystyrene. This material is commercialized by different companies with different commercial names, like for example the Natureworks_ PLA produced by Natureworks_ LLC (Blair, NB). Currently it is used in food packaging application only for short shelf-life.

1.10.2 Natural polymers

Environmental legislation as well as consumer demand has recently resulted in a renewed interest in natural materials, making recyclability and biodegradability important issues for the introduction of new materials and products. One of the more promising approaches to overcome these problems is the use of annually renewable resources, for obtaining biodegradable polymers useful for various applications in medical, agriculture, drug release and packaging fields. Among natural polymers, pectins are white, amorphous, complex carbohydrates that occur in ripe fruits and certain vegetables. Fruits rich in pectin are the peach, apple, currant, and plum (Coffin et al, 1994; Suvorova et al, 2003).

Structurally the pectic polysaccharides are a heterogeneous grouping, showing substantial diversity with botanical origin. They are based on chains of linear regions of 1,4-a-Dgalacturonosyl units and their methyl esters, interrupted in places by 1,2-a-L-rhamnopyranosyl units (Mitchell et al, 1998). Pectin is a secondary product of fruit juice, sunflower oil, and sugar manufacture. As food processing industry wastes, pectin is therefore a very good candidate for eco-friendly biodegradable materials. Poor water resistance and low strength, however, are limiting factors for the use of materials manufactured only from natural polymers, and hence they are often blended with other polymers (Kaczmarek et al, 2011; Kowalonek et al, 2010; Alves et al, 2010; Kaczmarek et al, 2007). An alternative way to overcome this problem is to modify natural polymers by incorporation of inorganic fillers, at nanometric level, that can further extend their applications in more special or severe circumstances. Several nanocomposites have been prepared and analysed utilizing pectins and different inorganic fillers (i.e. ZnO; clays; halloysite, hydroxyapatite) and physical properties studied (Shi et al, 2008; Jari et al, 2010, Mangiacapra et al, 2006; Cavallaro et al, 2011; Junjie Li et al, 2011). Interesting inorganic layered fillers are layered double hydroxides

(LDHs), that can act as host matrixes for the intercalation of anionic species (i.e. organic polymers or active molecules) in order to synthesize hybrid organic-inorganic nanocomposites (Herrero et al, 2011; Huang et al, 2011; Yuan et al, 2011; Wang et al, 2011; Kotal et al, 2011; Costa et al, 2011. Manzi-Nshuti et al, 2009; Bugatti et al, 2010 and 2011) They were prepared by intercalation of anionic pectins into LDH based of Zn and Al. The biopolymer-LDH nanocomposites have been incorporated in carbon paste or PVC matrixes for the development of potentiometric sensors, being tested as active phases of such devices for the recognition of calcium ions. In the present paper we report the preparation and characterization of model systems, formed by LDH intercalated with benzoate and benzoate derivatives: 2,4-dichlorobenzoate, p-hydroxybenzoate and o-hydroxybenzoate, having antimicrobial properties, and dispersed into a commercial pectin, for potential food packaging applications. The benzoate and benzoate derivatives are used as food preservatives and show toxicity at very high levels (maximum acceptable daily intake 5 mg/kg of body weight) (Joint FAO, 1961, Concise International Chemical Assessment Documents (CICADs), 2000; ISBN 924153026X.). It is well known that natural polymers, like pectins, generally do not melt on increasing the temperature, but undergo thermal degradation, then we utilized high energy ball milling to mix nanohybrids and pectin powders. Such technique has been yet succesfully used to prepare nano bio-composites pectins-clays with improved mechanical ad barrier properties (Mangiacapra et al, 2006).

Chapter II

Layered Double Hydroxides

II.1 Preparation of LDHs

Two methods of synthesis are used to prepare hydrotalcites: the method of urea and the one-step method of coprecipitation. The second one was preferred because faster, cheaper and suitable to industrial scale. The products obtained have revealed different structural features and have shown many different behaviours in different properties.

II.1.1 Synthesis of hydrotalcite (LDHBz and derivatives) by urea method

The hydrotalcite compounds are able to exchange counter-ions present in the interlayer with other counter-ions present in solution. The exchange reaction is governed by the selectivity of the host to the various counter-ions, by the concentration and the temperature of the solution. Recent studies reported the following scale of selectivity: $\text{CO}_3^{2-} \gg \text{OH}^- > \text{Cl}^- > \text{Br}^- > \text{NO}_3^-$. The anions nitrate counter-ions are not well withheld so the hydrotalcite precursors containing them are liable to exchange reactions with anions such

as carboxylic alkyl chains and aromatic. Based on these considerations has been synthesized a hydrotalcite Zn and Al in the form carbonate (LDHCO_3) then transformed into the first form of chloride (LDHCl) and finally into nitrate form (LDHNO_3).

a) Synthesis of carbonate form ZnAl-CO_3 :

The method used for the preparation of carbonate form is the hydrolysis of urea in the presence of a mixture of M (II) (Zn^{2+}) and M (III) (Al^{3+}). Solid urea is added to aqueous solutions of chlorides of metals (eg AlCl_3 and ZnCl_2)

b) Synthesis of chloride form ZnAl-Cl :

Titration with HCl 0.1M of LDH-CO_3 at $\text{pH} = 5$.

c) Synthesis of nitrate form ZnAl-NO_3 :

Ionic exchange reaction in the presence of excess NO_3^- ions.

d) Preparation of ZnAl-benzoate :

Intercalation of benzoate anion in LDH lamellae is an ionic exchange reaction of nitrate form with an aqueous organic anion solution 0.5mol/dm^3 .

From the elemental analysis were obtained the following compounds:

$[\text{Zn}_{0.65}\text{Al}_{0.35}(\text{OH})_2] \text{Bz}_{0.35} \cdot 1\text{H}_2\text{O}$ of which anion benzoate is 26% by weight of the total.

This synthesis consists of 4 steps, is more long, difficult and less suitable for the preparation of LDH at industrial scale.

II.1.2 Synthesis of hydrotalcite modified with active molecule by coprecipitation method

Were synthesized by coprecipitation method the hydrotalcites containing the following anions:

- 1) (LDH)-citrate
- 2) (LDH)-salicylate
- 3) (LDH)-benzoate
- 4) (LDH)-aleurate
- 5) (LDH)-pOH-benzoate
- 6) (LDH)-glycolate
- 7) (LDH)-serine
- 8) (LDH)-2.2-bis-hydroxymethyl-propionate

The procedure used was the following: a solution of two salts ($\text{Zn}(\text{NO}_3)_2 \cdot 6\text{H}_2\text{O}$ and $\text{Al}(\text{NO}_3)_3 \cdot 9\text{H}_2\text{O}$) is added quickly to a solution of anion (see materials) under stirring and nitrogen flow. The pH slowly reaches the value of 7.5 by adding 1M NaOH (about 8 hours). After the reaction time the mixture was filtered, repeatedly washed and dried. The product is characterized in terms of structural, thermal and elemental analysis (Frunza et al, 2008).

II. 2 Characterization and comparison of preparative methods

II.2.1 X-ray diffraction

Wide Angle X-Ray Diffractogram of the powders of LDH from coprecipitation is compared to the LDH obtained by the Urea method.

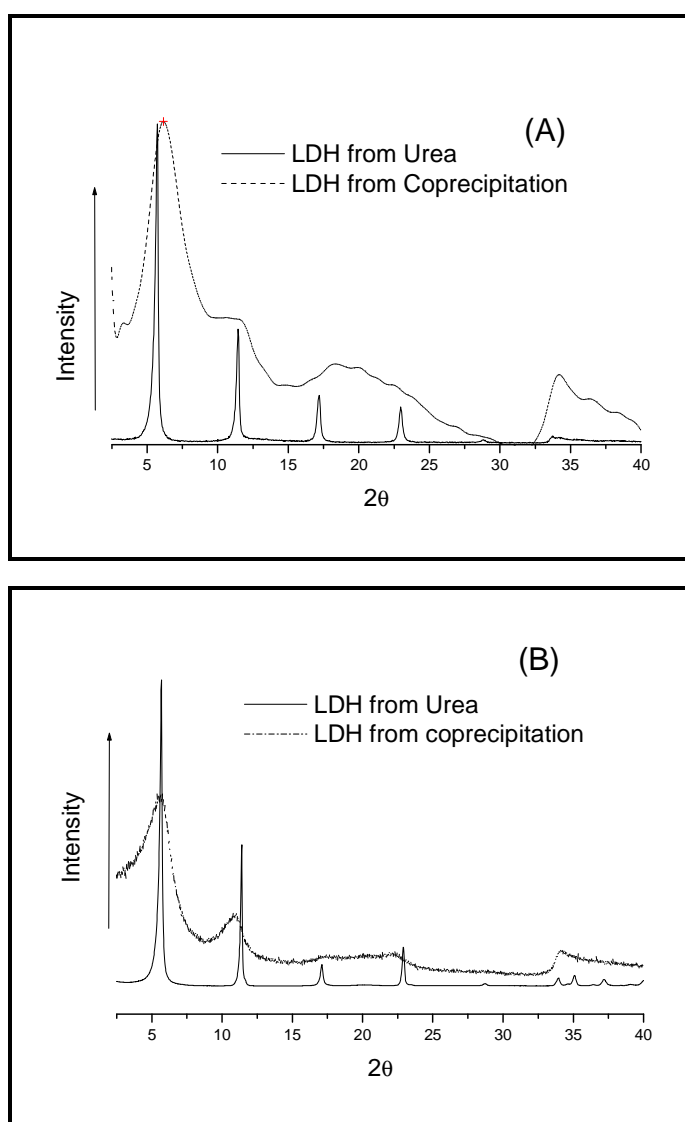


Figure II.1 Comparison between X-Ray spectra of LDH from Urea and from Coprecipitation for LDHsal (A) and LDHBz(B)

We observed that sharp and relatively symmetric reflections for the basal planes at 5.68 and 11.7 of 2θ are seen for the sample obtained by Urea. This result indicated that the material is crystalline, although constituted by small crystallites.

At variance, the powders obtained by co-precipitation showed broad peaks for the basal planes, centred at 5.6° and 11.2° of 2θ , indicating very small and disordered crystallites.

In figure II.1(A) for LDHsal and (B) for LDHBz it was showed that the structure of the lamellae is more ordered for hydrotalcite by urea while in the coprecipitation the structural order is less, then giving a broader distribution of interlayer distances (Vittoria et al, MI2011A/00192).

II.2.2 Infrared spectroscopy

FT-IR absorption spectroscopy of the LDH sample gived information on the presence of intercalated anions and the brucite-type layer. The spectrum of figure II.2, in both cases, showed a strong broad band in the $3000\text{-}3750\text{ cm}^{-1}$ range due to the stretching of the OH groups of the layer, involved in hydrogen bonds with hydration water molecules and carboxylate groups. Roughly below 650 cm^{-1} the lattice translational modes can be observed, while between 700 and 1000 cm^{-1} broad bands due to librational modes of the hydroxyl groups and water can be seen. The band at around 450 cm^{-1} has been ascribed to a condensed $[\text{AlO}_6]^{3-}$ group or as single Al-O bonds. In the case of Zn substitution of Mg this band is reported at 430 cm^{-1} (J.T. Kloprogge et al), as we observe in Fig. II.2. The sharp and intense bands at 1537 and 1390 cm^{-1} are ascribable to the asymmetric and symmetric stretching vibrations of the C-O bonds of COO- groups, confirming the presence of *o*-OH benzoate and benzoate into the inorganic galleries.

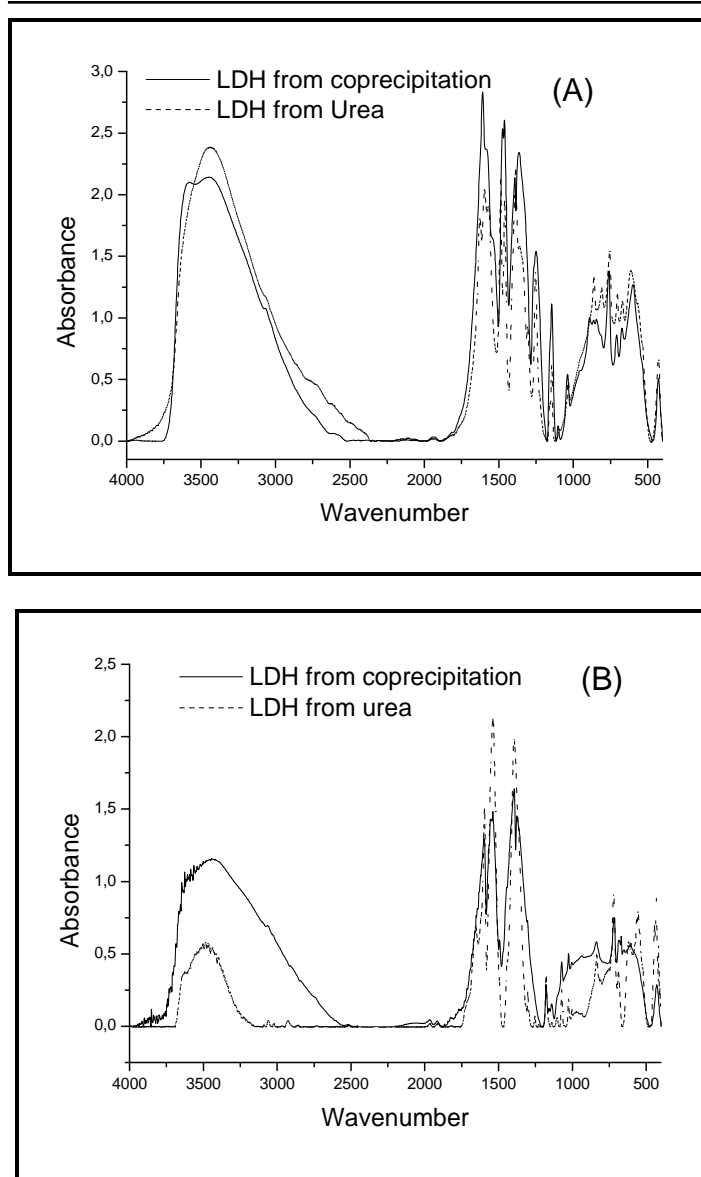


Figure II.2 Comparison between Infrared spectra of LDH from Urea and from Coprecipitation for LDHsal (A) and LDHBz(B)

II.2.3 Thermogravimetry (TGA)

Thermal behavior of the intercalate was investigated and the data are presented in figure II.3. The two endothermic weight losses, between 80 and 300 °C, are very likely related to the loss of co-intercalated water as well as water derived from dehydroxylation of the inorganic layers. The main

weight loss between 300 and 500 °C may be ascribed to endothermic decarboxylation of benzoate and to exothermal combustion of the residual organic part.

From the comparison of the two thermogravimetry it was found that both the temperatures of degradation of the inorganic compound are almost the same even if the amount of water of hydrotalcite from co-precipitation is less, as reported in figure II.3 (A) and (B).

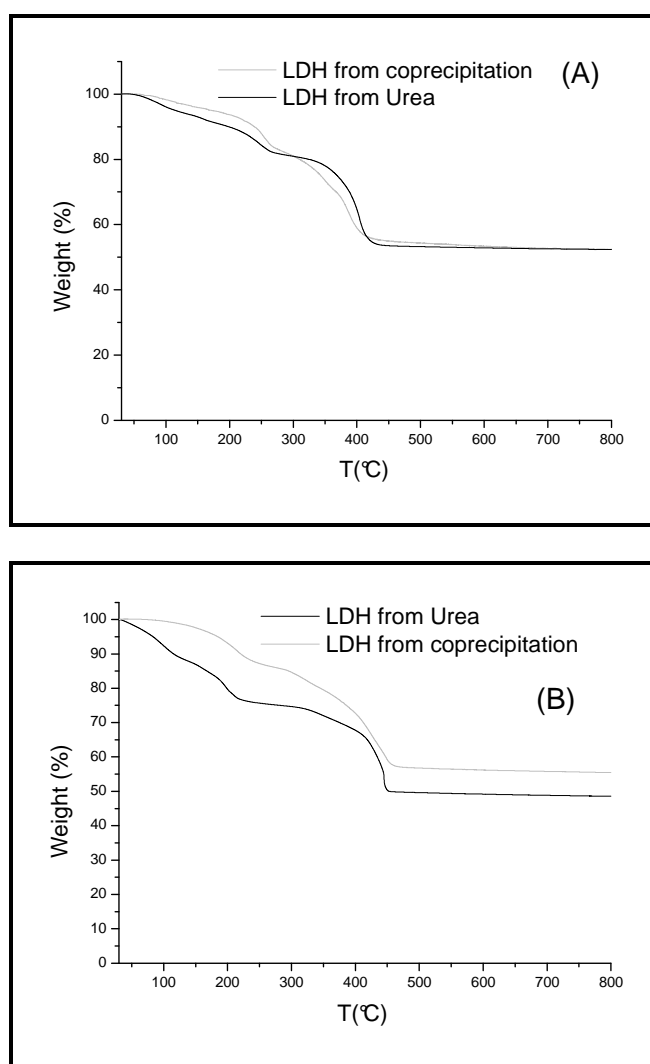


Figure II.3 Comparison between TGA of LDH from Urea and from Coprecipitation for LDHsal (A) and LDHBz(B) (thermal cycle from 30 to 800 °C at 5 °C / min, in air flow)

II.2.4 Elemental Analysis

The values of relative percentages and molar ratio are derived from solutions of 200mg of sample $[\text{ZnAl}(\text{OH})_2](\text{salicylate})$ dissolved in nitric acid concentrated, for Zn and Al by atomic absorption and C and H in a Elemental Analyzer. The results of elemental chemical analyses for Zn, Al, C, and H for the solids prepared, as well as some molar ratios, are given in Table II.1. The Zn/Al molar ratio in sample LDHsal is the same as in the starting solution of the Zn and Al nitrate:

Table II.1 Values for elemental analysis of LDHsal

	Zn	Al	C	H
%	29.9	5.7	16.32	2.43
Grams	29.9	5.7	16.32	2.43
Moles	0.45	0.21	1.36	2.43
Molar ratio	2.1	1	6.8	12

The chemical formula obtained from the elemental analysis was the following: $[\text{Zn}_{0.73}\text{Al}_{0.35}(\text{OH})_2] (\text{C}_7\text{O}_3\text{H}_5)_{0.34} \cdot 0.19 \text{H}_2\text{O}$ with value of the molar fraction $x = \text{M}^{\text{III}} / (\text{M}^{\text{III}} + \text{M}^{\text{II}})$ of 0.32 and molecular weight of 141.17g/mol; the salicylate intercalated amount in LDHsal is 32.9(w)% of the total. Therefore almost all the aluminium is co-precipitated with the zinc ions to obtain a solid with the stoichiometry of two Zn(II) for each Al(III). This corresponds to an ideal disposition in the brucite-like sheet of each aluminium atom surrounded by six zinc atoms.

Chapter III

Polycaprolactone composites

The following hydrotalcites incorporated on PCL, have been synthesized by the method of urea and characterized as described above, giving the compositions shown in the table III.1 (Costantino *et al*, 2009):

Table III.1 *Composition of hydrotalcites incorporated on PCL*

Anion	Composition
Bz	$[\text{Zn}_{0.65}\text{Al}_{0.35}(\text{OH})_2]\text{Bz}_{0.35} \cdot 1\text{H}_2\text{O}$
<i>o</i> -BzOH	$[\text{Zn}_{0.65}\text{Al}_{0.35}(\text{OH})_2]\textit{o}\text{-BzOH}_{0.27}(\text{NO}_3)_{0.08} \cdot 1\text{H}_2\text{O}$
<i>p</i> -BzOH	$[\text{Zn}_{0.65}\text{Al}_{0.35}(\text{OH})_2]\textit{p}\text{-BzOH}_{0.33}(\text{NO}_3)_{0.02} \cdot 0.85\text{H}_2\text{O}$
BzDCB	$[\text{Zn}_{0.65}\text{Al}_{0.35}(\text{OH})_2]\text{BzDC}_{0.32}(\text{NO}_3)_{0.03} \cdot 1\text{H}_2\text{O}$

III.1 PCL/nano-hybrids preparation

The incorporation of the nano-hybrids into polycaprolactone was achieved by High Energy Ball Milling (HEBM) method. Powders composed of PCL and the LDHs intercalation compounds of the four organic molecular anions (after vacuum drying 24h) were milled, in different percentages (wt/wt), at room temperature in a Retsch (Germany) centrifugal ball mill (model S 100). Samples mass were milled in a cylindrical steel jar of 50 cm³ with 5 steel balls of 10 mm of diameter. The rotation speed used was 580 r.p.m. and the milling time was 1 hour. The pure PCL, taken as reference, was milled in the same experimental conditions of the composites.

III.2 Film preparation

The milled powders, were molded in a Carver laboratory press between two teflon sheets, at 80°C, followed by a quick quenching in an ice-water bath (T=0°C). Films 100µm thick were obtained and analyzed. In the following, films by milling will be coded as “PCL/Nano-hybrid/X”, where X is the amount of the nanohybrid: ZnAl-Bz, ZnAl-BzDC, ZnAl-*o*-BzOH and ZnAl-*p*-BzOH, respectively, present in the composites.

III.3 X-Ray analysis

Are analyzed the structural features of the nano-hybrids into polycaprolactone, and here are recalled the main results. X-ray analysis was used to investigate the dispersion degree of the inorganic component into the polymeric matrix. The different interaction of the four anions in the inorganic lamellae had a significant consequence on their dispersion into the polymer, as it is evident in Figure III.1, where the X-ray diffractograms of all the nano-hybrids and their relative composites in the 2-40° interval of 2θ are shown.

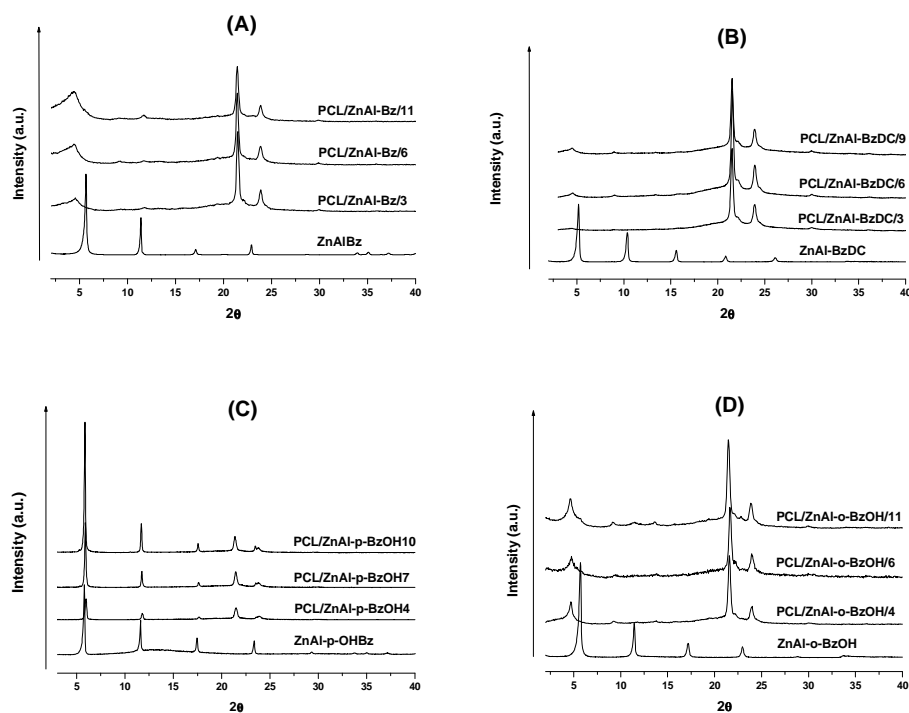


Figure III.1 X-ray powder diffraction patterns of: (A) ZnAl-Bz and composites; (B) ZnAl-BzDC and composites; (C) ZnAl-p-BzOH and composites; (D) ZnAl-o-BzOH and composites.

Figure III.1 (A) shows that the peak at $2\theta = 5.7^\circ$, corresponding to the basal spacing of the pristine nano-hybrid ZnAl-Bz ($d=1.55$ nm) is shifted in all cases at $2\theta = 4.55^\circ$ ($d= 1.94$ nm), indicating an increase of the interlayer distance as consequence of an expansion of the basal distance. The peaks are very broad, indicating a large distribution of distances and their intensity increases on increasing the inorganic content into the polymer. An intercalated composite was very likely obtained.

Figure III.1 (B) displays that in this case (dichlorobenzene) the basal peak of the pristine nano-hybrid is almost absent, and only a small trace, of very low intensity, is visible for the composite with 10% of inorganic ZnAl-BzDC, appearing at 4.7° of 2θ , corresponding to the interlayer distance of 1.88 nm. We can therefore assume that the inorganic with 2,4-dichlorobenzoate anion mixed by milling is mainly exfoliated into polycaprolactone.

In Figure III.1 (C) we observe that the peaks of the nano-hybrid ZnAl-p-BzOH were unchanged in the composites; their intensity is very high and they are even sharper than in the pristine sample. Therefore in this sample the

inorganic lamellae neither exfoliated nor intercalated the polymer: it is a microcomposite.

Figure III.1 (D) shows that the peak at $2\theta = 5.7^\circ$ ($d=1.55$ nm) corresponding to the interlayer distance of the pristine nano-hybrid ZnAl-o-BzOH was shifted in all the composites at $2\theta = 4.7^\circ$ ($d=1.88$ nm), indicating that the inorganic lamellae are partially intercalated with the polymer with an expansion of the basal distance.

In conclusion the less interacting anion (2,4-dichlorobenzoate) and the most interacting (para-hydroxybenzoate) with the inorganic layers of LDHs, showed opposite behaviour when mixed into PCL matrix, producing an exfoliated sample and a microcomposite, respectively. Intermediate behaviour was shown by the benzoate and ortho-hydroxybenzoate anions, forming intercalate composites.

Polycaprolactone in all the composites is crystalline, showing the peaks of its crystalline structure at $2\theta = 21.3^\circ$ and 23.9° well developed.

III.4 Water vapor barrier properties

In Figure III.2 the diffusion coefficients in the PCL composites with benzoate anions as a function of the concentration of water vapor are reported. We observe a linear dependence of diffusion on concentration for all the samples, that allowed us to extrapolate to zero vapor concentration and obtain the thermodynamic diffusion coefficient, D_0 , according to equation 1 (Vieth et al, 1974).

$$D = D_0 \exp(\gamma C_{eq}) \quad (1)$$

All the nanocomposites follow the same behaviour, so it was possible to derive the D_0 for the whole set of samples. The numerical values of D_0 (cm^2/s) are listed in Table III.2. Figure III.3 reports the D_0 (cm^2/s) as a function of the inorganic content for all the samples. It is observed a quite linear decrement of the thermodynamic diffusion coefficient with the inorganic percentage. The presence of the filler increases to a large extent the tortuosity of the system, leading to an expected large decrease in the value of the diffusion coefficient. Indeed for composites of polycaprolactone with inorganic fillers, as well as in the case of many other polymers, it was often found that the improvement of barrier properties is largely dominated by both the percentage and the shape of the inorganic filler dispersed in the polymeric matrix. (Osman et al, 2004). The improvement of the barrier properties, in terms of decrease of diffusion, is maximum for samples with the dichlorobenzoate, in the whole composition range. As already observed it is not the content of inorganic phase alone, but the type of dispersion (exfoliation and/or partial exfoliation) of the inorganic component in the

polymer phase that is important for improving the barrier properties of the samples (Bugatti *et al*, 2010).

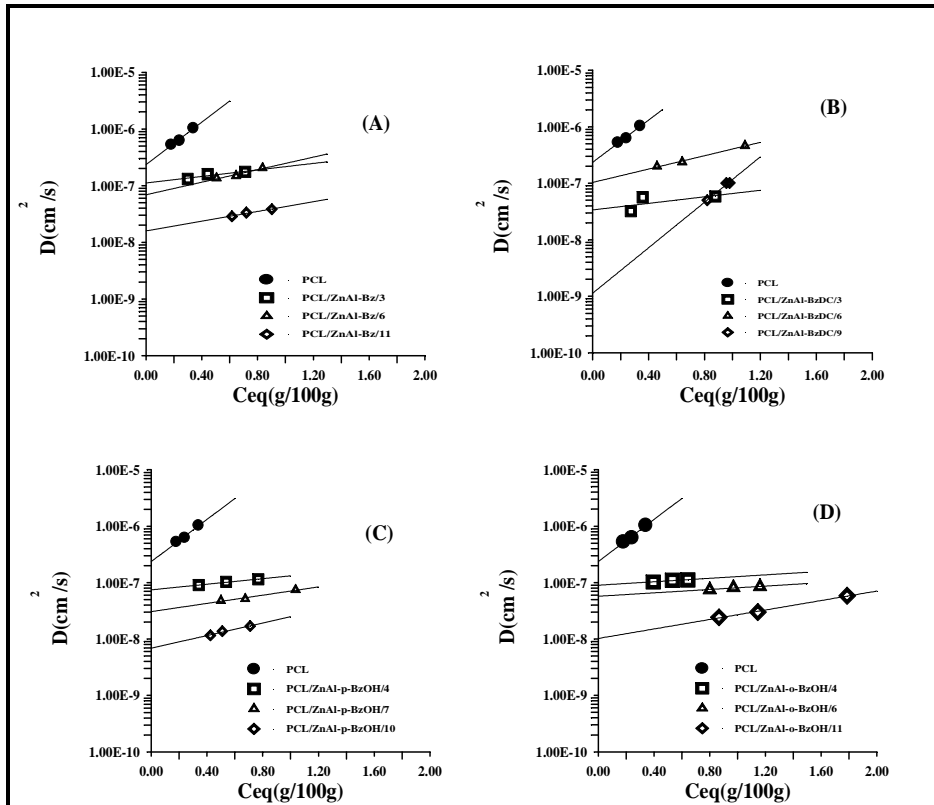


Figure III.2 Diffusion coefficient of water vapor for: PCL and PCL/ZnAl-Bz composites (A); PCL and PCL/ZnAl-BzDC composites (B); PCL and PCL/ZnAl-p-BzOH composites (C); PCL and PCL/ZnAl-o-BzOH composites (D).

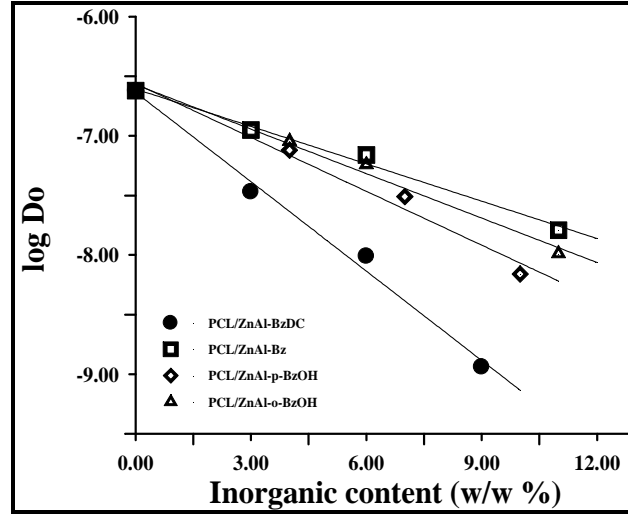


Figure III.3 The logarithm of thermodynamic diffusion coefficient, $D_0(\text{cm}^2/\text{s})$ versus the inorganic content of the nano-hybrid.

Table III. 2 Transport parameters for all the composites

Sample	Ceq(g/100g)	$D_0(\text{cm}^2/\text{sec})$
PCL	0.18	$2.36 \cdot 10^{-7}$
PCL/ZnAl-Bz/3	0.29	$1.11 \cdot 10^{-7}$
PCL/ZnAl-Bz/6	0.51	$6.92 \cdot 10^{-8}$
PCL/ZnAl-Bz/11	0.61	$1.59 \cdot 10^{-8}$
PCL/ZnAl-BzDC/3	0.27	$3.38 \cdot 10^{-8}$
PCL/ZnAl-BzDC/6	0.46	$9.77 \cdot 10^{-9}$
PCL/ZnAl-BzDC/9	0.82	$1.14 \cdot 10^{-9}$
PCL/ZnAl-p-BzOH/4	0.34	$7.47 \cdot 10^{-8}$
PCL/ZnAl-p-BzOH/7	0.42	$3.06 \cdot 10^{-8}$
PCL/ZnAl-p-BzOH/10	0.51	$6.91 \cdot 10^{-9}$
PCL/ZnAl-o-BzOH/4	0.39	$9.00 \cdot 10^{-8}$
PCL/ZnAl-o-BzOH/6	0.80	$5.76 \cdot 10^{-8}$
PCL/ZnAl-o-BzOH/11	0.86	$1.02 \cdot 10^{-8}$

III.5 Release kinetics

We proceeded to the preparation of polymeric films that have an effect antimicrobial or antioxidant on foods and drinks, to increase the shelf life of packaged products. The pack contains the active molecules anchored with ionic bonds to the inorganic lamellar solid dispersed in the polymer. The packaging, in contact with food may allow, under certain conditions, the release of the active ingredient and its diffusion in the food and then a slow-release and controlled, that is modular. The innovative system is that these active molecules, rather than being added directly to the food and all at once, are introduced in the same in a slow and controlled way, thus ensuring a better quality and greater durability.

III.5.1 Release of Benzoate

In a preliminary study, a comparison between the release of the benzoate, directly dispersed into the PCL matrix, and the nanohybrid, containing the benzoate dispersed in the same matrix, with the same benzoate concentration has been performed (Bugatti *et al* , 2011).

Fig. III.4 shows the release kinetic of benzoate ionically bonded to hydroxalcite structure and incorporated to the PCL sample (PCL/ZnAl-Bz/6). It is worth recalling that the Bz content is about 26% of the total ZnAl-Bz, and therefore the sample PCL/ZnAl-Bz/6 contains about 1.6% of drug. In the same figure also the release kinetic of a sample with benzoate anion directly dispersed into the polymer (PCL-Bz/1.6), obtained by milling of PCL and sodium benzoate salt, with the concentration of 1.6% of Bz anion, is shown. It is clearly evident that the release of benzoate (chosen as model antimicrobial species) from the lamellar solid incorporated into the polymeric matrix is much slower than the release of benzoate simply blended to the PCL. All the benzoate molecules from sodium benzoate dispersed into PCL are released in about 250 hours, whereas only 40% is released in the same time from the nanohybrid into PCL. Therefore such systems are very promising in the active packaging field, in which the antimicrobial drug has to remain anchored to the polymer for a long time, and not easily released.

It is worth noting that the release is performed in a saline solution, able to promote the exchange reaction. In the case of lower salt contents an even lower release is expected.

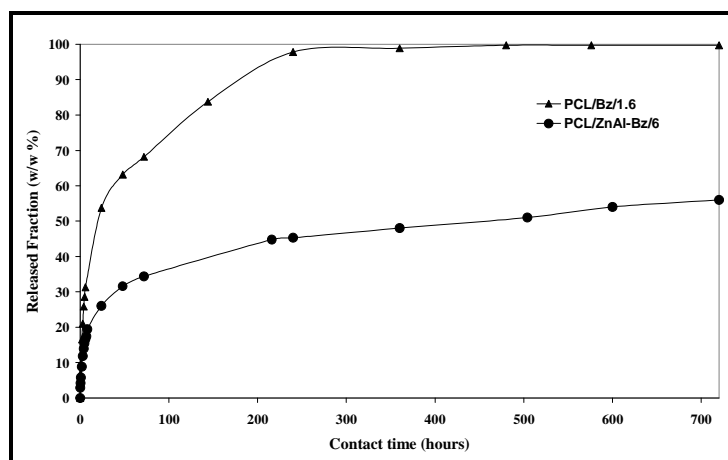


Figure III.4 Release kinetics of Bz anion from PCL/ZnAl-Bz6 and PCL-Bz/1.6 in a physiological saline solution, as a function of time.

As demonstrated in previous papers (Tammaro et al., 2005) the first stage of release is faster, due to the leakage of molecules anchored to the outer lamellae of inorganic or those not connected. In the second stage, the output of the molecule depends on the time of diffusion of counter-ions of saline solution (chloride ion) that enter the polymer, with the anion exchange, and the latter then diffuse into the polymer.

These phenomena are rather slow and the release can be prolonged for several months. This result demonstrates that these are promising nanohybrid as a slow and controlled release systems for application in active food packaging.

III.5.2 Comparison of PCL composites of hydroxaltes synthesized by different methods

The following samples were prepared both with hydroxaltes synthesized by the method of urea and by the method of coprecipitation. Are compared the structural properties and have been studied the kinetics of release of anions from PCL composites.

- Pcl +3% LDHsal
- Pcl +5% LDHsal
- Pcl +5% LDHBz
- Pcl +10% LDHsal

Data are reported only for the composition at 5% as representative of all other samples.

III.5.2.1 X-ray diffraction analysis

The X-Ray diffraction has been used with the aim of investigating a possible intercalation of the polymer inside the lamellae and any subsequent exfoliation of the inorganic phase.

The spectrum of figure III.5 A is related to composite PCL/5%LDHsal and it was possible to observe that the characteristic peak of hydrotalcite from coprecipitation (around $2\theta \approx 5.68^\circ$) is widened compared with the original filler because the structure is delaminated while the peak characteristic of hydrotalcite of urea is more evident and shifted to lower 2θ (about 4.5°) for greater intercalation of the polymer inside of the inorganic compound.

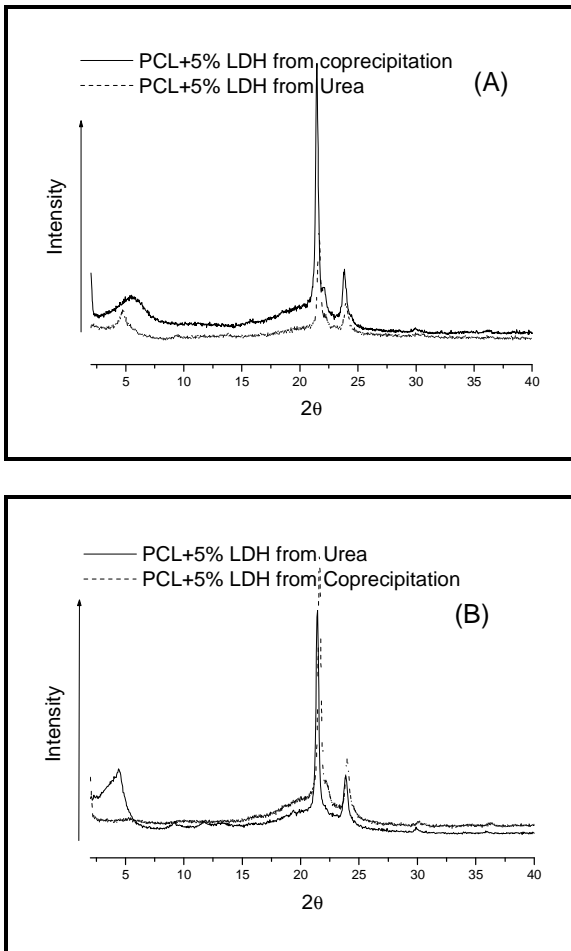


Figure III. 5 Comparison between X-Ray spectra of PCL/LDH from Urea and from Coprecipitation for LDHsal (A) and LDHBz (B)

The same behaviour is obtained for the composite PCL/5%LDHBz (Vittoria et al, MI2011A/00192).

III.5.2.2 Kinetics of release

Were carried out the release tests of salicylate and benzoate in saline solution (NaCl 0.9%) from the film Pcl/5%LDHBz and Pcl/5%LDHsal prepared with hydrotalcite synthesized by two different methods.

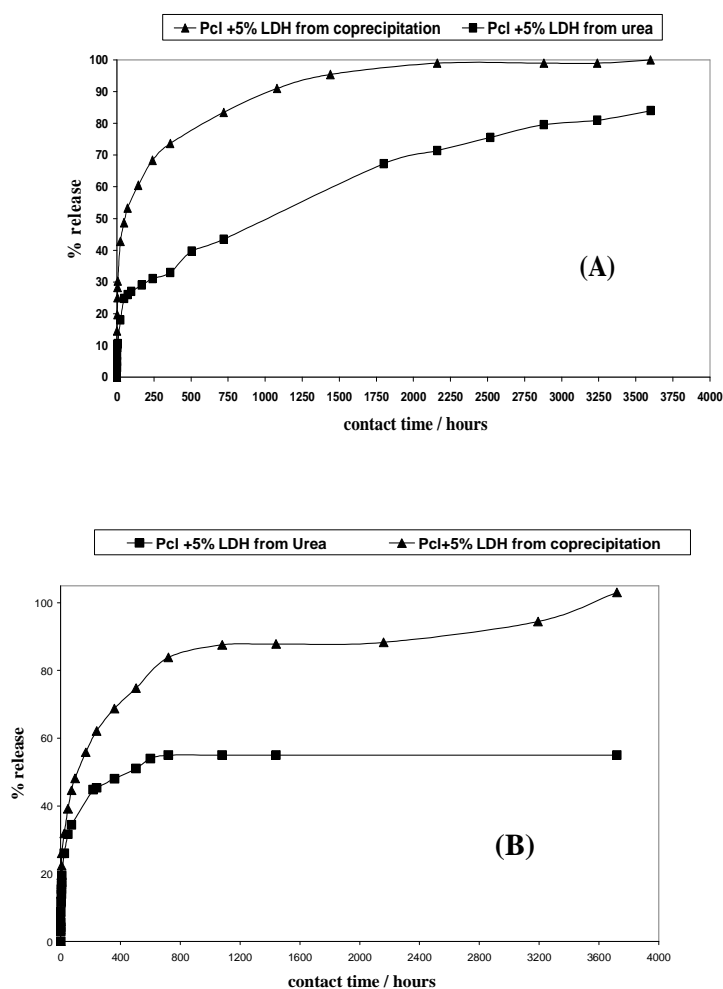


Figure III.6 Release kinetics as a function of time of Sal (A) and Bz (B) anions from PCL/LDH from coprecipitation and Urea composites

The samples were placed in 25ml of saline at room temperature. After specific time intervals, 1 ml of solution was collected and analyzed with spectrophotometry UV-visible, thanks to the chromophore nature of the organic molecule.

The Figures III.6 A e B show the release kinetics of salicylate and benzoate, anchored to the hydrotalcite LDHsal and LDHBz obtained by the two methods of synthesis and dispersed in the PCL.

As can be seen, the release of benzoate anchored to hydrotalcite by coprecipitation after 1200 is about 90% while from hydrotalcite by urea is only 50%, proving that the release kinetics of benzoate from hydrotalcite from coprecipitation is faster. This phenomenon is due to the exfoliated structure of lamellae in composites from LDH by coprecipitation.

The same has been for composites with LDHsal. In this way, depending on the method of synthesis it is possible to modulate the kinetics of release.

Chapter IV

Polyethyleneterephthalate composites

IV.1 Selection of filler used

Have been selected different types of inorganic fillers to improve oxygen barrier properties of PET.

Normally, for industrial application, are used laminated system such as PE/EVOH/PET and copolymers based on EVOH (ethylene-polyvinyl alcohol), designed to combine performance of polyvinyl alcohol (excellent gas barrier, but water barrier limited) and polyethylene (excellent barrier to water but gas barrier limited).

The use of EVOH in flexible packaging for perishable foods is very popular, especially after the introduction of modified atmosphere, which by their nature, can ensure a good oxygen barrier, aroma, and humidity (Jasse et al, 1997).

The filler selected to replace high barrier layer (EVOH) in poly laminate are:

1. LDH-citrate
2. LDH-salicylate
3. LDH-aleurate
4. LDH-pOH-benzoate
5. LDH-glycolate
6. LDH-serin
7. LDH-2.2-bis-hydroxymethyl-propionate

They are prepared by co-precipitation method, as above described.

The hydrotalcites have hydrophilic nature, for the presence of double hydroxides of aluminum and zinc and can therefore improve barrier properties of PET.

LDH-salicylate and LDH-pOHBz with the presence of the aromatic hydroxilic group and other fillers with aliphatic hydroxilic groups, can simulate the EVOH (Vittoria MI2011A/00192).

IV.2 Incorporation of modified inorganic fillers in PET by "High Energy Ball Milling" and characterization of PET composites

The technique used to incorporate the filler on PET was the High Energy Ball Milling (mixing for 1 hour at maximum speed in a mill with rigid balls at room temperature and in the absence of solvent).

Has been chosen as representative percentage of all compounds the 3% (w/w) of filler on PET.

Have been compared the structural, thermal and barrier properties for the following PET composites:

- PET+3% LDH-salicylate
- PET+3% LDH-aleurate
- PET+3% LDH-pOH-benzoate
- PET+3% LDH-glycolate
- PET+3% LDH-serina
- PET+3% LDH-2.2-bis-hydroxymethyl-propionate
- PET+3% LDH-citrate

IV. 3 PET composites characterization

IV.3.1 X-ray diffraction of PET-filler composites

The X-ray diffraction has been used with the aim of investigating possible intercalation of the polymer inside the blades and any subsequent exfoliation of the inorganic phase.

The Xray spectra of PET/3%LDHsal is reported as example.

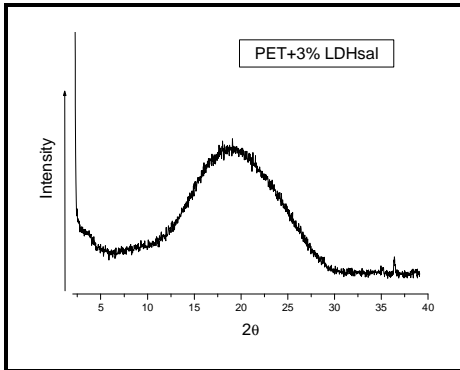


Figure IV.1 X-Ray diffraction patterns of PET/3%LDHsal composite

In all the X-ray spectrum of the composites the characteristic peak of hydrothermalite is widened, almost absent compared to the original filler. It is obtained for a delamination of the structure.

IV.3.2 Thermogravimetric Analysis of PET-filler Composites

The Thermogravimetric analysis confirmed the content of inorganic initially established in the preparation of the composite (3%) and showed a temperature of degradation for the composites like the original polymer.

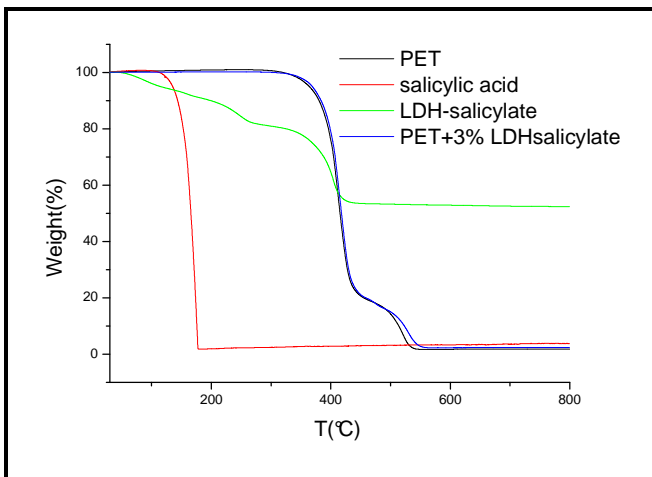


Figure IV.2 TGA curve of PET composite (thermal cycle from 30 to 800 °C at 5 °C / min, in air flow)

As can be seen from the figure IV.2 the temperature of degradation of the organic molecule increases by about 200 °C when it is ionically bound to hydrothermalite and dispersed in the polymer showing that inside of the

inorganic it is protected; for this reason it give the possibility to work with temperature sensible molecules even at high temperatures.

IV.3.3 Oxygen barrier properties

It was possible to obtain, using the microgravimetric technique, the transport parameters from a single experiment, using an experimental device (IGA, Intelligent Gravimetric Analyser).

In figure IV.3 is reported the oxygen sorption for PET composites expressed as $S = V_{O_2} \text{ (STP)} / \text{atm} * V_{\text{sample}}$ and it was possible to note an increase in sorption for all composites.

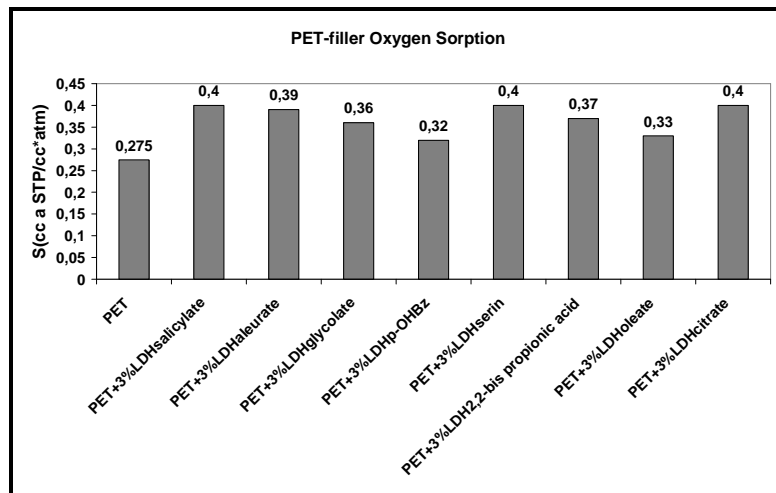


Figure IV.3 Oxygen sorption coefficients of PET composites

In figure IV.4 and IV.5 is reported the results of measurements of diffusion and permeability.

It has been obtained for all composites a small decrease of the values due to the presence of hydroxylic groups on aromatic rings and long aliphatic chains that make the material more hydrophilic and polar and therefore more resistant to oxygen.

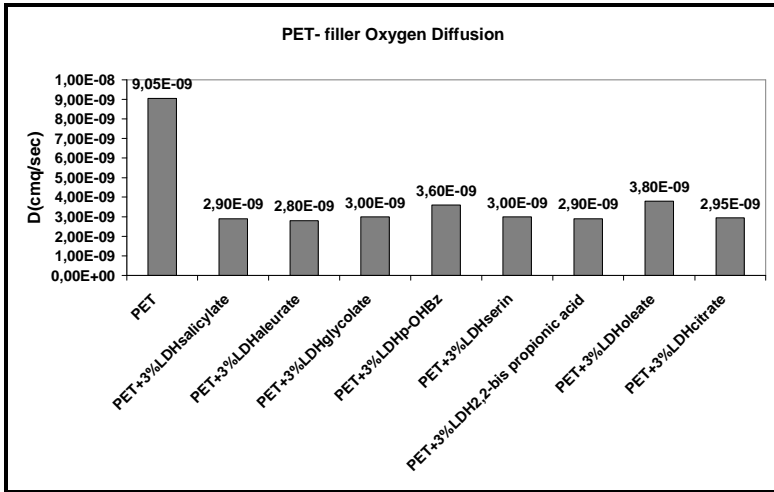


Figure IV.4 Oxygen diffusion coefficients of PET composites

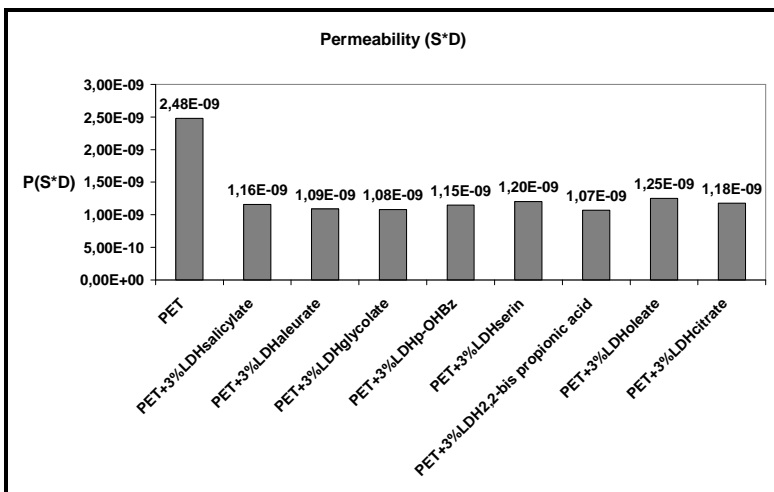


Figure IV.5 Oxygen Permeability coefficients of PET composites

Is reported in Figure IV.6, for example of the improved oxygen barrier properties of PET film/filler, an image of experiments carried out with apples contained in vials closed with films such as PET (number 1) and PET + filler (2, 3 and 4) after 6 months. (Vittoria MI2011A/00192).



Figure IV.6 Apples Test of PET composites

As it can be seen from the difference in color and aspect, the pieces of apple contained in vials closed with PET film + filler did not exhibit the signs of oxidation and molds that instead have been evident in the piece of apple contained in the vial number 1, being darker and moldy.

IV.4 Antimicrobial test of PET composites

The antimicrobial properties of sodium salicylate, benzoate derivative, is already known, being an inhibitor of gram-negative bacteria such as *Pseudomonas* and *E. coli*, the most responsible for the degradation of fresh foods such as meat, fish and dairy products; it was in any case interesting to do preliminary tests to prove that these properties are also present in the polymeric composite films.

The tests were performed with the organism *Escherichia coli* (DSM30083T) Gram negative bacterium, coliform, an indicator of faecal contamination in food. This is usually the bacterium most commonly used in the tests of antimicrobial activities described in scientific literature.

It was used the method of counting the CFU (colony-forming units). Are tested films prepared by HEBM (1 hour at maximum speed) of PET and PET LDHsalicylate at different percentages.

IV. 4. 1 Evaluation of antimicrobial activities of LDH-active molecule powder

Different amounts of LDH-salicylate powder (0,2-0,3-0,4grams) were weighed into flasks. Were added to each flask, 10 ml of Tryptic Soy Broth (TSB; liquid culture medium for bacterial growth). Everything was UV sterilized for 90 minutes. Then is added 1 ml of bacterial suspension of *E. coli*. The flasks were then incubated at 30 ° C in continuous agitation at 160

rpm. It was also prepared a flask of control where there was only the TSB and the bacterial suspension without the presence of the supposed antimicrobial agent.

At different incubation times were made and viable counts of live microorganisms present in the flasks. The medium used for plate count is the TBX, selective and differential culture medium, specific for the detection of *Escherichia coli*. The results of bacterial counts at different times of incubation are shown in the graph below.

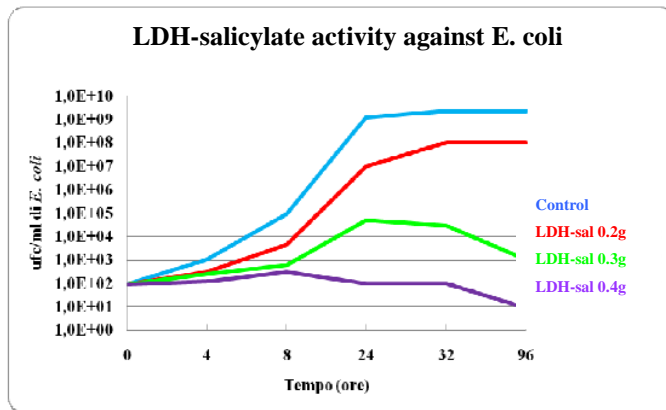


Figure IV.7 Antimicrobial activities of LDH-active molecule powder

Can be observed that the powder of LDH salicylate has bacteriostatic activity against *E. coli*. This activity was greater with increasing powder concentration in the broth culture. Can be seen that the minimum concentration of LDH-salicylate shows a substantial slowing microbial is 0.4 g/10 ml (4% w / v). At this concentration, the gap between control and test sample turns out to be, after 24 hours of incubation, amounting to 7 logarithmic orders that are maintained such substantially up to 72 hours of incubation at 30 ° C. At lower concentrations of LDH-salicylate control the gap tends to decrease due to lower bacteriostatic activity exercised by the powder.

The next step was to evaluate this activity on the PET film containing LDH-salicylate, trying to evaluate if the minimum concentration detected by the tests described above can also be transferred on the film.

IV. 4. 2 Evaluation of antimicrobial activities of LDH-salicylate in film

IV. 4. 2. 1 Contact between films and microorganisms in liquid

The operation method used was the following: were prepared squares of films of PET, and PET + LDHsalicylate at different percentages, of size (2x2) cm² and placed in sterile tubes containing 10ml of TSB medium (BD Tryptis Soy Broth) +100 µl (102 cfu / ml) of a fresh suspension of E. coli. The tubes were left at room temperature (25 ° C). The sowing took place in the plate according to the technique of dilutions that includes the following steps: the sample in examination was diluted of 10⁻¹, 10⁻², 10⁻³, diluting 1ml of sample to 10ml (adding 9 ml of saline), then diluting 1 ml of the latter back to this again and finally 10ml to 10ml. The 3 dilutions were added to the medium and then placed at 37 ° C for 24h.

Film examined:

- 1) PET
- 2) PET+20%LDH-SALICYLATE
- 3) PET+30%LDH-SALICYLATE
- 4) CONTROL: MEDIUM ONLY + E. coli

Counts were performed at the time t_0 , after 6h and 24h of incubation. The results are presented in Table IV.1.

Table IV. 1 *E. coli* counts after time of incubation for all the samples

Film tested	t_0	t= 6h	t= 24 h
PET		$3 \cdot 10^3$	$5 \cdot 10^8$
PET+20%LDHsalicylate		$3 \cdot 10^3$	$1.1 \cdot 10^9$
PET+30%LDHsalicylate		$2.5 \cdot 10^3$	$7 \cdot 10^8$
Control	$1 \cdot 10^2$	$1 \cdot 10^3$	$5.3 \cdot 10^9$

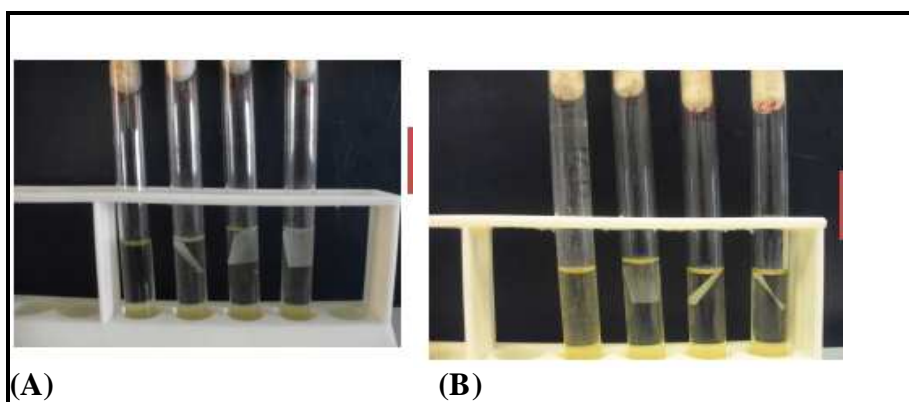


Figure IV.8 Antimicrobial activities of LDH-active molecule in film before (A) and after (B) incubation in liquid

The results in Table IV.1 and Figures IV.8 showed a uniform microbial growth independently of types of films, concluding that there wasn't any kind of inhibition.

IV. 4. 2. 2 Contact between films and microorganisms in solid

Are examined the following film:

- PET
- PET+20%LDH-SALICYLATE
- PET+30%LDH-SALICYLATE

The operation method used was the following: an agar containing a bacterial suspension of *E. coli* at a concentration from 10^7 to 10^4 cfu / ml is placed in contact with each film. The plates were incubated at 37°C for 24 hours.

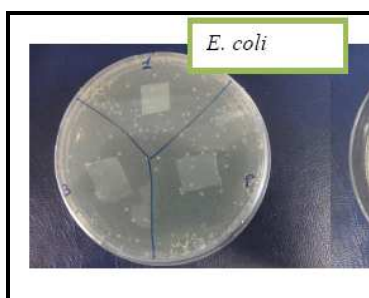


Figure IV.9 Antimicrobial activities in solid of LDH-active molecule in film

The results showed a uniform microbial growth independently of types of films for the bacteria tested.

To try to understand the non-inhibition of LDHsalicylate dispersed in the films against the bacteria analyzed it was studied the kinetics release in saline solution of the salicylate anion by LDH-sal dispersed in PET in different percentages.

IV. 5 Release kinetics

This part of thesis aims to observe and describe the release in an aqueous solution of the active molecule linked via ionic bonds to the inorganic compound dispersed in the polymer matrix. Has been carried out the release of salicylate in saline solution (NaCl 0.9%) from PET +20% LDHsal and PET+30% LDHsal.

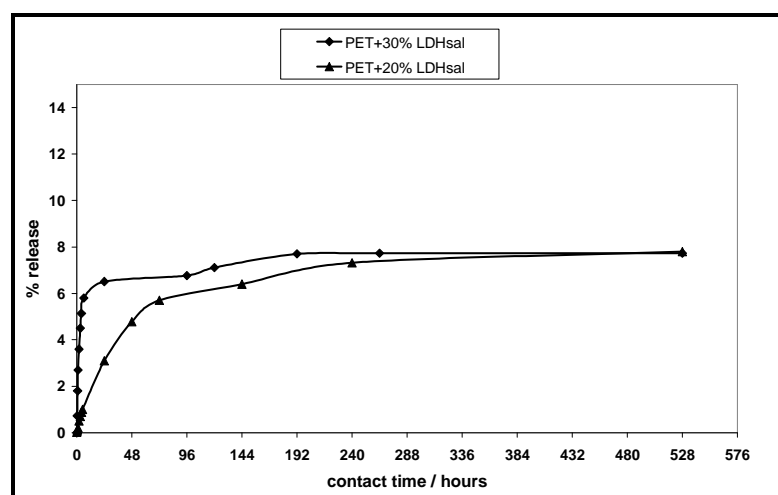


Figure IV.10 Kinetics of release of salicylate from PET composites

The samples were placed in 25ml of saline solution at room temperature. After specific time intervals, 1 ml of solution was collected and analyzed by UV-visible spectrophotometry, thanks to the chromophore nature of the organic molecule.

The release of salicylate anchored to the inorganic by PET is very slow. Infact, after 144 hours, the release of the molecule bound to hydrotalcite is only 7%.

It was possible to conclude that the release of salicylate from hydrotalcite dispersed in PET is so slow to not allow a release of a quantity that can inhibit the growth of the microorganism *E. coli* in the first 48 hours, as happens in the original hydrotalcite powder.

Chapter V

PET/hydrotalcites coating

Based on the results obtained from the antimicrobial tests and release kinetics of the composites it was found that the release of salicylate from hydrotalcite dispersed in PET is so slow as to not allow a release of a quantity that will inhibit the growth of the microorganism *E. coli* in the first 48 hours, as happens in the original hydrotalcite powder.

We decided to change method of dispersion of the inorganic filler on polymeric matrices: it was studied the dispersion of LDH-active molecule in an acrylic adhesive used in the food industry for sealable coating of polymers such as polyesters and polyolefins.

For the release of antimicrobial from coating on PET the phases of this part of project were:

- Preparation and characterization of films, dispersing the filler in the adhesive coating
- Application of the system PET-coating+LDH-active molecule on foods such as fresh mozzarella, grapes, cherries, milk and cheese to demonstrate the effectiveness of controlled-release on extending the shelf life of foods.

V.1 PET/ active filler coatings characterization

Were prepared PET film coating at different percentages of filler in acrylic adhesive. Were characterized in terms of structural and microbiological analysis and has been studied the release in saline solution. Are reported data for the PET/adhesive/12% LDH-salicylate.

The innovative system is that these active molecules, rather than being added directly to the food and all at once, are introduced in the same in a slow and controlled way, thus ensuring a better quality and greater durability (Vittoria MI2011A/00192)..

V.1.1 X-ray diffraction

The X-Ray diffraction was used with the aim of investigate the presence of inorganic phase in the acrylic resin.

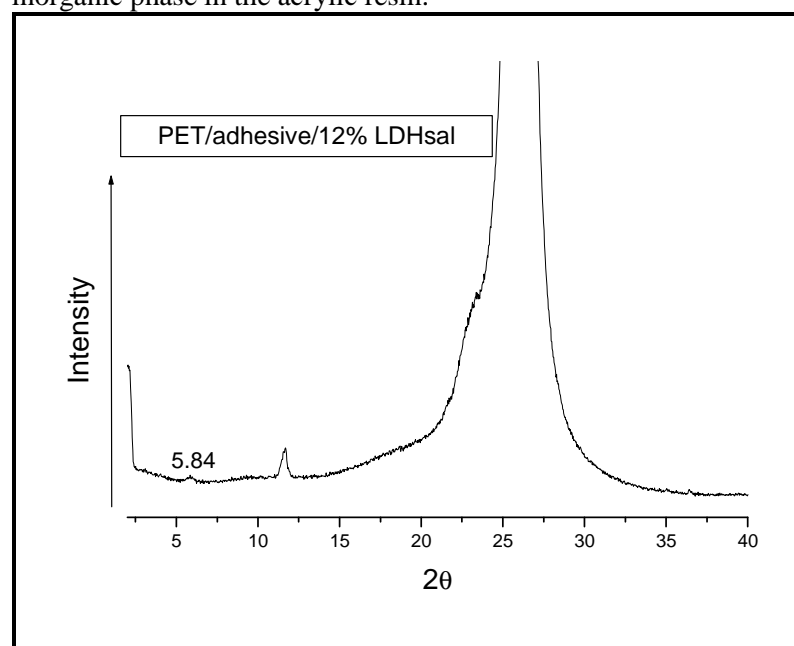


Figure V.1 X-ray diffraction patterns of PET/adhesive/12%LDHsal

In the X-ray spectrum of figure V.1 it was possible to see the characteristic peak of hydrotalcite LDHsal around $2\theta \approx 5.84^\circ$, evidence of presence of filler on the adhesive after dispersion on PET surface.

V.1.2 Release of salicylate from PET/adhesive/12% LDHsal

We have studied the release in an aqueous solution of the active molecule linked via ionic bonds to the inorganic compound dispersed in the acrylic adhesive. Has been carried out release of salicylate in saline (NaCl 0.9%) from PET film/adhesive/12%LDHsal according to the procedures given above.

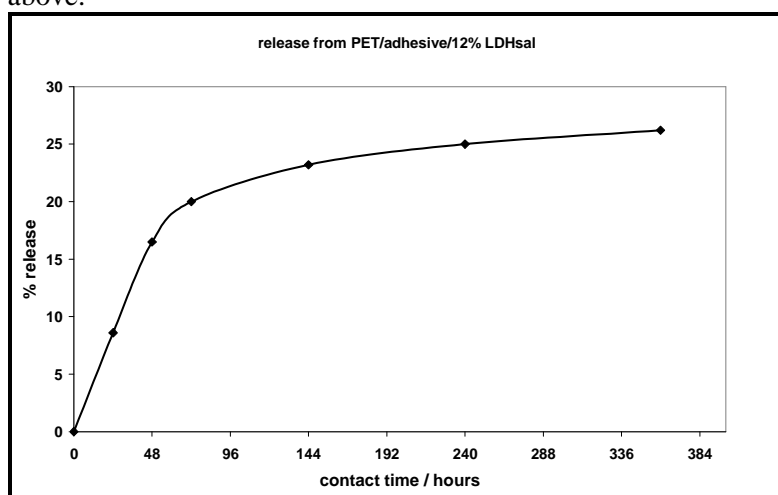


Figure V.2 kinetics of release of salicylate from PET/adhesive/12%LDHsal

From figure V.2 it is evident that the release of salicylate anchored to the inorganic, dispersed in the adhesive instead of dispersed in the polymer, it is faster. In fact, after 144 hours the release of the molecule bound to hydroxalcalite is 23% in comparison with the release of salicylate from PET+LDHsal composite where the release after the same time interval was only of 7%.

V.1.3 Microbiological Test of PET/adhesive/12 %LDHsalicylate

The tests were carried out by placing in a sterile tube 10 ml of TSB (culture broth), 4 cm² of film and 1 ml of microbial suspension (*Escherichia coli*). The tubes were incubated at 20-22 ° C and was carried out microbial counts in a timely manner.

As it can be seen from Figure V.3, there was a slight improvement of the antimicrobial activity of the PET /adhesive/12 %LDHsal) against *E. coli* compared to PET control.

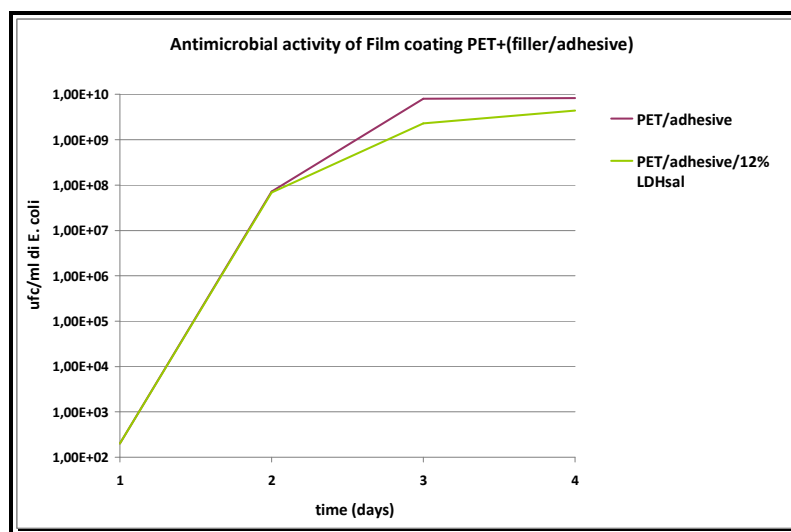


Figure V.3 Antimicrobial test of PET/adhesive/12%LDHsal film

Based on these promising results it was possible to use these system PET/adhesive/active filler to study of extension of the shelf life of foods, especially mozzarella, food that has been studied and analyzed.

V.2 Application of system PET/adhesive/LDHactive molecule on extending the shelf life of food

V.2.1 Mozzarella

We decided to apply the system film-coating + LDH-active molecule on foods such as fresh *mozzarella* to demonstrate the effectiveness of controlled-release from coating on extending the shelf life of food. (Altieri et al, 2005).

Fresh and aqueous foods such as dairy products, are very susceptible to bacteria growth such as Coliforms, *Pseudomonas* and Fungi, most responsible for their degradation (Laurienzo et al, 2008).

The determining factors on the preservation of the freshness of the *mozzarella* are different:

- pH;
- hydrolysis of casein;
- calcium;
- ratio of calcium / sodium;
- acidity;
- presence of microorganisms

This last point is crucial to maintain the freshness of the mozzarella, in fact coliforms, pseudomonas and fungi grow on the surface of the mozzarella, coming from the *governo* water; the coliforms test is an indicator of freshness. (Sinigaglia *et al*, 2008)

Coliforms grow rapidly during the first days of storage, producing lactic acid, acetic acid, formic acid, succinic acid, ethanol, CO₂ and causing swelling of the envelopes and a decrease in pH.

The pH is also an important factor. It affects the casein proteolysis, the amount of calcium, the ratio Ca-Na-Casein and organoleptic characteristics of *mozzarella* cheese (J. Dairy. Sci, 2007).

V.2.1.1 Project phases

The phases of this part of the project were:

1. Preparation of film for coating of PET+adhesive and PET+(adhesive/6% LDHsal-6%LDHcarbonate) useful to inhibit bacterial growth and to control the pH.
2. Preparation of bags with PET+adhesive film and PET + (adhesive / 6% LDHsal-6%LDHcarbonate) and packaging of each *bocconcino* dipped in a fixed amount of water (50 ml).
3. Storage of the bags at 18 ° C.
4. Water extraction and homogenization of the *bocconcino* at different times: at time t_0 , after 8h, 24h, 48h, 72h, 6 days, 10 days, 15 days, 20 days to 30 days.
5. Measuring the pH of the *governo* water and the *bocconcino*.
6. Analysis of the organoleptic properties (color, smell, taste)
7. Preparation of selective media for each type of organism (PCA, MRS, M17, VRB, Pseudomonas, YEPD)
8. Measurement of the total bacterial count, total coliforms, pseudomonas, streptococci, lactic acid bacteria, lactobacilli, yeasts and fungi.
9. Analysis of proteolysis of casein
10. Test on the elasticity of *bocconcino* (resistance and compression)

V.2.1.2 First results

As it can be seen from Figure V.4, the first data on pH measurements showed a pH differentiation on the *bocconcino* contained in the PET +adhesive and PET + (adhesive / 6%-LDHsal 6%-LDHcarbonate). The pH of the *bocconcino* contained into the bag with the antimicrobial and carbonate is more basic in the first 48h and between 48h and 72h there is a collapse to more acidic pH, due to the development of microorganisms that tend to acidify the system of the *mozzarella*.

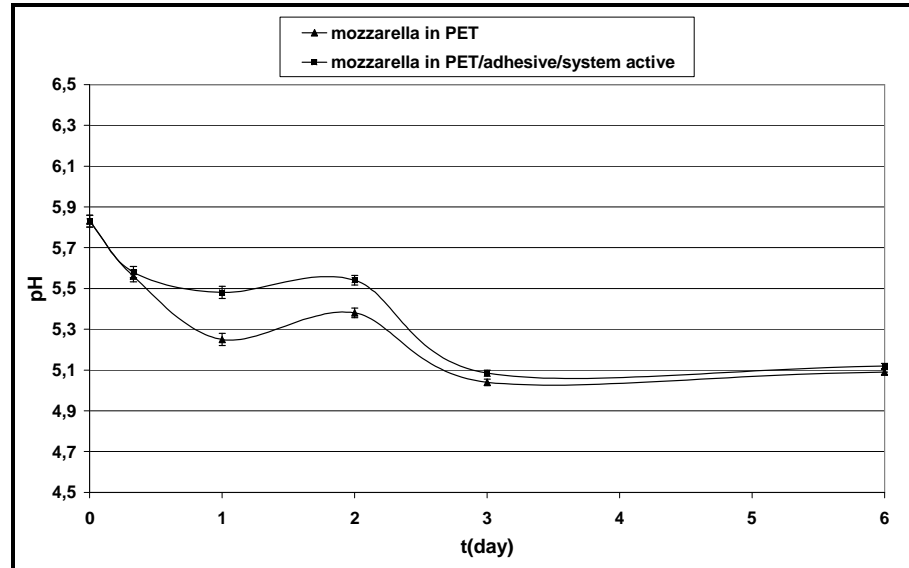


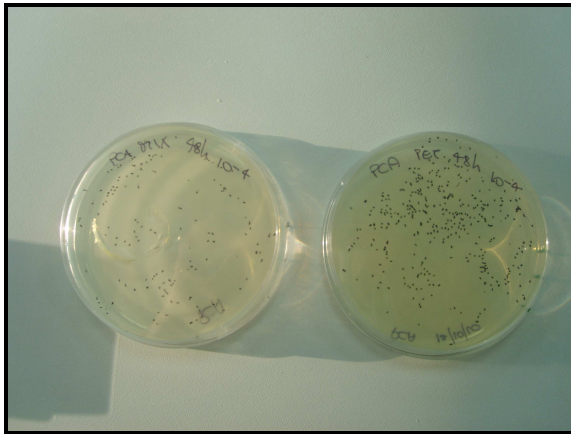
Figure V.4 pH variation for mozzarella in PET and in PET/active system

Regarding the growth of fungi and yeasts, as seen in Figure V.5, there was a strong inhibition by the antimicrobial agent released on the *bocconcino*.



Figure V.5 Yeast growth in PET (a) and in PET/active system (b)

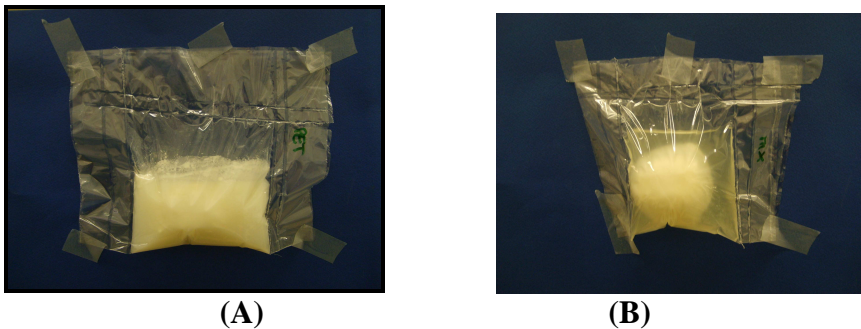
The total bacterial growth (Figure V.6) in the *bocconcino* inside the bag containing the active molecule is much less than that contained in PET.



(A) (B)

Figure V.6 Total bacterial growth in PET/active system (a) and in PET (b)

Also the organoleptic characteristics such as color and texture in the *bocconcino* on the bag with the antimicrobial agent are unchanged after 34days, as can be seen from Figure V.7.



(A) (B)

Figure V.7 Organoleptic characteristic for Mozzarella after 34days for the control (a) and antimicrobial agent (b)

V.2.2 Other foods

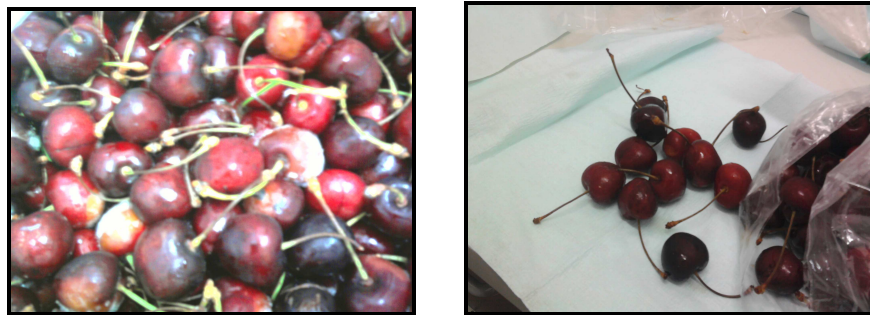
Was applied the system PET film-coating + LDH-active molecule dispersed on adhesive on other foods such as **grapes, cherries and cheese** to demonstrate the effectiveness of controlled-release on extending the shelf life of food. All the test showed a very good results. Infact after about 20 days the fruit and cheese inside the control film showed presence of mold and darkening in comparison with that in film with antimicrobial agent.



(A)

(B)

Figure V.8 Grapes after 21 days: control(A) and antimicrobial system (B)



(A)

(B)

Figure V.9 Cherries after 21 days: control(A) and antimicrobial system (B)



(A)

(B)

Figure V.10 Cheese after 21 days: control(A) and antimicrobial system (B)

V.2.2.1 Milk

To evaluate the freshness of milk it was used the Reductase methylene blue method. This method can quickly give an idea of the hygienic conditions of a sample of milk. It is based on the ability of microorganisms to decrease the redox potential of the medium in which they are, as result of their metabolic activity (oxygen consumption and reducing system). The addition of a redox indicator (such as methylene blue or resazurina) indicates, with its color change, the state of oxidation or reduction of the medium.

Methylene blue is blue in oxidized form and colorless in a reduction state: shorter is the reduction-time of indicator (blue to colorless) higher is the bacterial grow present and worse is the quality of milk.

In order to determine the activity of packaging films, have been measured the bacterial growth of milk by the methylene blue reductase. The tests were carried out at time zero (t_0), the day of expiry of the milk (t_1), to a one (t_2) and three days of the end (t_3), a week after the deadline (t_4).

Table V.1 Reduction time of blue methylene indicator on PET and PET/12 Mix samples

Sample	t_0	t_1	t_2	t_3	t_4
PET	>6h	3,5h	3h	2,5 h	<1h
PET/MIX 12	>6h	>6h	5,5h	5,5h	4,5h

Tests show that at the same conditions (time, temperature, size of the package) the bacteria growth appears to be less for milk packaged in PET/MIX12.

The final results of all these test are under patent so it wasn't possible to show all the data (Vittoria MI2011A/00192).

Chapter VI

Polylactic acid coating

VI.1 Objectives of this part of the project

Following the positive results obtained with PET coating system on shelf-life of fresh foods, the aim of this part of the project was the development and characterization of coatings system on biodegradable polymers (such as polylactic acid (PLA)) by a simple process deposition.

A simple coating method to plasma treated polymeric surfaces was developed, basing on electrostatic interactions between the positive charged surface of nanoparticles (Kaneda et al, 2010) and the charged polymeric substrate, leading to a stable and resistant coatings.

Using also nanoparticles with antimicrobial activity (silver nanoparticles or active organic molecules such as salicylate or phosphonium salts) it was possible to obtain an active multilayer coating useful to several application (food packaging, biomedical application) (Kim et al, 1998).

The objectives of the project were:

- Preparation of inorganic filler modified with active molecules
- Deposition of modified filler by coating on plasma treated polymeric surface for the realization of:
 - systems with antimicrobial activity
 - systems with improved barrier properties

These active systems are able to be used for food packaging, to protect and extending the shelf life of products.

The aim of the present work is to propose the use of layered double hydroxyde as an alternative to commonly used cationic clays and to combine

phosphonium ionic liquids to formulate PLA coatings with enhanced properties

VI. 2 Idea

The idea of the project came from a recent work realized in the lab of Professor Giannelis (Fang et al, 2010), Cornell University, Ithaca, NY where it was spent the period of PhD abroad (about 6 months), about a simple deposition process of positively functionalized silica nanoparticles (with ammonium group) on Plasma treated polypropylene (PP). It led to stable and solvent resistant multilayer coating and made the PP hydrophilic. Also have been used silver nanoparticles as antimicrobial (Pilati et al, 2009; Park et al, 2007; Takato et al, 2008).

We decided to apply this method to biodegradable polymer such as Polylactic acid (PLA) (Hirsjarvi, 2006), using active hydrotalcites (LDH) as positive nanoparticles, thanks to the positive charge of lamellae ($[M^{ii}_{1-x} M^{iii}_x(OH)_2]^{x+} A^{x-}$) and negative charges of PLA plasma treated.

The possible interaction between plasma treated polymeric surface and hydrotalcite nanoparticles can come from electrostatic forces, like showed in figure VI.1.

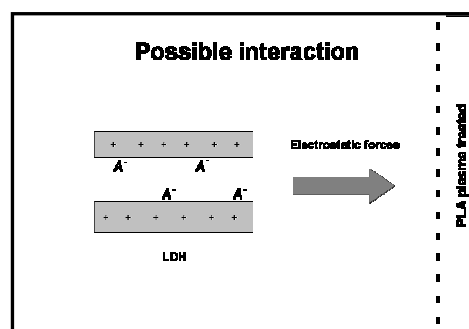


Figure VI.1 Possible interaction between hydrotalcites nanoparticles and Plasma treated surface PLA

VI.3 Research outline

Initially, the LDH with nitrate anions has been synthesized by coprecipitation method. Then, two different anions functionalized with long alkyl chains and based on phosphorous compounds are intercalated between the LDH layers by ion-exchange to make layered double hydroxyde more organophilic and contribute to the extension of interlayer distances which facilitates the dispersion of anionic clays. Finally, the modified-LDHs are

deposited on PLA surface and the final structure/properties relationships are also investigated in detail.

The principal steps of the project were:

- Hydrotalcite modified with organic molecules: synthesis and characterization (Tga, Rx, TEM)
- PLA characterization (Tga, Dsc, Rx)
- Study of the best plasma treatment conditions for PLA (power-time)
- Deposition process of hydrotalcite nanoparticles on plasma treated PLA
- Coating characterization (Xps, Contact angle, SEM, TEM, Tga, Dsc)
- Study of coatings durability and stability in different solvents
- Selection of LDH nanoparticles by 200nm filter to have more homogeneous deposition
- Water and oxygen permeability test
- Antimicrobial test

VI. 4 Advantages

This coating method can have several advantages for application on food packaging:

- Simplified method of dispersion of the inorganic active filler on polymers without using solvent and acrylic resin
- Dispersion of filler on polymeric surface
- A consequent more rapid kinetic of release
- Larger contact area to inhibit possible microorganism
- Higher antimicrobial activity
- Application to every kind of LDH and polymer
- Possibility of Industrial application

VI. 5 Organic molecules incorporated in the hydrotalcites

The organic molecules used to modify the hydrotalcite and give a target activity, are Polystyrenesulfonate (PSS) (Oriakhi, 1997, Aranda, 1995) and Phosphonium ionic salts (IL) (Daman'ska, 2007, Cumiencka, 2005, Kamazawa, 1994), to increase the hydrophobicity of PLA surface and to have an antimicrobial coating

VI.5.1 Phosphonium ionic liquid salts

The ionic liquid salts (ILs) are organic salts composed of cations and anions with a melting temperature less than 100°C. ILs can contain quaternary phosphorous cations, as shown in figure VI.2.

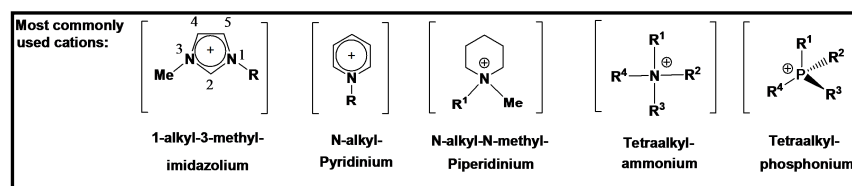


Figure VI.2 Ionic liquid (IL) salts structures

Ionic liquids (ILs) are organic salts composed of cations and anions, known for their excellent thermal stability, non-flammability, low vapor pressure and high ionic conductivity, not to mention that they are solvent environmentally benign. Moreover, these ionic liquids have already proven themselves as surfactant agents of layered silicates, as plasticizers, building blocks, lubricants or as compatibilizer of many polymers leading to a better dispersion of clay and ILs in the polymer matrix generally coupled with an increase of the final properties of the material. (Keskin et al, 2007; Kim et al, 2006; Rahman et al, 2006; Sanes et al, 2007 ; Livi et al, 2011).

ILs have several important properties that make these compounds very useful materials on organic and inorganic chemistry:

- Excellent thermal stability (> 300°C)
- Good ionic conductivity
- Solvents considered "green"
- Surfactant for polymers in suspension, organic inorganic charge, for porous materials
- Non-volatile plasticizers, Lubricants
- Antimicrobial activity

Ionic liquid phosphonium (IL) salts can give hydrophobic modification of layered double hydroxide (LDH) conducted by direct ion exchange reactions with two ionic liquids having the same phosphonium-based cation, but different anions, to improve barrier properties; also the physical adsorption of cationic phosphonium salt on hydrotalcite-like compounds (LDH) having positive structural charges, can give antimicrobial activity (Yanlia, 2007)

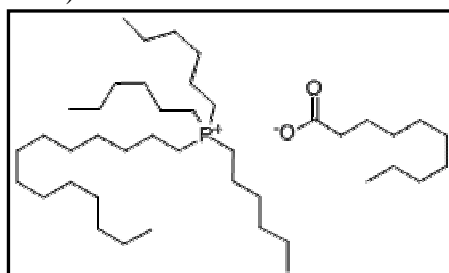


Figure VI.3 IL103:tetradecyl(trihexyl)phosphonium decanoate (P1) structure

One of ionic liquid used is the IL103: tetradecyl(trihexyl)phosphonium decanoate (P1) as shown in Figure VI.3.

The other one is IL201: tetradecyl(tributyl)phosphonium dodecylsulfonate (P2).

VI.6 Hydrotalcite (LDH) synthesis

The inorganic filler used on the project is the hydrotalcite as described above.

In this project are used two different method of synthesis of LDH modified:

- 1) Synthesis of hydrotalcite by the coprecipitation method, to synthesize LDH-nitrate and LDH-PSS, as the method explained above.
- 2) Phosphonium ionic liquids salts intercalation on LDH by ionic exchange from MgAlnitrate (AEC=3.35mmol/g) or MgAlcarbonate, using the following procedure:

Table VI.1 Reagents quantities for LDH ionic exchange reaction

Sample	M.W.	Molar ratio	mol	g	ml
MgAlNO ₃ or MgAlCO ₃	80.94	1	0.061	5	
IL 201or IL103	655	0.24	0.015	10	
water					100
THF					200

LDH was dispersed in 200 mL of a THF solution. The amount of surfactant added was about 2 AEC, based on the anion exchange capacity (AEC= 3.35 meq/g) of the LDH used. The suspension was mixed and stirred vigorously at 60°C for 24 h. Then, the precipitate was filtered, washed with THF. The solvent was removed by evaporation under vacuum. The modified-LDH was then dried at 80°C for 12 h. It was obtained 5g of product. Tga and Xray are used to characterize the sample.

VI. 7 Characterization of hydrotalcite LDH-active molecule

VI.7.1 X ray diffraction

The anionic exchange is clearly detectable by X-Ray Diffraction as shown in Figure VI.4. From X-ray spectra, for all the LDH modified by ionic exchange reaction, it was possible to realize the effective intercalation of PSS anion and phosphonium ionic liquid anions in the lamellae of LDH,

observing the shift from $2\theta=10.2$ to lower 2θ , of the characteristic peak of nitrate intercalated.

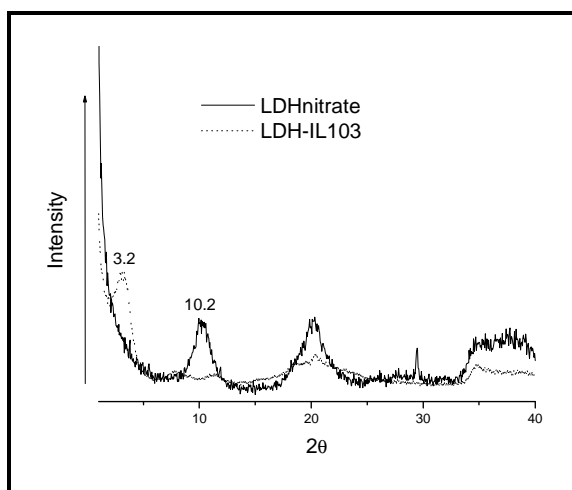


Figure VI.4 Comparison between X ray diffraction of LDHnitrate and LDH-IL103(P1)

In figure VI.4 is reported the spectra of LDH-IL103 (P1) as representative of all samples.

The larger dimensions of anions intercalated have increased the interlayer distance between the lamellae of LDH.

Before organic treatment, the basal spacing of the pure hydrotalcite *i.e.* LDH-NO₃ is 0.76 nm which corresponds to the diffraction peak $2\theta = 10.2^\circ$ and d-spacing of 7.7 nm, which is similar to that reported in the literature. After organic treatment by anionic exchange with phosphonium ionic liquids, the LDH-P1 and LDH-P2 shifted to the lower angle position. In fact, the LDH-P1 displays a (001) diffraction peak at $2\theta = 3.2^\circ$ corresponding to an interlayer distance of 2.7 nm whereas for LDH-P2, the diffraction peak at $2\theta = 2.6^\circ$ is significant of a distance of 3.4 nm. These distances obtained are very similar to one characteristic of a paraffinic conformation with trans-trans positions of the alkyl chain, frequently encountered in the case of cationic clays modified with imidazolium and phosphonium ionic liquids.

In conclusion, these increases of interlayer distances indicate the success intercalation of anions functionalized with long alkyl chains between the LDH layers. Moreover, these values are much higher than those obtained in different studies. In fact, the values are generally included between 1.4 nm and 2.9 nm. These new organophilic LDHs may facilitate the intercalation of polymer chains between the LDH layers during the preparation of nanocomposites and thus to improve the distribution of these organic fillers in the PLA matrix. (Chibwe et al, 1989; Bergaya et al, 2006).

VI.7.2 Thermogravimetric analysis (TGA)

After anionic exchange with the phosphonium ionic liquids, two organic species populations have been identified, the physisorbed species onto the layered double hydroxide surface and the intercalated ones which are located in the LDH galleries. To allow the identification of these two populations, the thermal degradation of the phosphonium treated-LDHs are reported.

From thermogravimetric analysis it was possible to evaluate the inorganic residual and degradation temperature for all the LDH, to understand the effective ionic exchange and intercalation of anions in LDHnitrate.

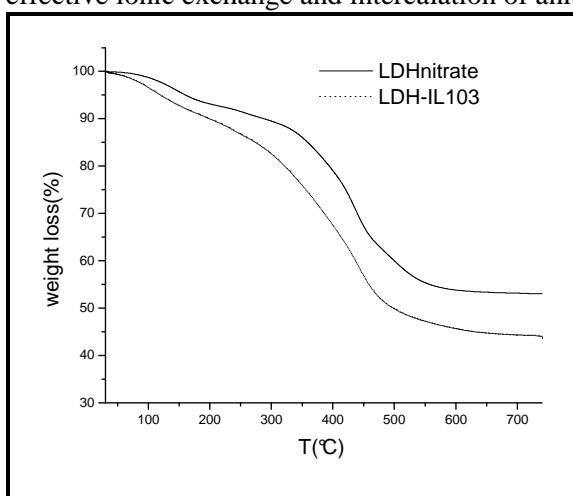


Figure VI.5 Comparison between Tga of LDHnitrate and LDH-IL103 (P1): [30-800°C at 20°C/minute under nitrogen]

Is reported the spectra of LDH-IL103 as representative of all samples.

In the case of LDH-NO₃, two steps of decomposition appear: in the first one, a weight loss of 10% at around 150-190°C, corresponds to the loss of absorbed water between LDH layers. In the second one, at a temperature range between 400-500°C, a weight loss of 30% can be described to the removal of nitrate anions as well as to the dehydroxylation of the LDH sheets. These results are consistent with the literature on the degradation of LDH and are also very similar to the results observed in the clays modified with organic cations where two kinds of interactions (Van der Waals and Ionic bonds) between inorganic clay and organic cations have been highlighted.

As for the anionic clays treated by decanoate and dodecylsulfonate anions and denoted LDH-P1 and LDH-P2, their decomposition is very similar to that of pristine LDH. In fact, two degradation peaks are observed at the temperature of 100°C and 420°C-500°C, respectively. According to the literature, the reduction of the degradation temperature of 150 ° C to 100 ° C corresponding to the water absorbed by the layered double hydroxide is due

to the decrease of the hydrogen bond interaction between water molecules. While the second peak at 420-530°C corresponds to the removal of dodecylsulfonate and decanoate anions combined with the degradation of phosphonium ionic liquids (340 °C for LDH-P1 and 450 °C for LDH-P2) adsorbed on the surface of layered hydroxides. In fact, an increase of the percentage of organic species is observed: 39% for LDH-P2 and 44% for LDH-P1 compared to 30% for LDH-NO₃.

In conclusion, these results confirm the excellent thermal stability of LDH modified with ionic liquids. Moreover, these new synthesized fillers have better thermal stability than montmorillonites modified with ammonium salts or treated with thermostable ionic liquids based on imidazolium and phosphonium cations commonly used as surfactants of layered silicates and which are degraded at a temperature 300°C. In addition, the presence of physisorbed ionic liquids can act as a compatibilizer in order to improve dispersion of fillers in the polymer matrix. (Zhao et al, 2002; Chen et al, 2003; Davis et al, 2004; Lv et al, 2009 ; Xie et al, 2002 ; Ngo et al, 2000 ; Livi et al, 2010).

VI. 8 PLA characterization

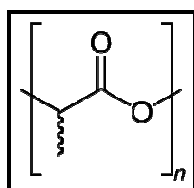


Figure VI.6 *PLA structure*

The PLA used in this project was a Natureworks polymer 7032D with melting temperature of 160°C, T_g of 55-60°C; degradation temperature of 379.9°C.

Film of 0.6mm of thickness were prepared by compression molding (200°C for 5 minutes).

VI.8.1 X ray diffraction

From X-ray spectra it was possible to observe an amorphous structure of PLA and calculate a crystallinity grade of 9%.

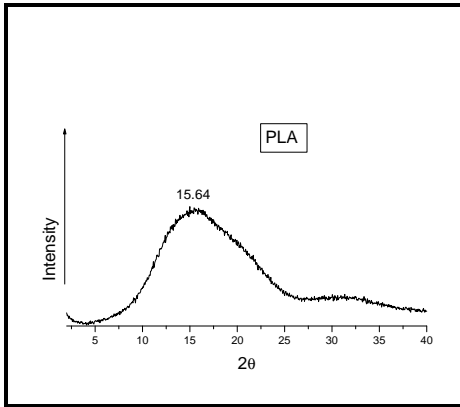


Figure VI.7 X-ray diffraction patterns of PLA

VI.9 Study of the best plasma treatment conditions for PLA

Before to apply the plasma treatment to PLA, being a soft polymer, film of 0.136 mm of thickness are used and the contact angle of the samples treated at different conditions was analyzed.

The substrate was treated with Ar-O₂ (50 : 50) mixed gas plasma.

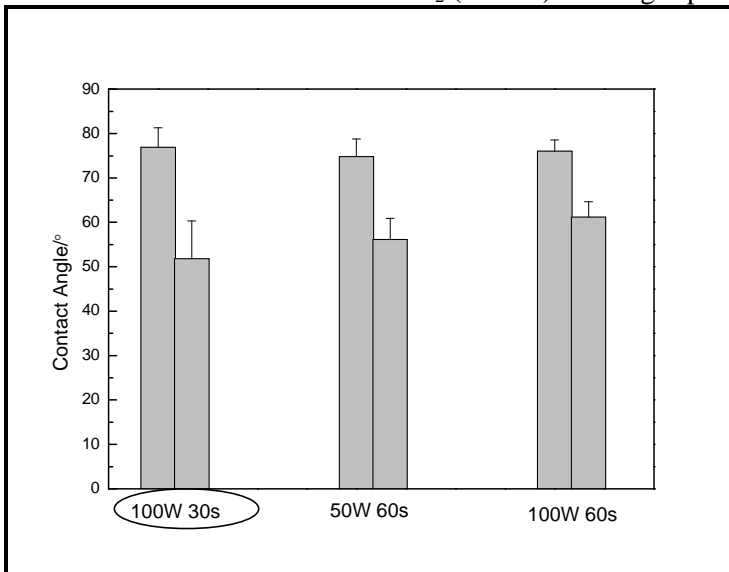


Figure VI.8 Contact angle (°) values for different conditions (power/time) of plasma treatment

The best power of plasma treatment is found to be 100W for 30sec because at these conditions the highest decrease of contact angle was obtained, evidence of the most surface modification.

Plasma treated PLA film with these conditions are prepared (100w- 30 sec).

VI.10 Deposition process of LDH nanoparticles on plasma treated PLA

The general procedure of deposition of LDH nanoparticles on plasma treated PLA is the following:

50ml of an aqueous solution of LDH (500mg) after 30 minutes in ultrasonic bath, was added to an oxygen plasma (100w 30sec) both side treated polylactic acid (PLA) film and left over night at room temperature, under stirring.

The PLA after coating was analysed by X-ray photoelectron spectroscopy (Xps), scanning electron microscope (SEM) and was studied the Contact angle;

VI.11 Coating characterization

VI.11.1 X-ray photoelectron spectroscopy

From Xps analysis it was possible to study the surface modification of PLA after plasma treatment (AP) and LDH deposition (AC) and it showed the presence of element that was expected.

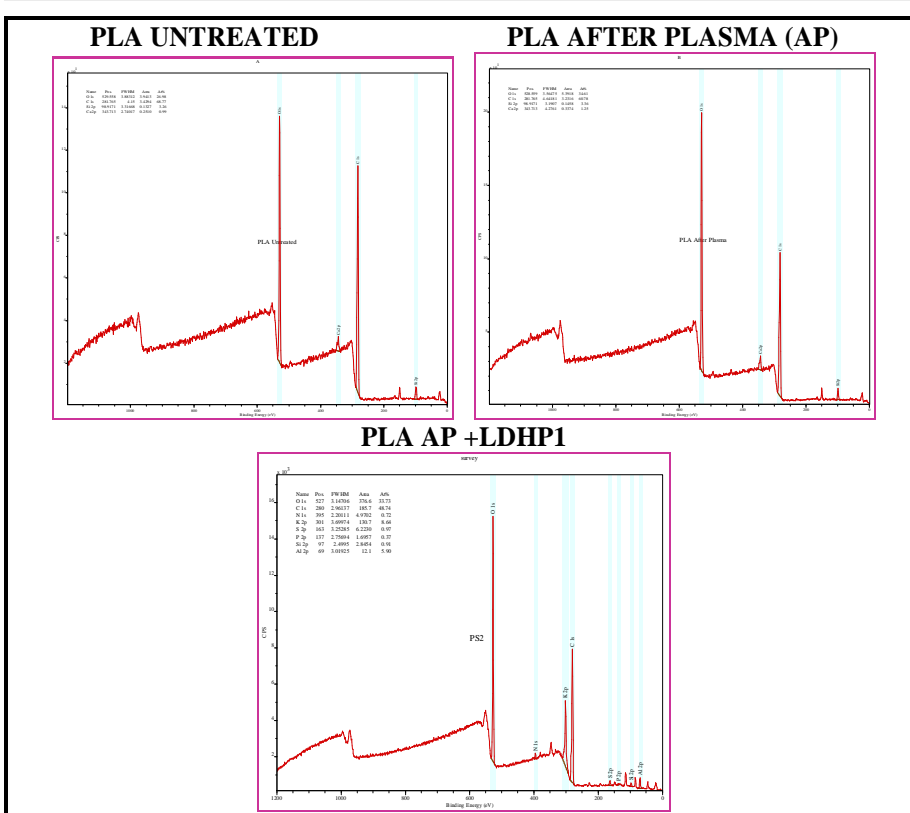


Figure VI.9 Xps spectra for PLA untreated, PLA after plasma (AP) and PLA after coating with LDHIL103(P1)

In fact in PLA after plasma (AP) there was an increase of percentage of Oxygen, evidence of plasma surface modification.

After deposition of LDH-P1 (AC) on PLA plasma treated, it was possible to note the presence of Mg, Al and phosphorus as elements, evidence of correct deposition of LDH on polymeric surface.

VI.11.2 Scanning electron microscope

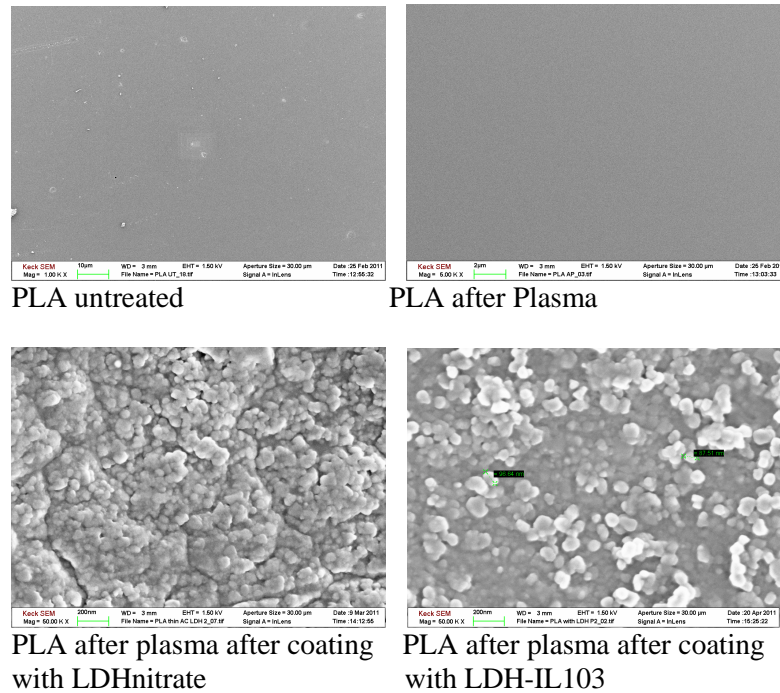


Figure VI.10 SEM images for PLA untreated, PLA AP, PLA after coating (AC) with LDHnitrate and LDH-IL103

From SEM analysis it was possible to observe an homogeneous deposition of nanoparticles for all the LDH coatings, even if for LDH-nitrate and LDH-P2 the deposition was more homogeneous than other. Between PLA untreated and PLA after plasma no difference wasn't observed.

VI.11.3 Contact angle

From contact angle analysis it was possible to note a decrease of value for PLA AP, evidence of an increase of hydrophilicity of PLA for the formation of negative charges on polymeric surface after Plasma treatment.

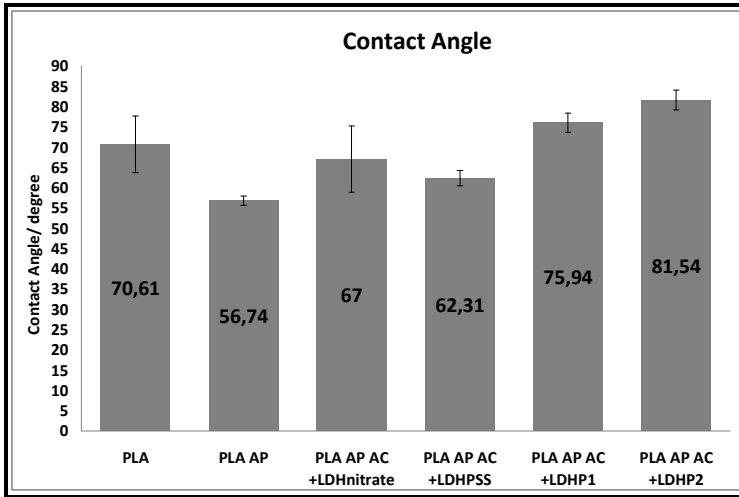


Figure VI.11 Contact angle (°) values for PLA, PLA AP and PLA after coating (AC) with different LDH

For all the film of PLA after coating of LDH nanoparticles there was an increase of value of contact angle, especially for LDHP1 and LDHP2. This was an evidence of increase of hydrophobicity of PLA surface, due to the intercalation of anion of phosphorus ionic liquid on LDH.

VI.11.4 Stability and durability

To evaluate their stability, the film of PLA after deposition of LDH, of thickness 0.6mm and treated at plasma on both side (100w-30sec) were subjected to ultrasonic field for 1 hour while being suspended in different solvents (water, acetone, ethanol). After this, SEM of samples in water and ethanol are analyzed (from acetone was not possible to have measures because PLA in acetone has swelled).

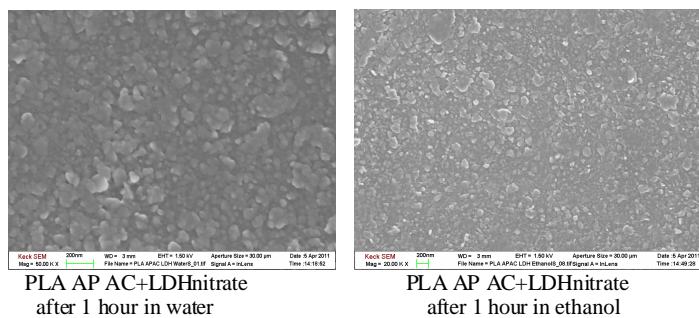


Figure VI.12 SEM images of PLA AP after coating with LDH after 1 hour in solvent

From SEM it was possible to observe an homogeneous deposition of nanoparticles of LDH even after 1 hour on solvent. As shown in Figure VI.12, even after 1 h of sonication while immersed in the solvents, the coatings resist detachment and are virtually unchanged.

VI.11.5 Selection of LDH nanoparticles

An aqueous solution of LDH-nitrate nanoparticles was filtered by a 200nm filter to have a selection and one more homogeneous dimension of nanoparticles, to give a better deposition. Film PLA of 0.2mm (plasma treatment 100w-30sec) are used.

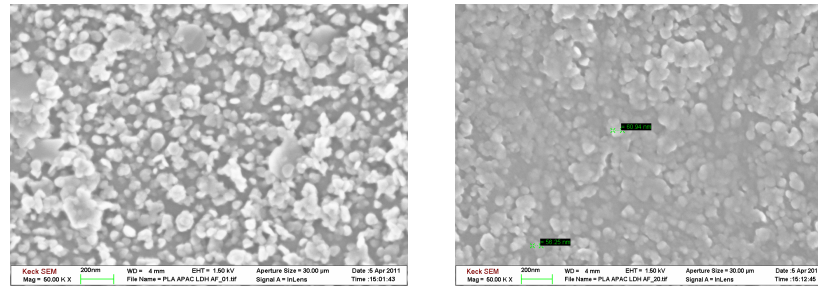


Figure VI.13 SEM images of PLA after coating with LDH nitrate filtered

After filtration, from SEM it was possible observe a better deposition and homogeneity of particles on PLA treated

VI.11.6 Water permeability

To evaluate the water permeability of PLA samples the following procedure was used:

Two PLA film of every samples are used to have an average of values. Area of film is of 0.003116m^2 , $\Delta P=1489\text{Pa}$ and 0.13 ± 0.03 mm of thickness.

The film has been left in a dryer on a saturated solution of $\text{Mg}(\text{NO}_3)_2$ ($a=0.53$).

The weight loss was reported in function of the time for sample PLA AP AC+LDHP1, reported as example of test. The permeability was expressed as $P= \text{g}/(\text{m}^*\text{s}*\text{Pa})$, following the formula (2):

$$\text{Permeability} = \frac{\text{Weight loss} \times \text{Thickness}}{\text{Time} \times \text{Film Area} \times \Delta \text{Vapor pressure}} \quad (2)$$

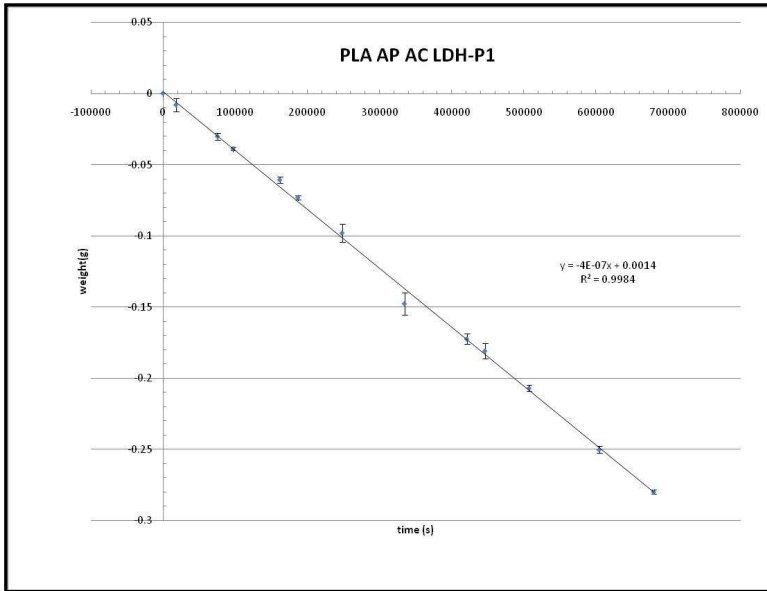


Figure VI.14 Weight loss in function of the time for sample PLA AP AC+LDHP1

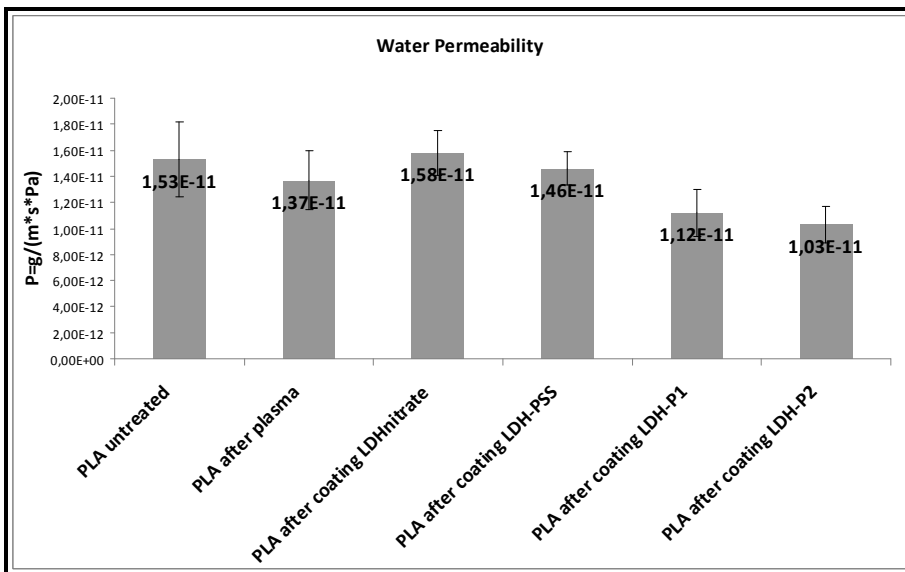


Figure VI.15 Water Permeability coefficients for PLA untreated, PLA AP and PLA after coating with different LDH

From water permeability test it was possible to note a decrease of value for all the film PLA AP AC+LDH especially for LDHP1 and LDHP2 (35%) to

demonstrate an increase of hydrophobicity of PLA surface, for the presence of anion of IL intercalated on LDH disperse on the coating, in accord with the changement of contact angle value.

VI.11.7 Thermal analysis

Thermogravimetric and DSC analysis are used to evaluate some variation of thermal properties of PLA film, coated with LDH nanoparticles modified with phosphonium ionic liquid.

Table VI.2 TGA of PLA and PLA coatings [30-800°C at 20°C/minute under nitrogen]

SAMPLE	Td(°C)
PLA	379.9
PLA AC+LDHP1	371.1
PLA AC+LDHP2	377.9

Table VI.3 DSC of PLA and PLA coatings [30-250°C at 10°C/minute under nitrogen]

SAMPLE	Tg(°C)	Tm(°C) (2 nd heating)
PLA	61.47	167
PLA AC+LDHP1	59.81	165.03
PLA AC+LDHP2	59.60	165.6

Observing the tables VI. 2 and VI. 3 about Tga and DSC analysis any important change was observed on thermal properties of coating.

VI.11.8 TEM

Are reported TEM images of LDHP1 and LDHP2 powders, to observe the real structure of lamellae.

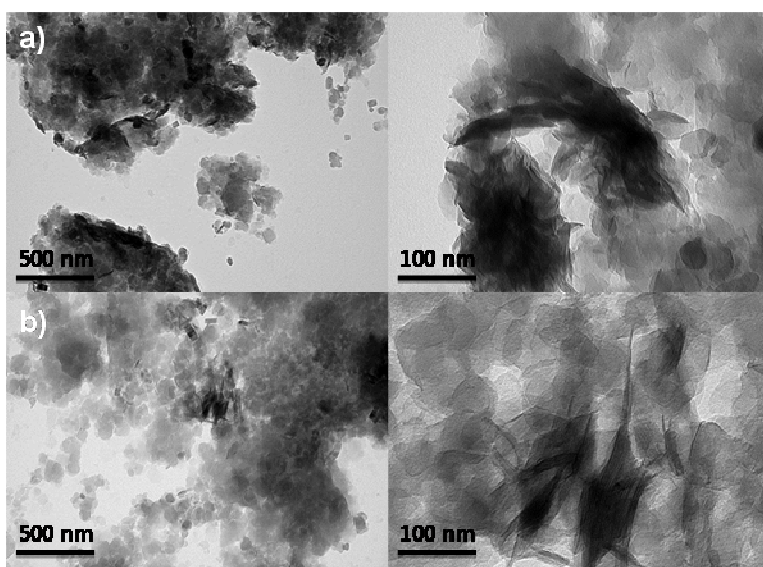


Figure VI.16 TEM images of LDH nanoparticles: (a) LDH-P1 (b) LDH-P2

Fig. VI.16 shows TEM micrographs of layered double hydroxides modified with different phosphonium ionic liquids. The morphologies obtained on LDH aggregates are quite similar. Nevertheless, in the case of LDH-P2, we were able to observe the interlayer space and using the software Image J, an interlayer distance of 3.2 nm has been determined on several agglomerates and confirms the results of X-Ray diffraction data.

Are reported TEM pictures of coating PLA+LDHP1 and LDHP2, to observe the effective thickness and homogeneity of deposition. (Ha et al, 2010; Zammarano et al, 2005).

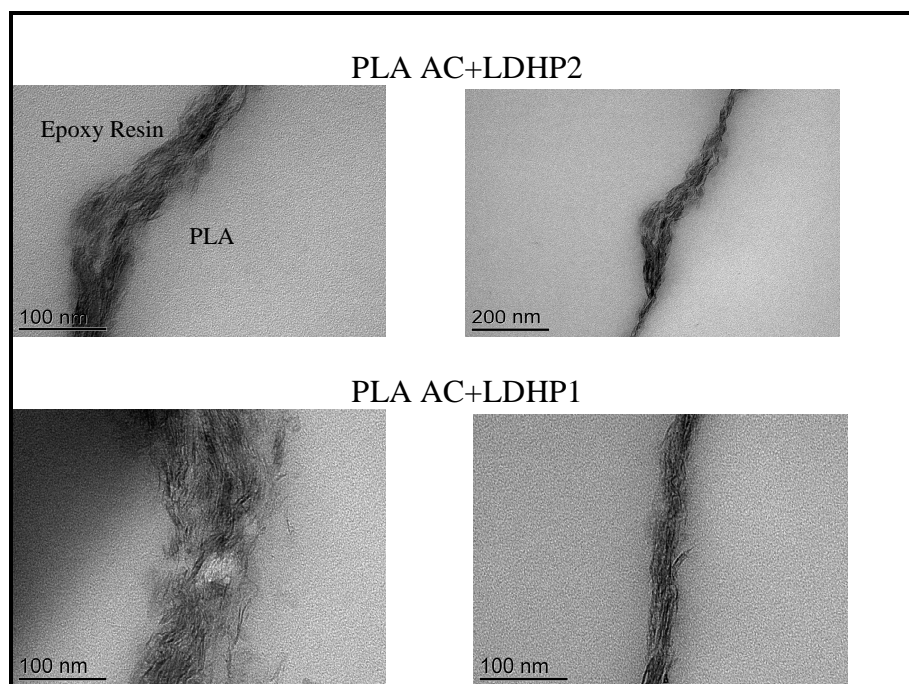


Figure VI.17 TEM images of the plasma treated PLA surfaces coated with a multilayer of LDH nanoparticles after a one-step deposition

It was possible to observe a complete and uniform coverage of polymer surface and a multilayer coating of nanoparticles of LDH on PLA surface. TEM pictures, shown in Figure VI.17, suggests a complete and uniform coverage along the periphery of the fiber. Cross-sectional TEM imaging indicates the formation of a multilayer coating.

Given that the nanoparticles do not show any tendency for agglomeration in solution, we believed that the multilayer coating consists of discrete nanoparticles and is not due to packing of larger aggregates

Chapter VII

Polylactic acid composites

VII.1 Materials preparation

The phosphonium salts used on PLA nanocomposites preparation are the same used for coating, as can be seen below:

- 1) IL 103: tetradecyl(trihexyl)phosphonium decanoate (P1)
- 2) IL 201: tetradecyl(tributyl)phosphonium dodecylsulfonate (P2)

Phosphonium ionic liquids intercalation on LDH was realized by ionic exchange from MgAl-nitrate and carbonate (AEC=3.35mmol/g) as described above. The PLA used for nanocomposites preparation is the same used for coating system.

The composites prepared are:

- PLA+2%LDH-carbonate
- PLA+2%LDH-nitrate
- PLA+2%LDH-IL103 from LDHnitrate and from LDHcarbonate
- PLA+2%LDH-IL201 from LDHnitrate and from LDHcarbonate

VII.2 PLA composites film preparation

PLA-composites preparation was realized by extrusion and injection molding:

The extrusion conditions were: 190°C for 3min at 100rpm, under nitrogen, using 20 g of PLA+2%LDH;

The Injection molding conditions were: T_{mold} of 60°C; T_{melting} of 206°C (Ahmed, 2010, Wilson, 1999, Jin Uk, 2010).

Nanocomposites based on PLA/organically modified layered double hydroxydes (2% by weight) were prepared under nitrogen atmosphere using a 15g-capacity DSM micro-extruder (Midi 2000 Heerlen, The Netherlands) with co-rotating screws. The mixture was sheared for about 3 min with a 100 rpm speed at 190°C and injected in a 10cm³ mould at 60°C to obtain dumbbell-shaped specimens

VII.3 Research outline

The phases of this part of research project were the following:

- X-ray diffraction analysis of PLA composites
- Thermogravimetric analysis of PLA composites
- DSC analysis of PLA composites
- Study of Mechanical properties of PLA composites
- Study of Barrier Properties: water permeability of PLA composites

VII.4 Characterization of PLA composites

VII.4.1 X-ray diffraction

From X-ray diffraction analysis it was possible to evaluate a delamination of structures for all the PLA composites, observing the disappearance of the characteristic peaks of LDH at low 2θ corresponding to the interlayer distance between lamellae.

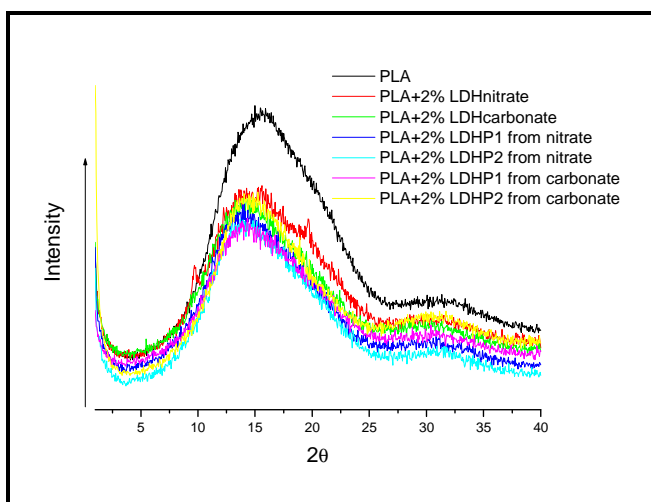


Figure VII.1 X-ray diffraction patterns of PLA composites

This occurred for all the PLA composites, except with LDH-nitrate that still showed the presence of characteristic peak at 10.2° of 2θ.

VII.4.2 Thermal analysis

To study the effect of phosphonium-modified layered double hydroxide (2 wt%) on the thermal stability of the nanocomposites, their thermal behavior was characterized by thermogravimetric analysis. Thus, the TGA results carried out on PLA and the PLA prepared with treated LDHs are presented in Table VII.1.

Table VII.1 Tga of PLA composites: [30-800°C at 20°C/minute under nitrogen]

SAMPLE	Td(°C)
PLA	379.9
PLA + 2% LDHNITRATE	354
PLA + 2% LDHCARBONATE	327
PLA + 2% LDHP1 FROM NITRATE	325
PLA + 2% LDHP2 FROM NITRATE	345
PLA + 2% LDHP1 FROM CARBONATE	331
PLA + 2% LDHP2 FROM CARBONATE	346

The polylactid acid polymer selected is already thermally stable as shown by its decomposition temperature of 380°C which corresponds to the values

found in the literature. In contrast, the addition of unmodified LDH or phosphonium modified-layered double hydroxide in the polymer matrix leads to a significant decrease in the thermal stability of PLA. In fact, the values of 354°C, 325°C and 345°C were determined for LDH-NO₃, LDH-P1 and LDH-P2 from nitrate, respectively. According to the literature, this decrease in the degradation temperature of PLA/LDH nanocomposites can be attributed to the low thermal stability of the dodecylsulphonate and decanoate anions, particularly in regard to the decanoate anion where a more pronounced catalytic effect is observed. However, another possible cause may be the presence of small amount of water contained in the LDH layers generating an acceleration of polymer decomposition. Indeed, this hypothesis has been confirmed in numerous studies.

In conclusion, the use of LDH modified with phosphonium ionic liquids induces a decrease in the thermal stability of nanocomposites in contrast to the results observed upon addition of ionic liquids treated-montmorillonites in various polymer matrices such as polyolefins. Nevertheless, the increase in thermal properties of PLA/LDH nanocomposites is possible: In fact, the drying of LDHs at high temperatures to remove water or the use of ionic liquids with heat-stable anions such as fluorinated anions, known to increase the intrinsic thermal stability of ILs are possible solutions (Zhou et al, 2008; Park et al, 2009; Fan et al, 2004).

Table VII.2 DSC of PLA composites: [30-250°C at 10°C/minute under nitrogen]

SAMPLE	Tg(°C)	Tm(°C) (2 ND heating)
PLA	61.47	167
PLA+2%LDHNITRATE	60.93	166.3
PLA+2%LDHCARBONATE	61.25	160.68
PLA+2%LDHP1 FROM NITRATE	58.61	159.41
PLA+2%LDHP1 FROM NITRATE	58.59	161.58
PLA+2%LDHP1 FROM CARBONATE	60.34	163.94
PLA+2%LDHP1 FROM CARBONATE	59.30	161.59

The DSC analysis didn't show any important change on the properties of composites in comparison with PLA. The glass transition and melting temperature decreased very slightly

VII.4.3 Mechanical properties

The analysis of data on stress-strain curves are reported for all the PLA composites and were determined elastic modulus, the tensile strength and tensile strain.

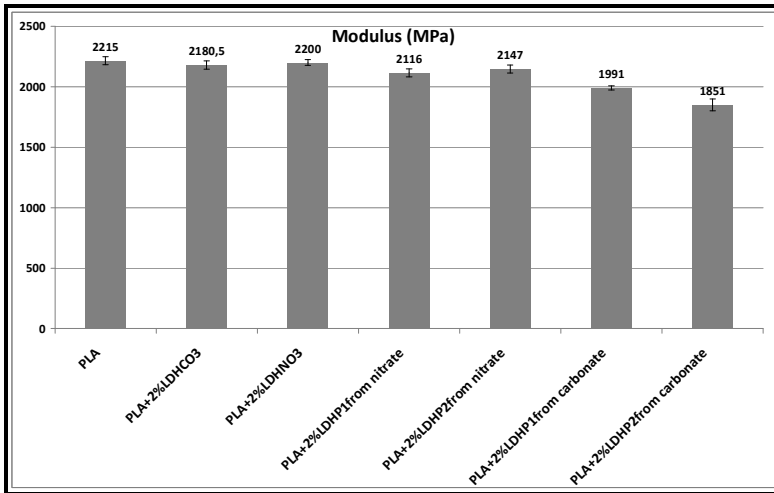


Figure VII.2 Elastic Modulus of PLA composites

About the elastic modulus analysis, there was a decrease of values for all the composites, especially for PLA+2%LDHP1 and P2 from LDHcarbonate, due to the presence of phosphonium ionic salts on PLA, acting as plasticizer.

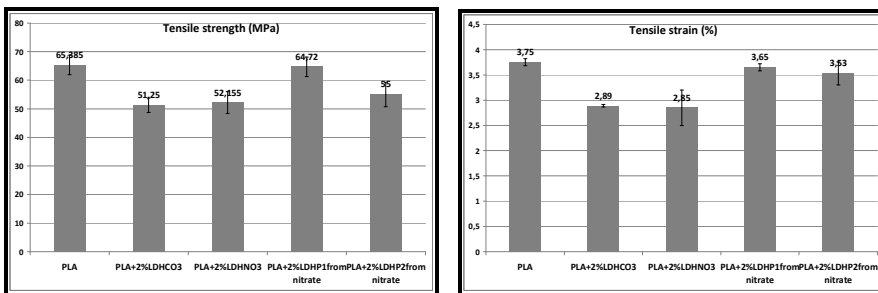


Figure VII.3 Tensile strength and Tensile strain of PLA composites

The tensile strength and strain for the composites prepared with LDHP1 and P2 from LDH-nitrate didn't show any important improvement but for the composites with LDHP1 and P2 from LDHcarbonate there was a very big improvement of properties. (Broz et al, 2003)

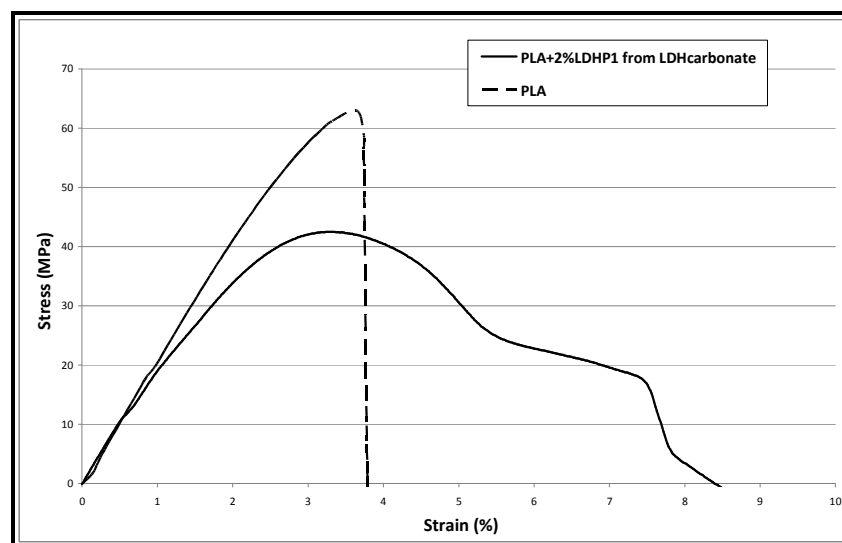


Figure VII.4 Stress-strain curve for PLA+2%LDHP1 composite

The stress-strain curve of PLA+2%LDHP1 from LDHcarbonate is reported as example, to show the effect of the presence of ILs on PLA as plasticizer (Martin et al, 2001).

In fact the value of tensile strain (%) for these samples is very increased (about 7.5%) in comparison with other composites and with PLA (about 4%). An increase in strain at break of 30% is obtained. This result can be explained by the effects of ILs (onto the surface of LDHs) on the crystallinity of the PLA matrix where it plays a role already described in the literature of plasticizer agent.

In the area of nanocomposites, the addition of 2 to 5% of ionic liquids modified-montmorillonites usually leads to significant increases in stiffness, but coupled with a significant decrease in strain at break while the ILs treated-LDH does not change the Young's modulus and generates a plasticizing effect of the polymer matrix (Scott et al, 2010; Giannelis et al, 1996; Schmidt et al, 2002).

VII.4.4 Barrier properties: water permeability

To evaluate the water permeability of PLA composites the following procedure was used:

Two films of every sample are used to have an average of values. The film has been left in a dryer on a saturated solution of $Mg(NO_3)_2$ ($a=0.53$). Area of film= $0.003116m^2$; $\Delta P=1489Pa$. 0.13 ± 0.03 mm of thickness; The weight loss was reported in function of the time as showed above.

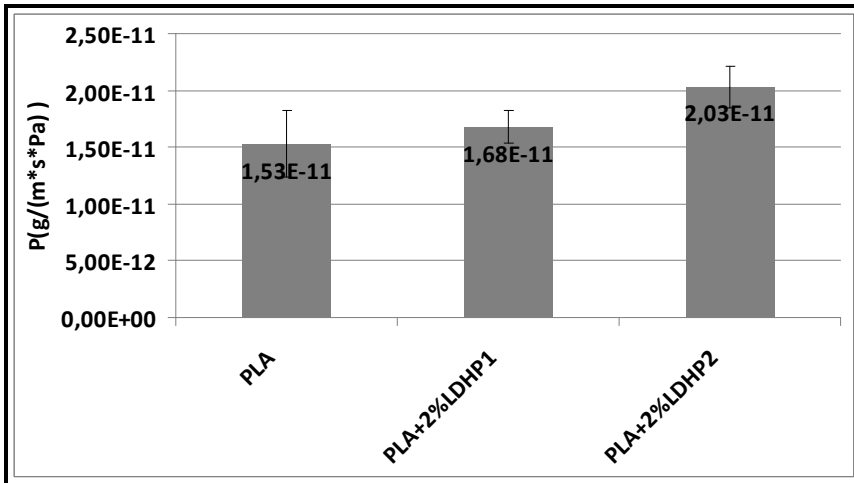


Figure VII.5 Water Permeability for PLA composites

The water permeability test reported the following results:

- PLA untreated: $P = 1.53 \pm 0.29 \cdot 10^{-11} \text{ g/(m*s*Pa)}$
- PLA+2% LDH-P1 composite: $P = 1.68 \pm 0.14 \cdot 10^{-11} \text{ g/(m*s*Pa)}$
- PLA+2% LDH-P2 composite: $P = 2.03 \pm 0.18 \cdot 10^{-11} \text{ g/(m*s*Pa)}$

The test didn't show any important improvement of water permeability for all the PLA composites, like in the case of the PLA coating system.

VII.4.5 Morphology of PLA/LDH nanocomposites

The distribution and dispersion of layered hydroxides in polylactid acid matrix were analyzed by transmission electron microscopy on the nanocomposites processed with 2%wt of phosphonium -modified LDHs. TEM images are reported in Figure VII.6.

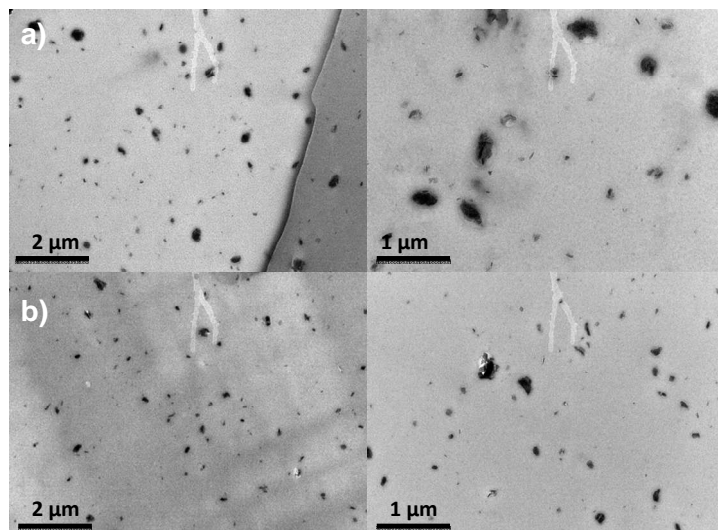


Figure VII.6 TEM images of (a) PLA/LDH-P1, (b) PLA/LDH-P2

The phosphonium-treated layered double hydroxides are usually well distributed in the form of isolated layers, despite the presence of small tactoids. However, differences exist depending on the alkyl chains length attached to anion. In fact, LDH-P2 is the modified layered hydroxide which displays the better dispersion in the PLA matrix. This result can be explained by the long alkyl chains (C12) which has increased the hydrophobicity of the LDH leading to a better compatibility between polymer matrix and anionic clay surface. Compared to the literature where the *in situ* polymerization is the most common method to generate quasi-exfoliated structures, we have shown that the melt intercalation also leads to an excellent dispersion of LDH layers in the PLA matrix (Berti et al, 2009; Czaun et al, 2008)

Chapter VIII

Pectin composites

VIII.1 Objectives

Nanohybrids of Layered Double Hydroxide (LDH) with intercalated active molecules such as Benzoate, 2,4-dichlorobenzoate, para-hydroxybenzoate and ortho-hydroxybenzoate, were incorporated into natural pectins *via* high energy ball milling in presence of water. Cast films were obtained and analysed.

X-ray diffraction analysis showed a complete destructurement of all nanohybrids into pectin matrix. Thermogravimetric analysis showed a better thermal resistance of pectin in presence of fillers. Mechanical and barrier properties showed an improvement in dependence on the intercalated active molecule. Active molecules showed antimicrobial properties into the composite films enlightening very good perspectives in the field of active packaging.

VIII.2 Composites and film preparation

Samples based on pectin and hydrotalcite (LDH) (vacuum dried for 24hrs) at 5% (w/w), were prepared by dissolving the powder of pectin and hydrotalcite modified with active molecules, in weight ratio 95:5 (pectin: LDH), in 30ml of distilled water and left stirring at 50 ° C for 15 minutes.

Nano-hybrids LDHs-Active molecules, the pectin powders and water, were milled at room temperature in a Retsch (Germany) centrifugal ball milling (model S 100). The powders were milled in a cylindrical steel jar of 50 cm³ with 5 steel balls of 10 mm of diameter. The rotation speed used was 580 r.p.m. and the milling time was 1 hour.

The mixtures obtained were made to evaporate slowly in culture dishes. The films of pectin alone were obtained by evaporating the solution quickly. The films were then dried in a vacuum oven at room temperature for 5 days.

VIII.3 Results and discussion

VIII.3.1 X-ray analysis

X-ray analysis, conducted on all nano-hybrids, showed a basal peak for Bz at $2\theta=5.7^\circ$ for DCBz at $2\theta=5.17$ for o-OHBz at $2\theta=5.68$ and for p-OHBz at $2\theta=5.7^\circ$ (Costantino et al, 2009). Figure VIII.1 showed the x-ray diffraction patterns of: (a) Pectin, (b) Pectin/LDH-Bz, (c) Pectin/LDH-DCBz, (d) Pectin/LDH-o-OHBz, (e) Pectin/LDH-p-OHBz. Pattern of film of pure pectin presented a broad peak located at about 13° of 2θ . Such structure is retained in all the composites.

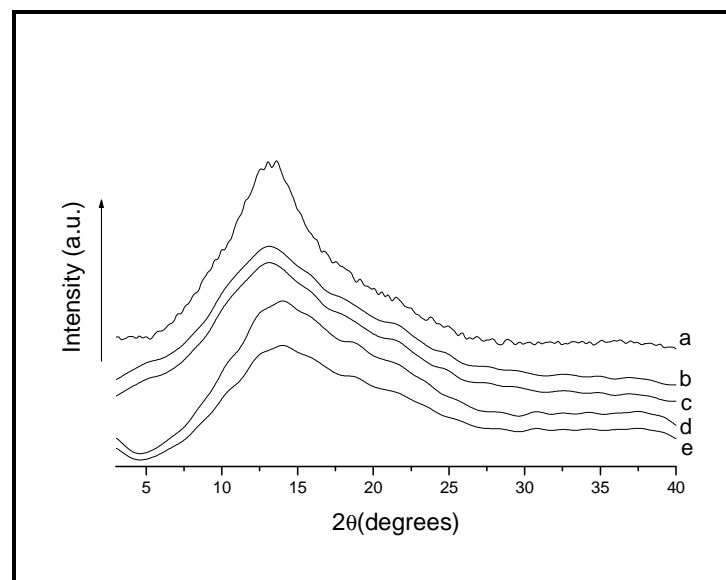


Figure VIII.1 X-ray diffraction pattern of (a) Pectin, (b) Pectin/LDH-Bz, (c) Pectin/LDH-DCBz, (d) Pectin/LDH-o-OHBz, (e) Pectin/LDH-p-OHBz

The absence of any other diffraction peak in the composites induces to affirm that, in the used milling conditions, complete delamination of LDH layers was reached for the four nanohybrids.

VIII.3.2 Thermogravimetric analysis (TGA)

Thermogravimetric analysis was performed, in air flow, on all the nanocomposites, as reported in figure VIII.2. The aim was to determine both the content of the inorganic component in the composites and the degradation temperatures. Pure pectin was also submitted to TGA test. The thermal degradation of pectin is a rather complex subject, depending on composition, molecular parameters and chemical modification (Einhorn-Stoll et al, 2009a and 2009b). Pure pectin presents a characteristic three-step thermal degradation: the first one, occurring at about 80°C, corresponds to the water loss and can be evaluated as 10% of the initial mass; then, it is followed by the second step, between 200 and 400 °C. In this temperature range, it has been reported that the degradation, covering about 60% of mass loss, is primarily derived from pyrolytic decomposition. It consists in a primary and secondary decarboxylation. The third step between 500 and 700°C corresponds to the oxidation region. In the nanocomposites we observed that the first step is slightly anticipated and reduced. This could be an indication that the composite samples have a lower amount of absorbed water in the same storage conditions as pure pectin, such water seems to be less bonded to the polymer. The second (after about 250°C) and the third degradation steps appear delayed in all the composites.

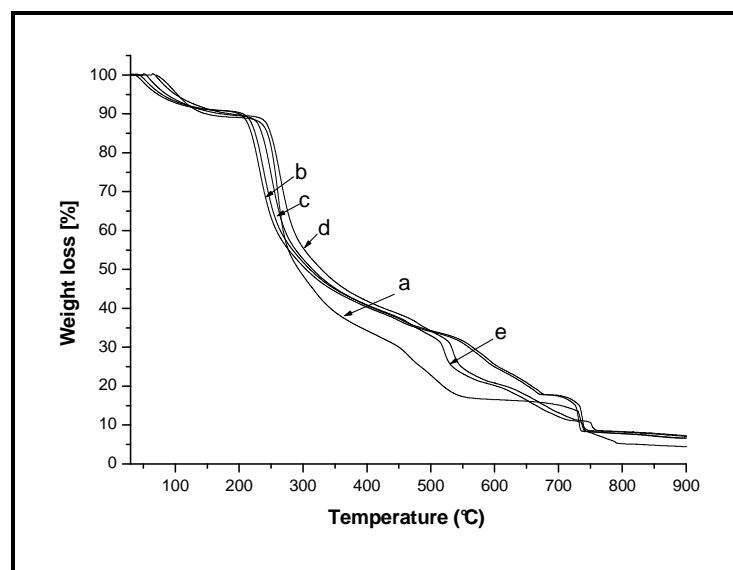


Figure VIII.2 TGA analysis of (a) Pectin, (b) Pectin/LDH-Bz, (c) Pectin/LDH-DCBz, (d) Pectin/LDH-o-OHBz, (e) Pectin/LDH-p-OHBz

The presence of the nanohybrids helps the pectin to degrade at higher temperatures. Table VIII.1 reports the degradation temperature at 50% of weight loss for all samples.

Table VIII.1 Degradation temperature ($^{\circ}\text{C}$) evaluated at 50% of weight loss from TGA

Sample	Td ($^{\circ}\text{C}$)
Pectin	293
Pectin/LDHBz	305
Pectin/LDH-DCBz	310
Pectin/LDH-p-OHBz	314
Pectin/LDH-o-OHBz	328

This behaviour is consistent with a protecting effect of LDHs increasing the thermal stability of the biopolymer.

VIII.3.3 Mechanical properties

The elastic modulus, E (MPa), of the milled pectin, and the pectin-nanohybrid composites are compared in Figure VIII.3. In general, the tensile modulus of a polymeric material has been shown to be remarkably improved when nanocomposites are formed with layered silicates. In the case of milled

samples, considering that the mechanical degradation of the chains backbone, due to the milling action, can be assumed equal for the five samples, we can observe the effect of the LDH-hybrids into the pectin matrix. It is evident an increasing of E (MPa) in all the nanocomposites. The higher value of elastic modulus is reached for nanohybrid having p-OHBz as active molecule. More likely, for the pectin nanocomposites, the extent of the improvement of the modulus does not depend only upon the degree of exfoliation, but from the interaction with the host molecule.

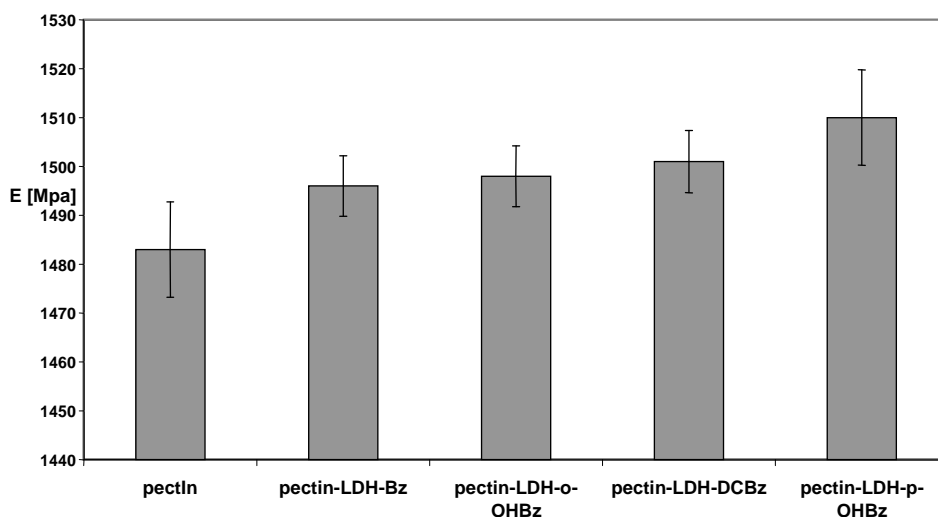


Figure VIII.3 Elastic moduli evaluated on pure pectin and nano composite films

The higher modulus exhibited from composites with LDH/p-OHBz filler could be attributed to the stronger interactions between pectin matrix and nanohybrid layers via formation of hydrogen bonds, better favoured by the p-OHBz molecule.

VIII.3.4 *Transport properties of water vapour*

Inorganic fillers are believed to increase the barrier properties by creating a more “tortuous path” that retards the progress of the small molecules through the polymeric matrix. The direct benefit of the formation of such a path is clearly observed in all the prepared nanocomposites by dramatically improved barrier properties (Gorrasi et al, 2003). The mean diffusion

coefficient from the linear part of the reduced sorption curve, is reported as C_t/C_{eq} versus square root of time (Vieth et al, 1974).

Figure VIII.4 reports the sorption isotherms of the composites with the different nano-hybrids in the range of vapour activity (P/P_0) between 0.2–0.6. For comparison the curve of pure pectin is also displayed. The sorption curve of the pure pectin follows the classical dual sorption behaviour: at low activity (up to $a = 0.2$), a rapid increase in vapour concentration, followed by a linear dependence indicates that besides the normal dissolution process the sorption of the polar solvent occurs on preferential sites, in which the molecules are adsorbed and/or immobilized. It is generally assumed that these specific sites on the matrix have a finite capacity. When the preferential sites are occupied, the isotherm becomes linear because of the normal vapour dissolution. At higher activities, the presence of water molecules determines the plasticization of the matrix, and we observe a transition in the curve, followed by an exponential increase in vapour concentration. The isotherms of the composites follow the same trend as pectin, although showing a higher water uptake in the whole investigated activity range. This behaviour is strictly related to the hydrophilicity of the inorganic lamellae, and determines a significant dependence of water sorption on the LDH content. The plasticization effect of water, above activity 0.4 is evident, according to Flory-Huggins mode of sorption. According to such mode of sorption there is preference for the formation of penetrant-penetrant pairs, so that the solubility coefficient continuously increases with activity. The first molecules sorbed tend to locally loose the polymer structure and make it easier for the following molecules to enter. These isotherms are observed when the penetrant effectively plasticizes the polymer, being a strong solvent or swelling agent for the polymer. The isotherms of the nanocomposites with the benzoate derivative active molecules behave in a similar way. Table VIII.2 reports the equilibrium concentration of water vapour C_{eq} ($g_{solvent}/100g_{polymer}$) at activity 0.2 for all the analyzed samples. Values for composites filled with LDH-Bz and LDH-DC-Bz and are significantly higher than the pure pectin, this is due to the high hydrophilic nature of hydrotalcites and to the fact that the mechanism of sorption, particular at low activity, is mainly influenced by the availability of the hydrophilic sites to the water molecules. Sorption at $a=0.2$ for LDH-o-OHBz is slightly higher than the pure pectin, and the same of the pure pectin for the sample filled with LDH-p-OHBz. Such trend is shown in all the investigated activity range. These results indicate a better interaction between active molecules having -OH groups and pectin matrix (in terms of hydrogen bonds), that reduce the availability of hydrophilic sites to water molecules.

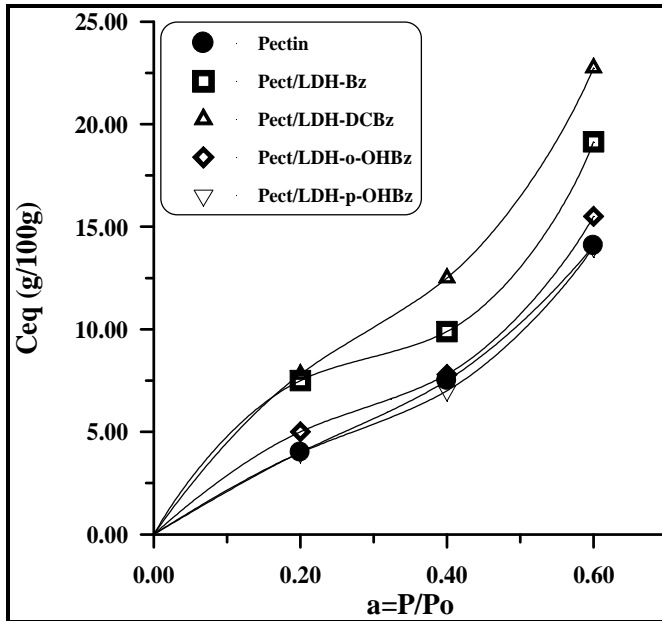


Figure VIII.4 Sorption isotherms of water vapour of pure pectin and composites with different nanohybrids

Figure VIII.5 reports the diffusion coefficients, $D(\text{cm}^2/\text{s})$, as function of C_{eq} (g/100g) of sorbed water for all samples. We observe a linear dependence of diffusion on concentration for all the samples, that allowed us to extrapolate to zero vapour concentration and obtain the thermodynamic diffusion coefficient, D_0 . All the samples follow the same behaviour, so it was possible to derive the D_0 . The numerical values of $D_0(\text{cm}^2/\text{s})$ are listed in Table VIII. 2. They tend to decrease with LDH-hybrids, reaching the minimum value for sample Pectin/LDH-p-OHBz. As already discussed, not only the amount of filler and degree of dispersion, but also the interaction of the continuous polymer phase has an important influence also on the kinetic parameter.

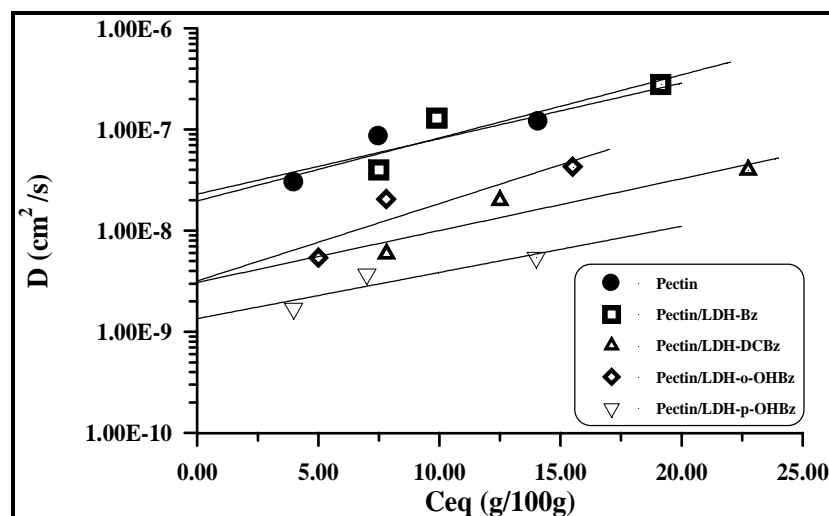


Figure VIII.5 Diffusion coefficients of water vapour as function of C_{eq} (g/100g) for pure pectin and composites with different nanohybrids

Table VIII.2 Transport parameters extracted from the curves of Figures VIII.4 and VIII. 5

Sample	C_{eq} (g/100g) at $a=0.2$	D_0 (cm^2/s)
Pectin	4.00	2.30×10^{-8}
Pectin/LDH-Bz	7.50	1.97×10^{-8}
Pectin/LDH-DCBz	7.81	3.10×10^{-9}
Pectin/LDH-o-OHBz	5.00	3.20×10^{-9}
Pectin/LDH-p-OHBz	3.98	1.35×10^{-9}

VIII.3.5 Antimicrobial behaviour

Figure VIII.6 shows pictures taken on pectin and nanocomposite films after 12 months of storage at room temperature and environmental humidity (about 60%). We observed the formation of mold on pectin film, soon after 2 weeks of storage in the described environmental conditions. Samples with nanohybrids containing active molecules, showed no appearance of any mold for so long period of storage.

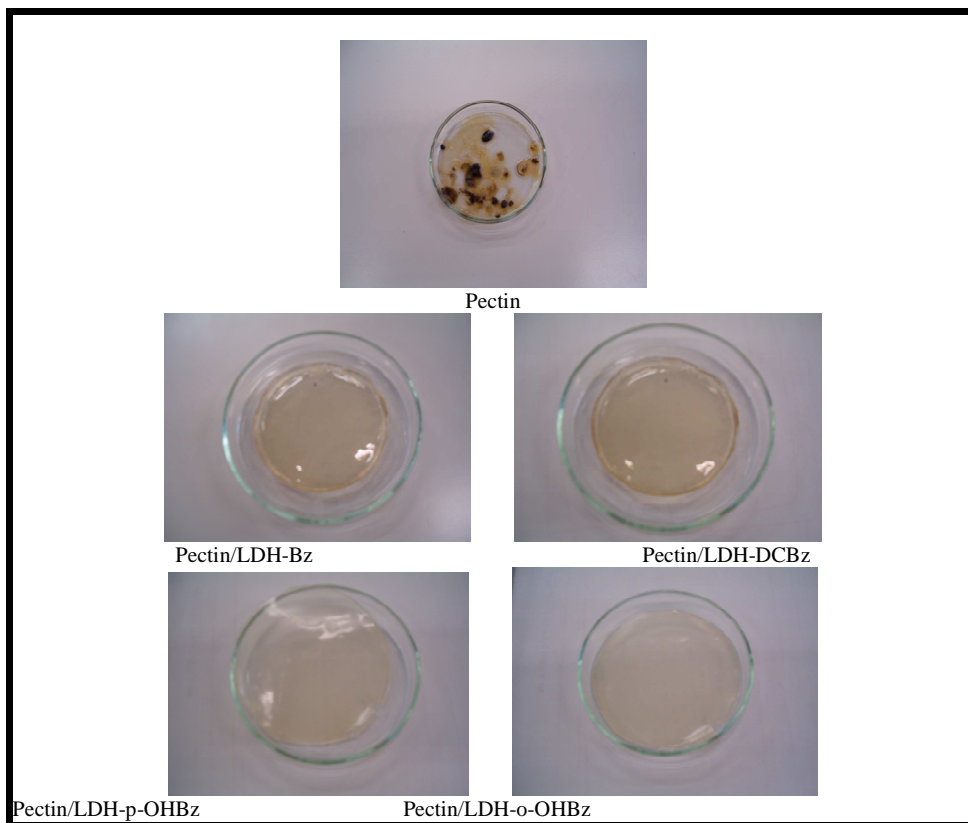


Figure VIII.6 Pictures from cast film of pectin and composites with nano hybrids after storage 12 months at ambient temperature

This is an important indication of the antimicrobial activity of the intercalated molecules.

Chapter IX

Methods of investigation

IX.1 High Energy Ball Milling (HEBM)

The incorporation of the inorganic compounds into polymeric matrices was achieved by High Energy Ball Milling method, following this procedure: powders composed of polymer and of LDHs modified with organic anions (vacuum dried for 24hrs) were milled in different percentages (wt/wt), at room temperature in a Retsch (Germany) centrifugal ball mill (model S 100). The powders were milled in a cylindrical steel jar of 50 cm³ with 5 steel balls of 10 mm of diameter. The rotation speed used was 580 r.p.m. and the milling time was 1 hour.

The Mixer used in this PhD thesis is a planetary mill, whose name describes the movement performed by the sample holder. The grinding jar, placed in an eccentric position on the main wheel of the mill, moves in the opposite direction to the direction of rotation of the wheel. The balls inside the jars are subjected to strong rotational movements called Coriolis forces. The combined action of these forces produces the high degree of refinement achieved by this type of mills.

IX.2 Twin screw extruder mini lab Haake

The twin-screw extruder used has conical screws converging, which, through their rotation, allow to molten material to move in a recirculating chamber, for a time t spent by the operator, and then, with the opening of an escape valve, it obtains small amounts of material in the form of "*spaghetti*" (7 cm^3 of polymer equivalent to 5g). The power of the material is supported by a twin-screw piston that reaches high pressure, which allows a more efficient compaction of the material inserted through a small hopper.

IX.3 X-ray powder diffraction (XRPD)

The X-ray diffraction measurements were made at room temperature with a powder diffractometer "bruker d8 advance", interfaced to a pc with software "diffrac-plus 2000 release" for data acquisition. The monochromatic radiation used was Cu $k\alpha$ of which has a wavelength $\lambda = 1.540619 \text{ \AA}$. The diffraction spectrum, which shows the intensity of scattering as a function of the diffraction angle 2θ , was performed with a scanning speed of 0.02 degrees per second.

IX.4 Thermogravimetric analysis (TGA)

The thermogravimetric analysis of samples were conducted in air with a Mettler TC 10 instrument interfaced to a PC with software for data acquisition Mettler, performing scans from 30 to 800 ° C with scan rate of 5 ° C / min.

IX.5 Differential scanning calorimetry (DSC)

The thermal analysis were carried out with a differential calorimeter Mettler Toledo (DSC 822). The differential scanning calorimetry is used to study what happens to polymers when subjected to heat treatment and especially the structural changes that occur during these treatments. The experimental data is reported as the difference between the heat capacity of the cell sample and that of the reference cell as a function of temperature.

IX.6 Infrared spectroscopy (FT-IR)

The infrared spectroscopy were carried out using a spectrophotometer Perkin Elmer 1600. Spectra are obtained with a resolution of 2 cm^{-1} collecting 32 scans per sample. The region of the spectrum was investigated between 500

and 4000 cm^{-1} and is registered in absorbance. This allows to directly obtain the spectrophotometer absorbance as a function of wave number.

IX.7 Ultraviolet spectrophotometry (UV)

UV-Visible spectrophotometry was used to quantify the percentage of organic molecule in the solution. In particular, UV-Visible spectrophotometry analyzes the selective absorption of molecules by radiation with a wavelength between 380 nm and 780 nm. This type of absorption involves the excitation of valence electrons, which requires much higher energies the larger the distance between the electronic levels of departure and to reach.

IX.8 Mechanical properties

The tool used to study the mechanical properties of the film was a dynamometer Instron 4301 equipped with a room temperature Instron 3119. The instrument is interfaced to a PC with a software "Series IX" for data acquisition. The machine has two terminals one of which is fixed and the other mobile which sets the standard so that the distance between terminals is 1 cm. The elastic modulus was evaluated at room temperature at a rate of 2 mm / min. Subsequently, on the same sample, was made a tensile test to failure at a constant speed equal to 10mm/min.

We analyzed the mechanical properties of nanocomposite materials by analyzing the stress-strain curves were determined and tensile module, the breaking strength and Elongation at break. The tensile test consists of subjecting a specimen to a deformation of a film at a constant speed by measuring the value of the load and the length of the specimen.

IX.9 Water vapor barrier properties

Transport properties of small molecules through polymeric nanocomposites is associated to the type and degree of dispersion of the inorganic filler. Indeed solubility and diffusivity can be simultaneously modified by the presence of the crystalline phase, by molecular orientation and by the presence of inorganic fillers. Inorganic fillers are believed to increase the barrier properties by creating a more "tortuous path" that retards the progress of the small molecules through the polymeric matrix.

Measuring the increase of weight with time, for the samples exposed to the vapor at a given partial pressure, it is possible to obtain the equilibrium value of sorbed vapor, $C_{eq}(g_{solvent}/100g_{polymer})$. Moreover, in the case of Fickian behaviour, that is a linear dependence of sorption on square root of time, it is

possible to derive the mean diffusion coefficient from the linear part of the reduced sorption curve, reported as C_t/C_{eq} vs square root of time, by the Equation (3):

$$\frac{C_t}{C_{eq}} = \frac{4}{d} \left(\frac{Dt}{\pi} \right)^{1/2} \quad (3)$$

where C_t is the penetrant concentration at the time t , C_{eq} the equilibrium value, d (cm) the thickness of the sample and D (cm^2/s) the average diffusion coefficient. All the samples showed a Fickian behaviour during the sorption of water vapor at different activities. Using Equation (1) it was possible to derive the coefficient, D , at every fixed vapor activity ($a=P/P_0$), and the equilibrium concentration of solvent into the sample $C_{eq}(\text{g}_{\text{solvent}}/100\text{g}_{\text{polymer}})$. For polymer-solvent systems, the diffusion parameter is usually not constant, but depends on the vapor concentration, according to the empirical equation:

$$D = D_0 \exp(\gamma C_{eq}) \quad (4)$$

where $D_0(\text{cm}^2/\text{s})$ is the zero concentration diffusion coefficient (related to the fractional free volume and to the microstructure of the polymer); γ is a coefficient, which depends on the fractional free volume and on the effectiveness of the penetrant to plasticize the matrix.

IX.10 Oxygen transport properties

It is possible to determine the transport parameters from a single experiment using the microgravimetric technique through the use of an experimental device (IGA, Intelligent Gravimetric Analyser 002, Hiden Isochema Ltd, Warrington, UK) on a microbalance principle of which is able to appreciate changes by weight of the order of 10⁻⁶ g.

The sample is suspended from a tungsten wire and placed in a closed reactor, connected to a vacuum pump and gas cylinder. After the pump has created a vacuum (<10 mbar) for 24 h, in experiments carried out by us, gas is introduced at a defined pressure and weight gain of the sample, due to absorption of the gas is followed in time with the analysis of a specific software. The unit of the solubility coefficient S ($\text{cc}_{\text{(STP)}} / \text{cm}^3 \cdot \text{atm}$) were obtained and knowing that this coefficient is equal to:

$$\frac{C_{eq} * \rho * V_{\text{molare}}}{PM(O_2) * \text{atm}} \quad (5)$$

where ρ is the density of the sample, V is the molar volume at standard conditions of temperature and pressure (STP) and PM is the molecular weight of the 'oxygen. Proceeding with the appropriate simplifications we obtain that:

$$S = \frac{V_{O_2}(STP)}{V_{Campione} * atm} \quad (6)$$

We report in diagram, the relationship between $C(t) / C(Eq)$ as a function of the square root of time. If the input gas into the material is of Fickian type will provide a first from the linear slope which can be derived, known thickness of the sample, the relationship between the diffusion coefficient and activity coefficient of steam or similar distribution and concentration of gas absorbed

IX. 11 Elemental analysis

The elemental chemical analysis was carried out at the Department of Chemistry of University of Salerno. The amount of Zn and Al was calculated by atomic absorption after dissolving the samples in nitric acid concentrated, using a Analyst 100 (Perkin Elmer). The amount of C, H and N was determined in a Flash EA 1112 (Thermo)

IX.12 Antimicrobial test

The tests were performed with the *Escherichia coli* (dsm30083t) gram negative bacterium. It usually turns out to be the bacterium most commonly used tests in the tests of antimicrobial activities described in scientific literature.

Generic liquid medium (TSB) containing the bacterial suspension of *E. Coli* at a concentration of 102 CFU / ml is placed in contact with each film. Incubation at 37 ° c for 24 hours. Films were prepared 2x2cm squares and placed in sterile tubes containing 10ml of tsb medium (bd tryptis soy broth) +100 μ l of a fresh suspension (overnight) of *E. Coli*. The tubes were incubated at room temperature (about 25 ° C). The sowing took place in the plate according to the technique of dilutions that includes the following steps: the sample was diluted in the examination of 10^{-1} , 10^{-2} , 10^{-3} , diluting 1 ml of sample to 10ml (then adding 9 ml of solution saline), then diluting 1

ml of the latter back to this again and finally 10ml to 10ml. The 3 dilutions were added to the soil and then placed at 37 ° C for 24h.

IX.13 Contact angle

Static and dynamic advancing contact angle measurements were carried out by means of a VCA Optima XE apparatus. The water droplets (deionized water from Millipore purification system, specific conductance 0.05 mS cm⁻¹, pH 5.5, droplet volume 0.5 mL) were monitored by a CCD camera and analyzed by standard drop-shape analysis methods.

VCA Optima Contact Angle: The VCA is able to measure the water contact angle on wafer surfaces up to 6 inch in diameter. It is a useful metrology tool for measuring the quality of surface treatments put down in the Applied Microstructures MVD100 tool.

IX.14 Plasma

The Glen 1000 system utilizes a oxygen plasma source for stripping of photoresist and other organics. The tool can be setup to give direct ion bombardment or in a downstream ion mode for lower surface damage.

The substrate was treated with Ar-O₂ (50 : 50) mixed gas plasma under 100 W for 30sec.

IX.15 X-ray photoelectron spectroscopy surface science instrument SSX-100 (XPS)

UHV system for X-ray photoelectron spectroscopy (XPS), also known as electron spectroscopy for chemical analysis (ESCA). Quantitative elemental analysis as well as chemical bonding information are possible on a variety of samples (films, polymers, ceramics, powders, etc.). Ion sputtering for depth profiling or contaminant removal; in-situ sample tilting. Remote access is available for real-time observation and control of the instrument.

IX.16 Leo 1550 FESEM (SEM)

SEM measurements were performed on a Keck Field Emission Scanning Electron Microscope (FE-SEM), LEO 1550 model.

Imaging at very high resolution (1 nm at 20 KeV and 2.5 nm at 5 KeV) is possible with certain types of specimens. Its superb performance, particularly at low accelerating voltages (i.e. 0.5 to 3 KV), makes it especially suitable for imaging the surface detail of polymeric, biological, and other low-density materials. Secondary Electron Imaging An in-lens

secondary electron detector enables a very short working distance and responds to the lowest voltage secondary electrons..

IX.17 FEI T12 TWIN (TEM)

TEM imaging was performed on FEI Tecnai T12 field emission electron microscope with an accelerating voltage of 80 kV. using microtomed epoxy-embedded ultrathin samples. This state-of-the-art equipment has 20-120kV high voltage and lanthanum-hexaboride(LaB6) thermoionic gun. It offers high performance, versatility, high productivity and ease of operation. The fully motorized eucentric goniometer stage (CompuStage®) can be tilted to $\pm 80^\circ$. The unit is also equipped with a high resolution, thermoelectrically (TE) cooled Gatan Orius® dual-scan CCD camera. It acquires 4008x2672 digital images, using Digital Micrograph(DM) software.

Transmission Electron Imaging TEM grids may be used in a special stage in conjunction with a detector below the specimen to obtain transmitted electron images

The samples were cut using an ultramicrotome equipped with a diamond knife to obtain 60 nm thick ultrathin sections. Then, the sections were set on copper grids.

Conclusion

With this PhD thesis were tested two techniques of dispersion of active inorganic fillers in polymer matrices, generating:

- 1) polymeric nanocomposites and
- 2) coatings of polymeric surfaces in order to realize systems with:
 - a) improved barrier properties to gases and vapors, and
 - b) active delivery system for food packaging, to increase the shelf life of foods. To this end was done a screening of different polymers from biodegradable to thermoplastic and natural, up to compare the effect of active fillers and the dispersion technique on the properties mentioned above.

1) Lamellar inorganic filler (LDH) modified with active molecules (antioxidants and antimicrobials) were prepared using two different synthesis methods (co-precipitation method and urea method), characterized and compared: the preparation by co-precipitation was found to be fastest, most versatile and applicable in industry and the reaction products showed a crystalline structure less ordered and which was shown to influence various properties of composites;

2) The modified fillers with antimicrobial molecules (benzoates and derivatives) were incorporated into polymeric matrices of polycaprolactone (PCL) with the innovative technique of High Energy Ball Milling (HEBM) in order to make composites materials:

- water barrier properties have been investigated: the diffusion was influenced by the very structure of the active molecule intercalated in the filler that has different behavior at the structural level so the type of dispersion (exfoliation and / or partial exfoliation) of the inorganic component in the polymer phase is important for improving the barrier properties of the samples.

- the kinetics of release of active molecules anchored to the hydrotalcite synthesized with 2 different methods and dispersed in the matrix of PCL, have been studied: these composites are possible candidates for application in the field of biodegradable food packaging since the release of the active molecule anchored to the inorganic filler and dispersed in polymeric packaging was slower and more controlled than directly dispersed in the polymer and a different method of synthesis of the filler can modulate the release to make it suitable to the needs of food preservation.

3) The fillers modified with organic molecules (antioxidant and antimicrobial) were incorporated into polymer matrices of polyethyleneterephthalate (PET) with the technique of ball milling (HEBM) in order to make composites materials and characterized;

- oxygen barrier were studied: selected filler with hydroxyl groups in the structure, to simulate the multilayer film of EVOH, as well as composites made all showed a small decrease in permeability to oxygen, especially with the filler having hydroxyl groups on aromatic rings;

- were studied antimicrobial properties of the films and the release of the antimicrobial compound: the release from PET was too slow in the early hours to inhibit bacterial growth of E. Coli tested, thus giving antimicrobial testing negative in both solid and in liquid for all composites tested

4) Were prepared and characterized Coating of PET film by dispersing the active filler in an adhesive used for food: the release of the active molecule and the antimicrobial activity of the films were better than those of composites

- The system PET-coating + LDH-active molecule is applied on fresh foods such as mozzarella, milk, grapes and cherries to demonstrate the effectiveness of controlled-release on lengthening the shelf life of food. These data are under patent so it was not possible to describe all but the tests

showed good results in terms of quality and durability of the organoleptic properties of foods examined.

5) During the PhD period spent at the laboratories of Prof. Giannelis, Cornell University, Ithaca, NY, has developed a new method of coating of polylactic acid (PLA) based on electrostatic forces between the positive charges of the hydrotalcite (LDH) and the negative charges created on the surface of the PLA plasma-treated. Were prepared and characterized antimicrobial coating stable and consistent, using phosphonium ionic liquids (IL) as anchored molecules to LDH and have been studied the barrier properties, resulting in a lowering of the water permeability of 35%.

With the same hydrotalcite modified with IL, were prepared by extrusion PLA composites, obtaining materials with improved mechanical properties by exploiting the capabilities of ionic liquid phosphonium salts as plasticizers.

6) Novel nanocomposites of apple peel pectin with 5%wt of nanohybrid fillers based on layered double hydroxide (LDH) containing molecules with antimicrobial activity: Benzoate (Bz), 2,4-dichlorobenzoate (DCBz), para hydroxybenzoate (p-OHBz) and orto hydroxybenzoate (o-OHBz) were prepared through high energy ball milling (HEBM) in presence of water. Milled composites and water were cast in Petri dishes and films obtained and analysed.

- X-ray analysis showed the absence of the peak corresponding to the basal spacing of the LDH hybrids in the composite samples, suggesting the exfoliation of the filler in all cases.
- Thermogravimetric analysis showed that the presence of the nanohybrids helps the pectin to degrade at higher temperatures for a protecting effect of LDH on the biopolymer.
- Elastic moduli of nanocomposites are higher than that exhibited from pure pectin and is higher composites with LDH/p-OHBz, probably for a stronger interactions between pectin matrix and nanohybrid layers via formation of hydrogen bonds, better favoured by the p-OHBz molecule
- Barrier properties to water vapour indicate the best improvement for composite with p-OHBz molecule, confirming that the interaction filler-continuous polymer phase has an important influence also on sorption and diffusion.
- Active molecules showed antimicrobial activity in all nanocomposite films stored at room temperature and environmental humidity. Such results indicate a potential application of the prepared composites in active packaging field

Conclusion

References

- Altieri, C. Scrocco, M. Sinigaglia, and M. A. Del Nobile, *J. Dairy Sci.* **2005**, 88:2683–2688.
- Alves, Vitor D.; Costa, Nuno; Coelho, Isabel M. **2010**, 79(2), 269-276;
- Ana Clarissa dos Santos Pires, Nilda de Fátima Ferreira Soares, Nélio José de Andrade, Luís Henrique Mendes da Silva, Geany Peruch Camilloto and Patrícia Campos Bernardes, *Packag. Technol. Sci.* **2008**; 21: 375–383.
- Appendini P, Hotchkiss JH. *Innov Food Sci Emerg* **2002**; 3(2): 113-126.
- Bergaya, B.K.G. Theng, G. Lagaly, *Handbook of Clay Science*, first ed., Elsevier, **2006**.
- Berti, C., Fiorini, M., Sisti, L., *Eur. Polym. J.* 45 **2009**, 70-78.
- Broz, M E, D L VanderHart, N R Washburn, *Biomaterials* 24, **2003** 4181–4190;
- Brun, C. D., Y. Hirata, V. Guillard, V. Ducruet, P. Chalier, A. Voilley; *J. Food Engineering*, 89 , **2008**, 217-226.
- Buchheit et al, **1985**
- Bugatti Valeria, Gorrasi, Montanari, Nocchetti, Tammaro, Vittoria; *Applied Clay Science* 52, **2011**, 34–40.
- Bugatti Valeria, Umberto Costantino, Giuliana Gorrasi, Morena Nocchetti, Loredana Tammaro, Vittoria Vittoria. *European polymer journal* 46 , **2010**, 418–427.

References

- Cabedo, Feijoo, Villanueva, Lagarón, & Giménez, **2006**
- Calvert, P., T. W. Ebbesen (Ed.) *Carbon Nanotubes*, CRC Press, Boca Raton, FL, 277-292, **1997**;
- Cavallaro, G., D. I. Donato, G. Lazzara and S. Milioto J. Phys. Chem. C **2011**, 115, 20491–20498;
- Chen, B.J. Qu, *Chem. Mater.* 15 **2003**, 3208.
- Chibwe, W. Jones, *Chem. Commun.* **1989**, 926.
- Christopher O. Oriakhi, Isaac v. Farr and Michael M. Lerner, *Clays and clay minerals*, vol. 45, no. 2, 194 202, **1997**;
- Cieniecka-Rosłonkiewicz Anna, Juliusz Pernak, Joanna Kubis-Feder, Alwar Ramani, Allan J. Robertson and Kenneth R. Seddon, *Green chem.*, **2005**, 7, 855–862
- Coffin, D. R., & Fishman, M. L. **1994**. *Journal of Applied Polymer Science*, 54, 1311–1320.
- Concise International Chemical Assessment Documents (CICADs). Benzoic acid and sodium benzoate; World Health Organization: Geneva, Switzerland, **2000**; ISBN 924153026X
- Costa, F. R.; Leuteritz, A.; Meinel, J.; Wagenknecht, U.; Heinrich, G. **2011**, 301 46-54.
- Costantino U, Marmottini F, Nocchetti M, Vivani R. *Eur J Inorg Chem* **1998**: 1439-1446.
- Costantino, U., Bugatti, V., Gorrasi G, Montanari F, Nocchetti M, Tammaro L, Vittoria V. *ACS Appl Mater Interfaces* **2009**; 1 (3): 668–677.
- Czaun, M. Rahman, M. Takafuji, M. Ihara, *Polymer* 49 **2008**, 5410-5416.
- Darder, M., M. López-Blanco, P. Aranda, F. Leroux, and E. Ruiz-Hitzky **2005**, 17, 1969-1977
- Davis, J.W. Gilman, T.E. Sutto, *Clay Clay Miner.* 52 (2) **2004**, 171.
- Del Nobile M.A., Piergiovanni L, Buonocore GG, Fava P, Puglisi ML, Nicolais L. Naringinase *J Food Sci* **2003**; 68: 2046-2049.
- Dubois Alexander, *Materials Science and Engineering*, 28, 1- 63 **2000**
- Einhorn-Stoll, b, U.; Kunzek, H. *Food Hydrocolloids* **2009b**, 23, 856–866
- Einhorn-Stoll, U.; Kunzek, H. *Food Hydrocolloids* **2009a**, 23, 40–52;
- Fan, H. Nishida, T. Mori, Y. Shirai, T. Endo, *Polymer* 45 **2004**, 1197-1205.
- Frunza et al., *J. Therm. Anal. Cal.*,93,**2008**
- Giannelis, *Adv. Mater.* 8 **1996**, 29.
- Giannelis, E. P., R. Krishnamoorti, E. Manias, *Adv. Polym. Sci.*, 118, 108-147, **1999**;

- Giavaresi G, Tschon M, Borsari V, Daly JH, Liggatt JJ, Fini M, Bonazzi V, Nicolini A, Carpi A, Morra M, Cassinelli C, Giardino R. *Biomed Pharmacother* **2004**; 58: 411-417.
- Goodburn, K. E. and Halligan, A. C., **1988**. modified-Atmosphere;
- Gorrasi G, Tortora M, Vittoria V, Pollet E, Lepoittevin B, Alexandre M, Dubois Ph. *Polymer* **2003**; 44(8): 2271-2279.
- Ha, M. Xanthos, *Applied Clay Science*, 47 **2010**, 303-310.
- Herrero, M.; Martinez-Gallegos, S.; Labajos, F. M.; Rives, V. *Journal of Solid State Chemistry* **2011**, 184(11), 2862-2869;
- Huang, Guobo; Zhuo, Anan; Wang, Liqiang; Wang, Xu. *Materials Chemistry and Physics* **2011**, 130(1-2), 714-720;
- Ionic liquids as modifiers for cationic and anionic nanoclays: acs symposium series; *american chemical society: washington, dc*, **2007**
- Jari Vartiainen, Tekla Tammelin, Jaakko Pere, Unto Tapper, Ali Harlin, *Carbohydrate Polymers* 82, **2010**, 989–996,
- Jasim Ahmed, Sunil K. Varshney, And Rafeal Aurasj *Food science*, vol 75, nr2, **2010**
- Jason Fang, Antonios Kelarakis, Luis Estevez, Yue Wang, Robert Rodriguez and Emmanuel P. Giannelis, *J. Mater. Chem.*, **2010**, 20, 1651-1653
- Jasse B, Seuvre A M, Mathlouthi M. (*Mathlouthi M.*, ed) **1997**; 1-22.
- Jay-Hyun Park, H Shin, *Materials letters* 61, **2007**, 156–159
- Jin Uk H, Marino Xanthos, *Applied clay science* 47 , **2010**, 303–310
- Joint FAO/WHO Expert Committee on Food Additives. Evaluation of the toxicity of a number of antimicrobials and antioxidants, Geneva, Switzerland, June 5-12, **1961**.
- Junjie Li, Hong Sun, Da Sun, Yuli Yao, Fanglian Yao, Kangde Yao, **2011**, 885–894
- Kaczmarek, Halina; Bajer, Krzysztof; Galka, Piotr; Kotnowska, Barbara. *Polymer Degradation and Stability*, **2007**;
- Kaczmarek, Halina; Dabrowska, Aldona; Vukovic-Kwiatkowska, Irena. *Journal of Applied Polymer Science* , **2011**, 122(3), 1936-1945;
- Kanazawa, A., T Ikeda and T Endo, *Antimicrobial agents and chemotherapy*, may **1994**, p. 945-952 vol. 38, no. 5
- Keskin, D. Kayrak-Talay, U. Akman, O. Hortaçsu, *J. of Supercritical Fluids* 43 **2007**, 150-180.
- Kester J J, Fennema O R. *Food Technol.* **1986**; 40: 47-59.
- Kim, S.V. Malhotra, M. Xanthos, *Microporous and Mesoporous Materials* 96 **2006**, 29-35.

References

- Kim, T. N, Q. L Feng, J. O Kim, J Wu, H Wang, G. C Chen and F. Z Cui,: *Journal of materials science: materials in medicine* 9, **1998** 129-134
- Kiyotomi Kaneda, Takato Mitsudome, Tomoo Mizugaki and Koichiro Jitsukawa, *Molecules* **2010**, 15, 8988-9007
- Klopogge J.T. and R.L, Ed. Vicente Rives, *Nova Science Publishers, Inc. New York*, **2001**
- Kotal, Moumita; Srivastava, Suneel Kumar; Bhowmick, Anil Kumar; Chakraborty, Sunity Kumar. *Polymer International*, **2011**, 60(5), 772-780;
- Kowalonek, Jolanta; Kaczmarek, Halina. **2010**, 46(2), 345-353;
- Laurienzo, P., M. Malinconico, G. Mazzarella, F. Petitto, N. Piciocchi, R. Stefanile, and M.G. Volpe, *J. Dairy Sci.* **2008**, 91:1317–1324
- Livi, J. Duchet-Rumeau, J-F. Gérard, *Chem Comm* 47 **2011**, 3589-3592.
- Livi, J. Duchet-Rumeau, T.-N. Pham, J.-F. Gérard, *J. Colloid Interface Sci.* 349 **2010**, 424.
- Lu Y, Chen SC. *Adv Drug Del Rev* **2004**; 56: 1621-1633.
- Lv, W. Zhou, H. Miao, W. Shi, *Progress in Organic Coatings*, 65 **2009**, 450-456.
- Mangiacapra P, Gorrasi G, Sorrentino A, Vittoria V. *Carbohydr Polym* **2006**; 64 (4): 516-523.
- Manzi-Nshuti, Charles; Songtipya, Ponusa; Manias, E.; Jimenez-Gasco, Maria M.; Hossenlopp, Jeanne M.; Wilkie, Charles A. *Polymer*, **2009**, 50(15), 3564-3574.
- Martin, O, L. Averous, *Polymer* 42, (**2001**), 6209
- Mikhail L. Zheludkevich, Dmitry G. Shchukin, Kiryl A. Yasakau, Helmut Mo'hwald, and Mario G. S. Ferreira; *Chem. Mater.* **2007**, 19, 402-411
- Milena Sinigaglia, Antonio Bevilacqua, Maria Rosaria Corbo, Sandra Pati, Matteo Alessandro Del Nobile, *Dairy Journal*, 18, **2008**, 624–630.
- Ming-Feng Chiang, Tzong-Ming Wu, *Composites science and technology* 70, **2010**, 110–115
- Mitchell, J. R., Hill, S. E., & Ledward, D. A., **1998**. Functional properties of food macromolecules (2nd ed.
- Ngo, K. Le Compte, L. Hargen, A.B. McEven, *Thermochim. Acta*, 97 **2000**, 357–358.
- Osman A M, Mittal V, Lusti H R. *Macromol Rapid Commun* **2004**, 25: 1145-1149

- Paola Fabbri, Massimo Messori, Monica Montecchi, Stefano Nannarone, Luca Pasquali, Francesco Pilati, Claudio Tonelli, Maurizio Toselli, *Polymer* 47, **2006**, 1055–1062
- Park, K., Xanthos, M., *Polym. Degrad. Stab.* 94 **2009**, 834-844.
- Piergiovanni, L. and Fava, P. 1994. Imballaggio funzionale per una migliore qualità degli alimenti confezionati. Milano 3-4 Febbraio **1994**. *Arti Poligrafiche Europee*;
- Piergiovanni, L. and Fava, P., **1987**. Il confezionamento alimentare in atmosfera modificata. *Arti Poligrafiche Europee* Publ. Milano;
- Pilar Aranda, Wen-Janq Chen, Charles R. Martin, *Journal of membrane science* 99, **1995**, 185-195
- Pilati et al *J Polym Environ*, **2009**, 17:10–19:
- Rahman, C.S. Brazel, *Polym. Degrad. Stab* 91 **2006**, 3371-3382.
- Ravi Kumar M N V, Kumar N. *Drug Dev Ind Pharm.* **2001**; 27: 1-30.
- Robertson G L., *Marcel Dekker* **1993**; 79-110.
- Salame M, (Finlayson K M, ed) *Technomic* **1989**; 132-145.
- Salame M, *John Wiley & Sons* **1986**; 48-54
- Samuli Hirsjärvi, Leena Peltonen, Jouni Hirvonen, *Colloids and surfaces b: biointerfaces* 49, **2006**, 93–99
- Sanes, F.J. Carrión, A.E. Jiménez, M.D. Bermúdez, *Wear*, 263 **2007**, 658-662.
- Schmidt, D. Shah, E.P. Giannelis, *Current Opinion in Solid State and Materials Science*, 6 **2002**, 205-212.
- Scott, M. Rahman, C.S. Brazel, *Eur. Polym. J*, 39 (**2010**) 1947-1953.
- Shi, L., S. Gunasekaran Preparation of Pectin–ZnO Nanocomposite *Nanoscale Res Lett*, **2008**, 3:491–495;
- Soroka V. Institute of Packaging Professionals, Herndon, VA, USA, **1995**.
- Sorrentino A, Gorrasi G, Tortora M, Vittoria V, Costantino U, Marmottini F, Padella F. *Polymer* **2005**; 46(5): 1601-1608.
- Sorrentino A, Gorrasi G, Tortora M, Vittoria V. *Polymer Nanocomposites* **2006**; 11: 273-292 .
- Suryanarayana, C., *Progress in Materials Sciences*, 46, 1-184, **2001**;
- Suvorova, A. I., Tyukova, I. S., Smirnova, E. A., & Peshekhonova, A. L. **2003**. Viscosity of blends of pectins of various origins with
- Takato Mitsudome, Yusuke Mikami, Hisashi Funai, Tomoo Mizugaki, Koichiro Jitsukawa, and Kiyotomi Kaneda, *Angew. Chem. Int. Ed.* **2008**, 47, 138 –141:
- Tammaro, L., Tortora M, Vittoria V, Costantino U, Marmottini F. *J Polym Sc Part A: Polym Chem* **2005**; 43: 2281-2290.
- Tammaro, L., U. Costantino, M. Nocchetti, V. Vittoria *Applied Clay Science*, **2009**, 43, 350-356;

References

- Urszula Doman´ska, and Lidia M. Casa´s, *J. Phys. Chem. B* **2007**, 111, 4109-4115
- Valcheva-Traykova, M.L., N.P. Davodova and A.H. Weiss, *J. Mater. Sci.* 28, **1993**, 215
- Vicente Rives Editor, *Nova Science Publisher, INC.*New York, **2001**
- Vieth W.R, Amini MA. In: *Hopfenberg*, Plenum Press. London, **1974**. p. 49-61
- Vittoria V, Gorrasi G., Sorrentino A, Tammaro L, Bugatti V, Costantino U, Nocchetti M., **2007**. (SA2007A/000031)
- Vittoria V, Gorrasi G., Sorrentino A, Tammaro L, Bugatti V, Costantino U, Nocchetti M., **2008**. (SA2008A/000024)
- Vittoria V.; Sorrentino A.; Gorrasi G.; Tammaro L.; Bugatti V.; Costantino U.; Nocchetti M.. *WO 2010/016034 A2* (11.02.2010)
- Vittoria V.; Tammaro L.; Bugatti V.; Bianchi R. **2011** (N. MI2011A/00192)
- Wang, Linjiang; He, Xuejun; Lu, Hongdian; Feng, Jianxiang; Xie, Xiangli; Su, Shengpei; Wilkie, Charles A. **2011**, 22(7), 1131-1138;
- Wilson O.C, Jr.a, T Olorunyolemi, A Jaworski, L Borum, D Young, A Siriwat, E Dickens, C Oriakhi, M Lerner, *Applied clay science* 15, **1999**. 265–279,
- Xie, R. Xie, W.P. Pan, D. Hunter, B. Koene, L.S. Tan, R. Vaia, *Chem. Mater.* 14 **2002**, 4837.
- Yan Lia, Wan-Guo Houa, Wei-Qun Zhu, *Colloids and surfaces a: Physicochem. Eng. Aspects* 303, **2007**, 166–172,
- Yuan, Yan; Zhang, Yong; Shi, Wenfang. *Applied Clay Science* **2011**, 53(4), 608-614;
- Zammarano, M. Franceschi, S. Bellayer, J. W. Gilman, S. Meriani, *Polymer*, 46 **2005**, 9314-9328.
- Zhao, F. Li, R. Zhang, D.G. Evans, X. Duan, *Chem. Mater.* 14 **2002**, 4286.
- Zheludkevich, M.L., S.K. Poznyak, L.M. Rodrigues D. Raps, T. Hack, L.F. Dick , T. Nunes, M.G.S. Ferreira; *Corrosion Science* 52, **2010**, 602–611
- Zhou, **2008**. Ph. D. Dissertation, New Jersey Institute of Technology, Newark, NJ, USA.
- Zweers MLT, Engbers GHM, Grijpma DW, Feijen J. *J Control Release* **2006**; 114: 317-324.